

# **AGE-RELATED CHANGES IN THE OPTICS OF HUMAN EYE WITH ACCOMMODATION**



Thesis submitted to The University of Manchester for the degree of  
Doctor of Philosophy (PhD) in the Faculty of Biology, Medicine and  
Health

2017

**Irene Sisó Fuertes**

Division of Pharmacy and Optometry

“Blank page”

# THESIS CONTENTS

<b>THESIS CONTENTS</b>	<b>3</b>
<b>LIST OF FIGURES</b>	<b>7</b>
<b>LIST OF TABLES</b>	<b>13</b>
<b>LIST OF EQUATIONS</b>	<b>14</b>
<b>LIST OF ABBREVIATIONS</b>	<b>15</b>
<b>ABSTRACT</b>	<b>17</b>
<b>DECLARATION</b>	<b>18</b>
<b>COPYRIGHT STATEMENT</b>	<b>19</b>
<b>ALTERNATIVE FORMAT</b>	<b>20</b>
<b>ACKNOWLEDGEMENTS</b>	<b>21</b>
<b>DEDICATION</b>	<b>23</b>
<b>1 INTRODUCTION</b>	<b>25</b>
<b>1.1 ACCOMMODATION MECHANISM</b>	<b>26</b>
1.1.1 INFLUENCE OF OTHER OCULAR STRUCTURES ON ACCOMMODATION	28
<b>1.2 THEORIES OF PRESBYOPIA DEVELOPMENT</b>	<b>29</b>
1.2.1 LENTICULAR THEORIES	30
1.2.2 EXTRALENTICULAR THEORY	32
1.2.3 CURRENT SOLUTIONS FOR PRESBYOPIA CORRECTION	34

<b>1.3</b>	<b>STRUCTURAL CHANGES IN THE CRYSTALLINE LENS</b>	<b>38</b>
1.3.1	STRUCTURAL CHANGES WITH ACCOMMODATION	38
1.3.2	CHANGES IN REFRACTIVE INDEX	41
1.3.3	STRUCTURAL CHANGES WITH AGE	43
1.3.4	STRUCTURAL CHANGES WITH ACCOMMODATION AND AGE	44
<b>1.4</b>	<b>OPTICAL CHANGES</b>	<b>45</b>
1.4.1	OPTICAL CHANGES WITH ACCOMMODATION	45
1.4.2	OPTICAL CHANGES WITH AGE	47
1.4.3	OPTICAL CHANGES WITH ACCOMMODATION AND AGE	49
<b>1.5</b>	<b>DYNAMIC CHANGES</b>	<b>51</b>
1.5.1	DYNAMICS OF ACCOMMODATION	52
1.5.2	DYNAMICS OF ABERRATIONS	54
1.5.3	DYNAMICS OF ACCOMMODATION WITH AGE	56
<b>1.6</b>	<b>RATIONALE AND GENERAL AIMS</b>	<b>57</b>
1.6.1	SPECIFIC OBJECTIVES	59
<b>1.7</b>	<b>REFERENCES</b>	<b>61</b>

**2 CORNEAL CHANGES WITH ACCOMMODATION USING DUAL SCHEIMPFLUG PHOTOGRAPHY**

	<b>CONTRIBUTIONS AND PUBLICATION</b>	<b>75</b>
<b>2.1</b>	<b>ABSTRACT</b>	<b>76</b>
<b>2.2</b>	<b>INTRODUCTION</b>	<b>77</b>
<b>2.3</b>	<b>METHODS</b>	<b>79</b>
2.3.1	SUBJECTS	79
2.3.2	MEASUREMENT SYSTEM	80
2.3.3	MEASUREMENT PROCEDURE	80
2.3.4	STATISTICAL ANALYSIS	82
<b>2.4</b>	<b>RESULTS</b>	<b>82</b>
<b>2.5</b>	<b>DISCUSSION</b>	<b>90</b>
<b>2.6</b>	<b>REFERENCES</b>	<b>97</b>

**3      RELATIONSHIP BETWEEN ACCOMMODATIVE RESPONSE FUNCTION AND CILIARY  
MUSCLE CHARACTERISTICS      103**

<b>CONTRIBUTIONS AND PUBLICATION</b>	<b>103</b>
<b>3.1 ABSTRACT</b>	<b>104</b>
<b>3.2 INTRODUCTION</b>	<b>105</b>
<b>3.3 METHODS</b>	<b>109</b>
3.3.1 SUBJECTS	109
3.3.2 ACCOMMODATIVE RESPONSE	111
3.3.3 CILIARY MUSCLE IMAGES	112
3.3.4 STATISTICAL ANALYSIS	118
<b>3.4 RESULTS</b>	<b>118</b>
<b>3.5 DISCUSSION</b>	<b>127</b>
<b>3.6 REFERENCES</b>	<b>136</b>

**4      CHANGES IN ACCOMMODATIVE FLUCTUATIONS WITH AGE AND MULTIFOCAL  
CONTACT LENSES      139**

<b>CONTRIBUTIONS AND PUBLICATION</b>	<b>139</b>
<b>4.1 ABSTRACT</b>	<b>140</b>
<b>4.2 INTRODUCTION</b>	<b>142</b>
<b>4.3 METHODS</b>	<b>145</b>
4.3.1 <u>EXPERIMENT 1: AGE-RELATED CHANGES IN ACCOMMODATION</u>	145
4.3.1.1 Subjects	145
4.3.1.2 Protocol	146
4.3.1.3 Static accommodative response measurements	147
4.3.1.4 Dynamic accommodative response measurements	148
4.3.2 <u>EXPERIMENT 2: ACCOMMODATION THROUGH MFCLs</u>	152
4.3.2.1 Contact lenses	153
4.3.2.2 Static and dynamic accommodative response measurements	153
4.3.3 STATISTICS	154
<b>4.4 RESULTS</b>	<b>154</b>
4.4.1 <u>EXPERIMENT 1</u>	154
4.4.2 <u>EXPERIMENT 2</u>	167

<b>4.5</b>	<b>DISCUSSION</b>	<b>172</b>
<b>4.6</b>	<b>REFERENCES</b>	<b>180</b>
<b>5</b>	<b><u>ACCOMMODATION AND OCULAR ABERRATIONS WITH TWO GENERATIONS OF MULTIFOCAL CONTACT LENSES</u></b>	<b>186</b>
	<b>CONTRIBUTIONS AND PUBLICATION</b>	<b>186</b>
<b>5.1</b>	<b>ABSTRACT</b>	<b>187</b>
<b>5.2</b>	<b>INTRODUCTION</b>	<b>188</b>
<b>5.3</b>	<b>METHODS</b>	<b>190</b>
5.3.1	SUBJECTS	190
5.3.2	CONTACT LENSES	191
5.3.3	EXPERIMENTAL PROCEDURE	192
<b>5.4</b>	<b>RESULTS</b>	<b>194</b>
<b>5.5</b>	<b>DISCUSSION</b>	<b>199</b>
<b>5.6</b>	<b>REFERENCES</b>	<b>205</b>
<b>6</b>	<b><u>FINAL SUMMARY AND FUTURE WORK</u></b>	<b>210</b>
<b>6.1</b>	<b>REFERENCES</b>	<b>215</b>
	<b><u>APPENDIX</u></b>	<b>216</b>

**Final word count: 46,146**

## LIST OF FIGURES

- Figure 1.1:** An illustration of the structure and growth of the lens. The fibres extend from the anterior to the posterior pole and originate as epithelial cells at the outer boundary of the lens body that will lose their nuclei and be covered by newer cells. (Source: Koretz and Handelman, 1988<sup>2</sup>) \_\_\_\_\_ 25
- Figure 1.2:** Schematic drawing demonstrating that all the zonules (AZ) on either side of the lens equator are tense in unaccommodated state (A) and relaxed lens in accommodated state (B). (Source: Rohen, 1979<sup>8</sup>) \_\_\_\_\_ 27
- Figure 1.3:** Summary of methods of presbyopia correction based on ophthalmic or optical devices. \_\_\_\_\_ 35
- Figure 1.4:** Change in anterior lens thickness and ACD during accommodation in a 29 year-old female. (Source: Dubbelman and Van der Heijde, 2005<sup>83</sup>) \_\_\_\_\_ 39
- Figure 1.5:** Contour plots of the refractive index distribution obtained in (A) young, unaccommodated; (B) young, accommodated, and (C) older crystalline lenses \_\_\_\_ 42
- Figure 1.6:** Higher-order RMS error of the eye expressed in micrometers ( $\mu\text{m}$ ) as a function of age for a 5.9 mm pupil diameter. The wavefront aberration and the associated point spread function (PSF) for one young and one older subject are also shown as an illustrative example. (Source: Artal et al., 2002<sup>110</sup>) \_\_\_\_\_ 49
- Figure 2.1:** The mean anterior and posterior corneal curvature keratometry, mean total corneal power, and mean pachymetry at different accommodative demands for the 3 corneal zones (central, mid, and peripheral). \_\_\_\_\_ 83
- Figure 2.2:** Anterior and posterior corneal keratometry, TCP, and pachymetry for the 3 corneal zones (central, mid, and peripheral) with the assumption that they are

constant with accommodation. Boxplots with medians (lines), 25% to 75% quartiles (boxes), ranges (whiskers), and outliers (+). \_\_\_\_\_ 86

**Figure 2.3:** The mean anterior and posterior corneal keratometry, TCP, and pachymetry for the 3 corneal zones (central, mid, and peripheral) with accommodation. \_\_\_\_\_ 87

**Figure 2.4:** Mean defocus  $Z(2,0)$  and spherical aberration  $Z(4,0)$  at different accommodative demand \_\_\_\_\_ 88

**Figure 3.1:** Schematic diagram of the laboratory set up for imaging the ciliary muscle with Visante AS-OCT. \_\_\_\_\_ 113

**Figure 3.2:** Example of a ciliary muscle segmentation by using the MATLAB code developed. Red line delimits the ocular structure and blue line the ciliary muscle region along with the pigmented epithelium. Transversal blue lines normal to the ciliary muscle curvature represent the thickness measurements taken with the custom software. \_\_\_\_\_ 116

**Figure 3.3:** Linear regression fitted to Kao et al.<sup>24</sup> data from mean CMT2 and mean CMT3. Black and red lines and dots represent data from Kao's et al.<sup>24</sup> algorithm data with a refractive index of  $n = 1$  and  $n = 1.38$ , respectively. Mean CMT values at 1 mm from the scleral spur empirically obtained by Kao et al.<sup>24</sup> were  $1.15 \pm 0.09$  and  $0.92 \pm 0.09$  for  $n = 1$  and  $n = 1.38$ , respectively. \_\_\_\_\_ 117

**Figure 3.4:** CMT relationship with age at the three different accommodative demands for a sample of 49 subjects. Dots, solid and dashed lines represent the CMT values, linear regression and confidence intervals for a 0.05 of significance level. Black colour corresponds to CMT2, grey to CMT25 and blue to CMT3. The



linear equations for the three respective CMT linear regressions are also displayed on top of each graph. \_\_\_\_\_ 119

**Figure 3.5:** CMT relationship with age at the three different accommodative demands for a sample of 18 subjects. Dots, solid and dashed lines represent the CMT values, linear regression and confidence intervals for a 0.05 of significance level. Black colour corresponds to CMT2, grey to CMT25 and blue to CMT3. The linear equations for the three respective CMT linear regressions are also displayed on top of each graph. \_\_\_\_\_ 120

**Figure 3.6:** CMT at three different accommodative stimulus. Boxplots with medians (lines), 25 % to 75 % quartiles (boxes), ranges (whiskers) and outliers (+). \_\_\_\_\_ 121

**Figure 3.7:** CMT for age groups 1 (red boxes), 2 (blue boxes) and 3 (green boxes) at three different accommodative stimulus. Boxplots with medians (lines), 25 % to 75 % quartiles (boxes), ranges (whiskers) and outliers (+). \_\_\_\_\_ 122

**Figure 3.8:** Mean CMT (open dots) and standard deviation for the 3 different points of the ciliary muscle at which thickness was measured and extrapolation of the mean CMT (solid dots) and standard deviation at 1 mm from the scleral spur. Data for the three age groups (red: age group 1, blue: age group 2 and green: age group 3) is shown. Solid lines represent the linear fit to the mean CMT data in each group. Linear equations and p-value for each of the regressions is displayed on top of each graph for the three age groups. \_\_\_\_\_ 124

**Figure 3.9:** Accommodative response slope and absolute value of the CMT slope for the 3 different points of the ciliary muscle at which thickness was measured and age groups (red dots: age group 1, blue dots: age group 2 and green dots: age group 3). Solid lines represent the linear fit to the data in each group. Linear equations and p-

value for each of the regressions is displayed on top of each graph for the three age groups. \_\_\_\_\_ 127

**Figure 4.1:** Example of dynamic accommodative response measurement when a 2.5 D stimulus was presented to a young subject (age group 1). Red lines in the graph are the portions of sustained accommodative response. Green asterisks delimitate the transition zones between accommodative states. \_\_\_\_\_ 149

**Figure 4.2:** Accommodative and disaccommodative amplitude for the 3 age groups and two different accommodative stimuli (blue boxplots: 2.5 D and red boxplots: 4 D). Boxplots with medians (lines), 25 % to 75 % quartiles (boxes), ranges (whiskers) and outliers (+). \_\_\_\_\_ 157

**Figure 4.3:** RMS deviation of the paraxial M for the 3 age groups (red boxplots: age group 1, blue boxplots: age group 2 and green boxplots: age group 3) and two different accommodative stimulus. Boxplots with medians (lines), 25 % to 75 % quartiles (boxes), ranges (whiskers) and outliers (+). \_\_\_\_\_ 158

**Figure 4.4:** RMS deviation of the HOA and SA for the 3 age groups (red boxplots: age group 1, blue boxplots: age group 2 and green boxplots: age group 3) and two different accommodative stimuli. Boxplots with medians (lines), 25 % to 75 % quartiles (boxes), ranges (whiskers) and outliers (+). One spurious data point in the HOAs – 2.5 D graph was deleted ( $0.52 \mu\text{m}$ ) for 0 D stimulus (initial resting state) to expand the scale. \_\_\_\_\_ 160

**Figure 4.5:** Accommodative and disaccommodative time constants for the 3 age groups and two different accommodative stimuli (top and bottom left boxplots: 2.5 D and top and bottom right boxplots: 4 D). Boxplots with medians (lines), 25 % to 75 % quartiles (boxes), ranges (whiskers) and outliers (+). \_\_\_\_\_ 161

**Figure 4.6:** Accommodative response slope and RMS deviation of the paraxial M for the 3 age groups (red dots: age group 1, blue dots: age group 2 and green dots: age group 3) and two different accommodative stimulus. Solid lines represent the linear fit to the data in each group. Linear equations and p value for each of the regressions is displayed on top of each graph for the three age groups. \_\_\_\_\_ 162

**Figure 4.7:** Accommodative response slope and RMS deviation of the paraxial M for age group 1. Subjects are divided according to their refractive error (blue dots: myopes (<-0.50 D), magenta dots: emmetropes (-0.50 to +0.50 D)) and two different accommodative stimulus. Solid lines represent the linear fit to the data in each subgroup. Linear equations and p value for each of the regressions is displayed on top of each graph for the two subgroups. \_\_\_\_\_ 164

**Figure 4.8:** Accommodative response slope and time constant for the 3 age groups (red dots: age group 1, blue dots: age group 2 and green dots: age group 3) and two different accommodative stimulus. Solid lines represent the linear fit to the data in each group. Linear equations and p value for each of the regressions is displayed on top of each graph for the three age groups. \_\_\_\_\_ 165

**Figure 4.9:** Accommodative response slope and time constant for age group 1. Subjects are divided according to their refractive error (blue dots: myopes (<-0.50 D), magenta dots: emmetropes (-0.50 to +0.50 D)) and two different accommodative stimulus. Solid lines represent the linear fit to the data in each subgroup. Linear equations and p value for each of the regressions is displayed on top of each graph for the two subgroups. \_\_\_\_\_ 167

**Figure 4.10:** Slope of the accommodative response for the 3 conditions (purple boxplots: without contact lenses, blue boxplots: PureVision 2 and orange boxplots:

Proclear). Boxplots with medians (lines), 25 % to 75 % quartiles (boxes), ranges (whiskers) and outliers (+). \_\_\_\_\_ 168

**Figure 4.11:** RMS deviation of the paraxial M for the 3 conditions (purple boxplots: without CLs, blue boxplots: PureVision2 and orange boxplots: Proclear) and two different accommodative stimuli. Boxplots with medians (lines), 25 % to 75 % quartiles (boxes), ranges (whiskers) and outliers (+). \_\_\_\_\_ 169

**Figure 4.12:** Accommodative and disaccommodative time constants for the 3 conditions tested and two different accommodative stimuli (top and bottom left boxplots: 2.5 D and top and bottom right boxplots: 4 D). Boxplots with medians (lines), 25 % to 75 % quartiles (boxes), ranges (whiskers) and outliers (+). \_\_\_\_\_ 171

**Figure 4.13:** Accommodative response slope and time constant for the conditions tested (purple boxplots: without contact lenses, blue boxplots: PureVision 2 and orange boxplots: Proclear) and two different accommodative stimulus. Solid lines represent the linear fit to the data in each group. Linear equations and p value for each of the regressions is displayed on top of each graph for the three conditions. \_\_\_\_\_ 172

**Figure 5.1:** Mean CDVA and mean DCNVA in photopic conditions for subjects wearing the two types of simultaneous vision MFCLs. Error bars represent standard error. \_\_\_\_\_ 194

**Figure 5.2:** Mean stimulus-response function for each MFCL. The lines represent the best linear trend for each condition. Blue line refers to the PureVision High Add and red line represents the PureVision 2 High Add. Linear equations for each of the regressions is displayed on top of the graph for both conditions. Error bars represent standard error of the means. \_\_\_\_\_ 195

**Figure 5.3:** Mean Zernike aberration coefficients when the three accommodative stimuli (0 D, 2.5 D and 4 D) were presented for the PureVision High Add and PureVision 2 High Add, respectively. Error bars represent standard error of the means. \_\_\_\_\_ 197

**Figure 5.4:** Mean Zernike aberration coefficients when the two types of simultaneous vision MFCLs were worn for the three accommodative stimuli (0 D, 2.5 D and 4 D), respectively. Error bars represent standard error of the means. \_\_\_\_\_ 198

## LIST OF TABLES

**Table 1.1:** Anatomical changes (mean value and standard deviation) per dioptre of accommodation using Scheimpflug imaging. (Source: Dubbelman and Van der Heijde, 2005<sup>83</sup>) \_\_\_\_\_ 40

**Table 2.1:** Mean anterior and posterior corneal surface keratometry, TCP, and pachymetry for the different accommodative demands. Two-way repeated ANOVA results statistical significance (P Value) and substantive significance (Partial Eta Squared). \_\_\_\_\_ 85

**Table 2.2:** Mean of Zernike polynomials for the different accommodative states. Repeated ANOVA results and significance. \_\_\_\_\_ 89

**Table 3.1:** Demographic data. \_\_\_\_\_ 110

**Table 3.2:** Mean and standard deviation for CMT2, CMT25 and CMT3 at the different accommodative demands. P-value for Friedman and Wilcoxon tests for the different comparisons. Asterisks (\*) indicate statistically significant differences ( $p < 0.05$ ) in CMT with accommodation. \_\_\_\_\_ 121

**Table 3.3:** Mean and standard deviation for CMT1, CMT2, CMT25 and CMT3 at the different accommodative demands and age groups. P-value for the linear relationship between the empirically obtained CMT and the distance it was measured at each accommodative demand presented, is also shown. Asterisks (\*) indicate statistically significant differences ( $p < 0.05$ ) in CMT. \_\_\_\_\_ 125

**Table 3.4:** Comparison of CMT results at 3 different distances from the scleral spur (1, 2 and 3 mm) in disaccomadated state from previous publications with the results from the present study for the particular age group tested. The region of the ciliary muscle assessed in each publication is included: N (Nasal), T (Temporal). \_\_\_\_\_ 133

**Table 4.1:** Number, distribution and demographics of subjects and continuous accommodative response measurements included in the study. \_\_\_\_\_ 156

**Table 5.1:** Demographic information for all 8 subjects. \_\_\_\_\_ 191

## LIST OF EQUATIONS

**Equation 4.1:** RMS deviation, where  $n$  is the number of values,  $x_i$  is each individual value and  $\bar{x}$  is the mean value. \_\_\_\_\_ 151

**Equation 4.2:** Time constant calculation.  $t_{10}$  and  $t_{90}$  are the times in seconds at which the accommodative response was 10% and 90% of the accommodative amplitude, respectively. The difference is divided by the natural logarithm of 9 in order to obtain the time constant ( $\tau$ ) in seconds. \_\_\_\_\_ 152

**Equation 5.1:** Surface fitting procedure that minimizes the RMS of the wave aberration using the second-order Zernike coefficients.<sup>21</sup> \_\_\_\_\_ 193

## LIST OF ABBREVIATIONS

ACD: Anterior Chamber Depth

ANOVA: Analysis Of Variance

AS-OCT: Anterior Segment Optical Coherence Tomography

CCT: Central Corneal Thickness

CDVA: Corrected Distance Visual Acuity

CL: Contact Lens

CMT: Ciliary Muscle Thickness

CMT2 : Ciliary Muscle Thickness at 2 mm from the scleral spur

CMT25 : Ciliary Muscle Thickness at 2.5 mm from the scleral spur

CMT3 : Ciliary Muscle Thickness at 3 mm from the scleral spur

DCNVA: Distance Corrected Near Visual Acuity

DoF: Depth of Focus

GRIN: Gradient of Refractive Index

HFC: High Frequency Component

HOA: Higher Order Aberration

IOL: Intraocular Lens

LFC: Low Frequency Component

M: Equivalent Refraction

MFCL : Multifocal Contact Lens

MRI: Magnetic Resonance Imaging

MTF: Modulation Transfer Function

OCT: Optical Coherence Tomography

PCI: Partial Coherence Interferometry

PSF: Point Spread Function

RMS: Root Mean Square

SA: Spherical Aberration

SD: Standard Deviation

TCP: Total Corneal Power

VA: Visual Acuity



# ABSTRACT

## Age-related changes in the optics of human eye with accommodation

Irene Sisó Fuertes

A thesis submitted to The University of Manchester for the degree of Doctor of Philosophy (PhD), 2017

**PURPOSE:** The mechanism of accommodation together with its age-related changes is complex and still not fully understood. The objective of this PhD thesis is to extend this knowledge and evaluate the accommodative performance with some options for presbyopia correction available at present.

**METHODS:** The latest technology was used to assess the accommodative function both from a structural and optical point of view. Corneal and ciliary muscle changes with accommodation were evaluated in the first two experimental chapters. Chapter 3 combined imaging data of the ciliary muscle with information of the optical response to different accommodative demands in an age divided cohort, whose accommodative response was analysed in a static and dynamic way in Chapter 4. Fluctuations in accommodation and dissaccommodation and time constants were measured in natural conditions. Additional dynamic (Chapter 4) and static (Chapter 5) assessment of the accommodative performance was done for young subjects fitted with multifocal contact lenses (MFCLs).

**RESULTS and CONCLUSION:** Cornea is stable during accommodation while the ciliary muscle thickness varies at different accommodative demands but not as a consequence of ageing. Microfluctuations in accommodation show highly intra-subject variability, but a trend to play a role in accommodation control can be observed. In general, a bigger magnitude of fluctuations is found when accommodation is more accurate. Ageing has a significant effect on the accommodative fluctuations when a small stimulus (2.5 D) is presented but not on time constants. Subjects in the third decade of life present the highest magnitude of accommodative fluctuations as their accommodative system is more stressed. Multifocal contact lenses fitted in young subjects do not affect the accommodative dynamics. Some improvements have been seen when different generations of multifocal contact lenses are assessed.

The applicability of this research to the improvement of solutions capable of restoring the accommodative ability in older eyes, widens the future scope of this research.

## **DECLARATION**

I hereby declare that no portion of the work referred to in this thesis has been submitted in support of an application for another degree or qualification of The University of Manchester, or any other university or institute of learning.

## COPYRIGHT STATEMENT

- i. The author of this thesis (including any appendices and/or schedules to this thesis) owns certain copyright or related rights in it (the “Copyright”) and s/he has given The University of Manchester certain rights to use such Copyright, including for administrative purposes.
- ii. Copies of this thesis, either in full or in extracts and whether in hard or electronic copy, may be made only in accordance with the Copyright, Designs and Patents Act 1988 (as amended) and regulations issued under it or, where appropriate, in accordance with licensing agreements which the University has from time to time. This page must form part of any such copies made.
- iii. The ownership of certain Copyright, patents, designs, trademarks and other intellectual property (the “Intellectual Property”) and any reproductions of copyright works in the thesis, for example graphs and tables (“Reproductions”), which may be described in this thesis, may not be owned by the author and may be owned by third parties. Such Intellectual Property and Reproductions cannot and must not be made available for use without the prior written permission of the owner(s) of the relevant Intellectual Property and/or Reproductions.
- iv. Further information on the conditions under which disclosure, publication and commercialisation of this thesis, the Copyright and any Intellectual Property University IP Policy (see <http://documents.manchester.ac.uk/display.aspx?DocID=24420>), in any relevant Thesis restriction declarations deposited in the University Library, The University Library’s regulations (see <http://www.library.manchester.ac.uk/about/regulations/>) and in The University’s policy on Presentation of Theses.

## **ALTERNATIVE FORMAT**

Permission was conceded by the Faculty of Biology, Medicine and Health to submit this thesis in alternative format in accordance with the rules and regulations of The University of Manchester. This thesis is composed of a series of related publications that had already been either published, or prepared for submission to peer-reviewed journals. The author's contribution along with the publication status of the work presented in each chapter is identified on the first page of each chapter.

The thesis begins with a general introduction which reviews the current state of the art on the short and long term changes affecting accommodation (Chapter 1), followed by Chapters 2 to 5 presented as journal style manuscripts and ends with a final summary of the entire thesis and future work (Chapter 6)

## **ACKNOWLEDGEMENTS**

Foremost, I would like to express my sincerest gratitude to my supervisor Dr. Hema Radhakrishnan for her support, understanding, guidance and encouragement during the years of the PhD.

I am deeply thankful to my family for their endless encouragement and continuous and unparalleled love and support. I would also like to thank Felipe for showing me the bright side of things during the last and toughest part of my PhD.

My gratitude to all my fellow PhD candidates and friends in Spain and UK. They, either virtually or personally listened to me and gave me the necessary distractions from my research making my stay in Manchester memorable.

My thanks also go to all the staff in Optometry for the assistance provided throughout my project.

Finally, I would like to thank all the participants involved in the studies.

This project has received funding from the European Union's FP7 research and innovation programme under the Marie Curie Initial Training Network AGEYE (FP7-PEOPLE-ITN-2013), grant agreement No 608049



*To my parents, Blanca Fuertes Bona and Jose Miguel Sisó Espitia  
for their endless love and warm support in all walks of life.*

“Blank page”



# 1 INTRODUCTION

The human eye can be understood as a compound optical system whose principles of image formation are the same as for many man-made optical systems. The crystalline lens contributes to around one third of the total power of the eye's optical system. The lens has a biconvex form with aspheric surfaces and it is known to be a highly variable structure and unique in that it grows throughout life by the addition of new cells.<sup>1</sup>

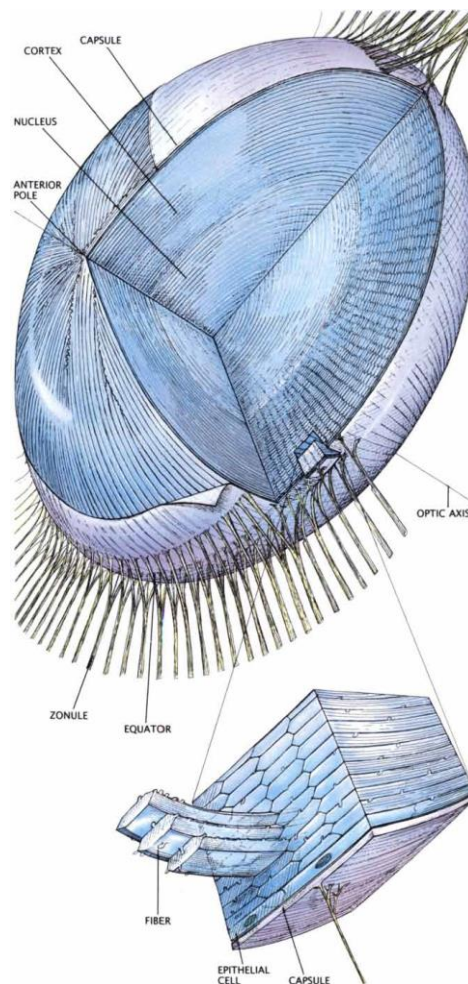


**Figure 1.1:** An illustration of the structure and growth of the lens. The fibres extend from the anterior to the posterior pole and originate as epithelial cells at the outer boundary of the lens body that will lose their nuclei and be covered by newer cells. (Source: Koretz and Handelman, 1988<sup>2</sup>)

Hence, a lot of the long term changes are produced as a consequence of ageing. Moreover, the crystalline lens is able to change its shape to accommodate. This allows the eye to bring near objects into focus in young subjects and therefore produce short term changes in its performance due to the accommodation ability. Accommodation is usually treated as a static process but has been proved to continuously change and exhibit fluctuations over time.

## **1.1 Accommodation mechanism**

The human accommodation mechanism has been widely studied since the 17th century. Scheiner<sup>3</sup> already showed the presence of a mechanism capable of focusing at different distances on looking through a double pin-hole.<sup>4</sup> Later in 1637, in his *Traité de l'Homme*, Descartes also accepted the view that in order to permit viewing of objects at different distances, the lens changes its shape; and conjectured that it must be controlled by muscles. Although he lacked experimental evidence his hypothesis was found to be correct in 1801 by Young. Young demonstrated by examining aphakic patients, that despite his suppositions about the possible influence of a decrease in corneal radius and an increase in the distance between the lens and the retina, in the mechanism of accommodation; most of this process is attributed to the changes in the crystalline lens.<sup>5</sup>

In 1855 Helmholtz first proposed his classical theory of accommodation. He stated that the increase in thickness and curvature of the crystalline lens leads to a rise in optical power during accommodation.<sup>6, 7</sup> This is a consequence of a contraction of the annular ciliary muscle which pulls the ciliary body forward and causes a

reduction of tension in the zonular fibers attached on either side of the lens equator<sup>6,7</sup> (Figure 1.2).

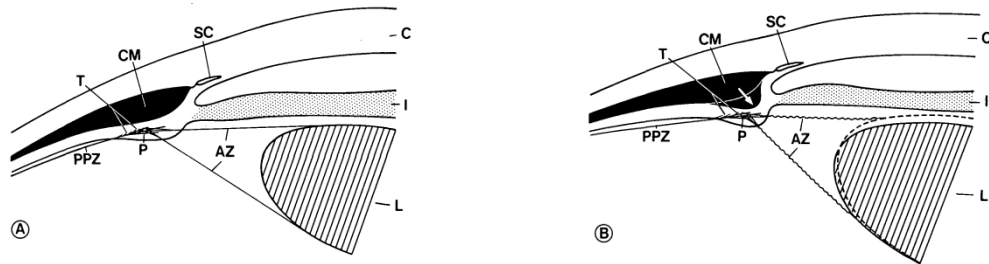


**Figure 1.2:** Schematic drawing demonstrating that all the zonules (AZ) on either side of the lens equator are tense in unaccommodated state (A) and relaxed lens in accommodated state (B). (Source: Rohen, 1979<sup>8</sup>)

This statement was expanded by Gullstrand<sup>9</sup> who asserted that the extracapsular changes described by Helmholtz account for around two-thirds of the refractive power increment. Thus the remaining third is due to the intracapsular rearrangement of the lens fibers. During accommodation, the zonular insertion points are separated by the increase in thickness of the lens which involves a dislocation of particles, which also results in changes in the substance of the lens. These changes explain the connection between the structure and the total variation of the refractive index occurring in the course of the accommodation process.<sup>10</sup> Despite the fact that this is challenged by some authors who state completely the opposite<sup>11,12</sup>, it is the most accepted theory of accommodation.<sup>7,13-15</sup> However, this mechanism still remains unclear and therefore numerous studies about the structural changes during accommodation of the lens are reviewed next.

### 1.1.1 Influence of other ocular structures on accommodation

Another suggestion that has been queried is whether there are any other ocular parameters or structures such as vitreous, choroid or cornea that could affect accommodation. Regarding the vitreous implications, it is clear that there is a bowing-relaxation movement of the hyaloids membrane during the accommodation process due to the closeness of structures.<sup>16-19</sup> Clinical studies with vitrectomized eyes conclude that the vitreous is not essential for the human eye to efficiently accommodate and for the lens anterior pole to move forward.<sup>20, 21</sup> As far as the choroid is concerned, there are very few investigations. A thinning of the choroid layer has been evidenced<sup>22-24</sup> during accommodation and suggested to be a possible cause of the axial length increase observed during accommodation<sup>23, 24</sup> what was previously neglected by Young.<sup>5</sup> In order to understand these features, further studies should be done utilising simultaneous measurements of ocular optics and ocular biometrics during near tasks. When it comes to the corneal changes during accommodation, there is some controversy and diversity of measurement methods in the published literature. The corneal implications in accommodation come from the assumption that the ciliary muscle must affect the cornea, mostly in the periphery, due to its anatomical proximity to the limbus.<sup>25, 26</sup> Thus, when the corneal periphery (7 mm) has been assessed, a steepening of the corneal topography in the maximum and minimum keratometric values<sup>26, 27</sup>, an increase in refraction<sup>26</sup> and a change in corneal volume as well as in corneal aberrations with accommodation<sup>25</sup>; have been found. Other studies suggest that the origin of corneal changes with accommodation is due to significant cyclotorsion

produced in the corneal topography when changing focus.<sup>27, 28</sup> When this rotation is corrected and the central portion of the cornea is considered, the corneal changes are found to reduce considerably and are not statistically significant.<sup>27-29</sup> Only Ni et al.<sup>25</sup> and Yasuda et al.<sup>26</sup> have evaluated these changes in presbyopic patients. The latter study found no association between age and changes in corneal refraction, suggesting a more important role in presbyopes compared to younger patients.<sup>26</sup> This is because presbyopic subjects have reduced amplitude of accommodation, the increase in corneal refraction becomes more important in supporting the remaining accommodating function.<sup>26</sup> Thus, this is an area worthy of further investigation.

## **1.2 Theories of presbyopia development**

Another fundamental factor that contributes to the crystalline lens long term changes is ageing. Donders and Moore<sup>30</sup> noticed that the range of distances for which the eye is able to focus clearly, progressively declines with age and subsequently other authors have found that the decrease is almost linear and it reaches zero at about 50 years of age.<sup>31-34</sup> Hence, presbyopia becomes manifested when the near point no longer coincides with the normal near working distance.

While Helmholtz's theory of accommodation has attained general support from the optometric community, the same cannot be said about the theories of presbyopia evolution. There is a large range of theories that have been developed, however the causal factors of age-related accommodative loss leading to presbyopia still remain undefined. Despite this fact, the more relevant theories are described as lenticular (including mechanical and geometric theories) or extralenticular theories.<sup>35</sup>

### 1.2.1 Lenticular theories

As described before, lenticular anterior and posterior surfaces' radii of curvature and the distribution of the index gradient change with age.<sup>2, 36</sup> This suggests that there is a progressive increase in the mass, thickness, hardness and volume of the lens and also changes in the insertion point of the zonules to the crystalline lens.<sup>2, 36</sup> Apart from a decline in light transmission associated with an increased dispersion, an increase in spectral absorption and an increase in fluorescence are also found in the crystalline lens.<sup>36, 37</sup> These structural changes that occur in the lens with ageing are further described below. Regarding lenticular theories of the causes of presbyopia, Hess<sup>38</sup> – Gullstrand<sup>39</sup> and Duane<sup>40</sup> – Fincham<sup>41</sup> theories are the two most important, mutually exclusive variations. They deal with the mechanical resistance in the lens and capsule due to the increase in hardness of the lens, assuming that the ciliary muscle preserves its power.<sup>13, 35, 42-44</sup> The Hess-Gullstrand theory is different from the Duane-Fincham theory in that, it stated that ciliary muscle contraction is constant throughout life for the same dioptric accommodation, but as age increases and amplitude of accommodation diminishes there is a latent proportion of contraction that won't produce any accommodative change.<sup>35, 42</sup> This theory has been described more recently by some authors<sup>13, 35, 44</sup> as an oversimplification, since Fisher<sup>45</sup> provided overwhelming evidence against it. They<sup>45</sup> measured directly on cadaver eyes, the change in the force of ciliary muscle contraction which is required to produce a given change in power at a certain age and found that it progressively rises from 30 years old on due to the increase of the

lens resistance to deformation, and starts declining by the age of 50 years. Thus, contradicting the Hess-Gullstrand assumption.

The Duane-Fincham theory, has been also treated as two different theories.<sup>35</sup>

Duane<sup>46</sup> had an extralenticular vision of the causes of presbyopia and thought that “the activity of the ciliary muscle diminishes with age, and that in advanced life only a comparatively small amount of ciliary energy can be put into play”; while Fincham did not.<sup>35, 41, 42, 47</sup> Fincham<sup>41, 47</sup> reasoned that as the eye ages and lens hardness increases, the amount of ciliary muscle contraction also increases in order to deform the lens upon a given accommodative effort. Thus, at the maximum amplitude of accommodation, the ciliary muscle will be maximally contracted too.<sup>35, 42, 46</sup> This is in agreement with the early findings of Fisher et al.<sup>45</sup> and the most recent from Shao et al.<sup>48</sup> who also disagree with the Duane<sup>46</sup> theory.

When it comes to the geometric theory, it is based on changes in the shape and size of the lens. With increasing age, the relationship between crystalline lens and the surrounding structures changes. Using cadaver eyes, Farnsworth and Shyne<sup>49</sup> suggested that causes of presbyopia could be partially attributed to the changes in the suspension geometry of the lens. Later, Koretz, Handleman et al.<sup>50</sup> and Koretz and Handleman<sup>2</sup> helped by Brown’s slit lamp photographs, provided more insight into this theory. On the basis of these photographs they created a mathematical model and determined that as a result of lens growth, both the point and the angle of application of the zonular forces is altered in older eyes. This alteration makes the zonules to be more tangential to the lens capsular surface, so they can cause less tension.<sup>51</sup> Schachar<sup>44</sup> who has been a staunch defender of his own mechanism of accommodation theory, agreed with this explanation, but maintaining his theory

of accommodation in which accommodation is caused by an increase in zonular tension rather than a decrease as in the Helmholtz theory.<sup>6,7</sup>

The most recent publications support Koretz and Handleman's theory who envisioned that lens growth is the causal factor in the development of presbyopia as it leads to a more complex mechanism involving age related changes in the geometric relationship between the lens and surrounding accommodative structures.<sup>2, 13, 52</sup> Strenk et al.<sup>13, 53</sup> have proposed The Modified Geometric Theory of presbyopia development. They suggest that presbyopia results in an age-related mechanical change in the lens material but it is not caused by it. Hence, they describe accommodative loss as an effect of lens growth. The Modified Geometric Theory states that as the lens continually thickens with age, it applies forces to the iris causing and anterior and inward movement of the uvea (that acts at a unit) as well as the constriction of the pupil. This ciliary muscle movement causes the circumlental space to reduce, while maintaining its asymmetry<sup>54</sup>, resulting in a decrease in zonular tension. This lack of zonular tension prevents any change in lens shape, although the ciliary muscle still contracts.<sup>13, 53</sup>

### **1.2.2 Extralenticular theory**

On the other hand, the extralenticular theory refers to the weakening of the ciliary muscle (suggested by Duane<sup>46</sup>) or loss of elasticity of its components as the main cause of presbyopia. Nonetheless, the development of imaging technologies such as magnetic resonance imaging (MRI) and optical coherence tomography (OCT), have rejected this theory. Using MRI, that allows visualisation of the ciliary muscle



and processes in the eye without optical distortions, Strenk and colleagues<sup>52, 55-57</sup> have found that there isn't any change in ciliary muscle contraction with age and besides, it maintains its mobility throughout life. Assessment of the ciliary muscle in the human eye is difficult since the iris blocks direct observation. Many attempts to study the ciliary muscle behaviour have been made with rhesus monkeys, finding that though there is a decrease in accommodation function with age in this species too, presbyopia develops very differently from humans.<sup>13</sup> Examining human beings through MRI, a decrease in the ciliary muscle ring diameter (probably due to the ciliary body thickening) that leads to a decline in circumlental space with age<sup>53, 54</sup>; has been found. This reduction in circumlental space has potential effects in reducing zonular tension.<sup>53, 57, 58</sup> Thus, supporting the geometrical theory of presbyopia and rejecting the extralenticular theory. This overall anterior-inwards shift of the ciliary muscle as well as the preservation of its contractility, even in presbyopes, is consistent with the *in-vivo* findings of Sheppard and Davies<sup>59</sup> using anterior segment OCT (AS-OCT). They found the expected thickening of ciliary muscle with age but just in the anterior portion (first 25% of overall length from the scleral spur) and they also detected a progressive asymmetric thinning the point 75% of the overall length posterior to the scleral spur.<sup>59</sup> To get these data they relied on correction algorithms for optical distortion and assumed refractive indexes. Richdale et al.<sup>60</sup> used AS-OCT, ultrasonography and high resolution MRI to measure the ciliary muscle and lens of their participants. However, only lens thickness was measured with the three approaches resulting in very similar values. Correlation of results was not calculated between methods for any of the parameters measured; hence, correlation measurements of both MRI and OCT

ciliary muscle data should be made to provide consistency and a new standpoint on presbyopia development. The findings of these two last studies<sup>59, 60</sup> which are the only ones that look into the ciliary muscle characteristics in a presbyopic cohort, also contradict the extralenticular theory of presbyopia, yet agree with a lensocentric-geometric model as a consequence of anterior zonular migration. This also suggest that the still unknown presbyopia development has a multifactorial origin as Weale et al.<sup>61, 62</sup> alluded to. Due to the paucity of ciliary muscle data in people older than 50 and the increased use of presbyopia correction methods that rely on the ciliary muscle functionality, this is an area worth of further investigation. The most common methods of presbyopia correction previously mentioned and available at present will be reviewed next.

### **1.2.3 Current solutions for presbyopia correction**

Longevity and in consequence the percentage of older people (30 % men and 14 % women) active in the labour force has increased in the last years. Besides, vision loss caused by refractive errors is within the first 8<sup>th</sup> causes of disability among older people globally. Therefore any correction involves supplying a solution to restore or enhance the accommodative ability of those people suffering presbyopia. Currently, there are many developed non-invasive and invasive (surgery) approaches available. Only the ones that rely on ophthalmic or optical devices to correct presbyopia are reviewed and are summarized in the following flowchart (Figure 1.3).

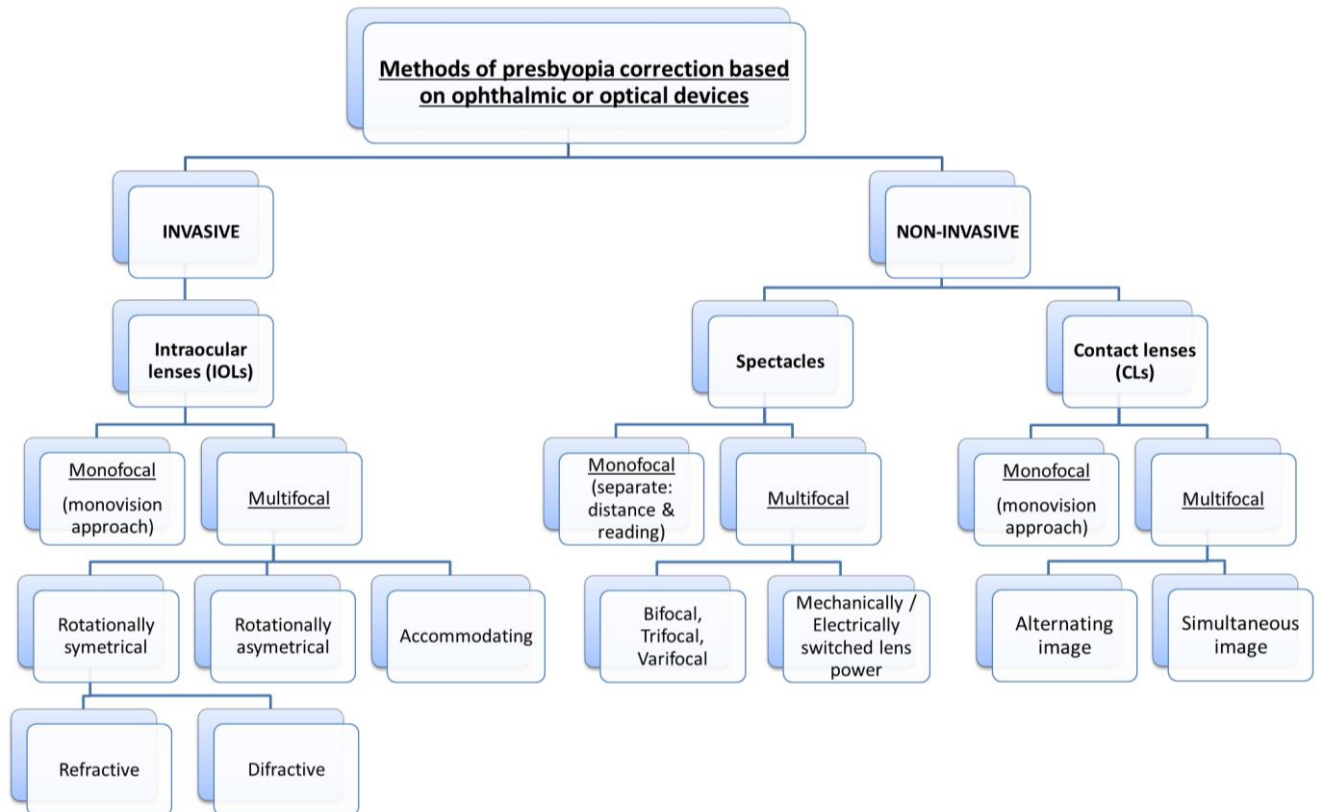


**Figure 1.3:** Summary of methods of presbyopia correction based on ophthalmic or optical devices.

Invasive methods of presbyopia correction through lenticular approaches comprise different options such as phakic and pseudophakic intraocular lenses (IOLs).<sup>63, 64</sup> The latter are commonly prescribed due to their higher safety and low rate of complications compared to the phakic IOLs (i.e. the intraocular lens is implanted into the eye but the natural crystalline lens being preserved).<sup>64</sup> When it comes to pseudophakic IOLs, they could be divided into monofocal and multifocal. Monofocal IOLs for presbyopia correction are usually implanted following a monovision approach to produce reasonable degree of spectacle independence which is also the ultimate goal of all the multifocal designs.<sup>63</sup> Most of the multifocal designs available in the market are rotationally symmetrical and according to their optical

design can be refractive or diffractive. Refractive IOLs have different powers distributed in circular, concentric refractive zones while diffractive IOLs possess diffractive zones (microscopic steps) that direct the light towards the distance, near and also intermediate foci in the case of the trifocal designs. Rotationally asymmetrical IOLs are also being implanted and consist of a IOL which is segmented for near vision.<sup>64</sup> Accommodating IOLs were designed in order to avoid the optical side effects of multifocal IOLs such as glare or haloes that produce bothersome visual disturbances and can affect the quality of life.<sup>65</sup> There are different concepts but all of the accommodating IOLs rely on the action of the ciliary muscle to produce an axial movement of the optic in order to change the dioptric power of the eye. Hence, the importance of understanding the functionality of the ciliary muscle when looking at different distances especially in people older than 50 years.

Non-invasive presbyopia correction methods include spectacles and contact lenses (CLs). In terms of the spectacles, aside from the conventional bifocal or varifocal lenses, there are other type of lenses capable of mechanically or electrically switching the lens power to provide the needed dioptric amount at each distance.<sup>66</sup> Monofocal CLs have also been extensively used for presbyopia correction by creating monovision. However, multifocal contact lenses (MFCLs) have gained more popularity in the last few years.<sup>67</sup> They can be alternating image MFCLs in which the near correction is located in the lower half of the CL or simultaneous image MFCLs that have both distance and near powers located within the pupillary area. While the alternating image ones rely on a translation of the CL to change its position with respect to the pupil depending on gaze position; patients wearing

simultaneous image MFCLs need to suppress the blurred image out of all the images created, to choose the clearest one for that particular task. In consequence, there is a monocular degradation of the image that leads to the reported reduction in contrast sensitivity for MFCLs when compared to monofocal CLs or spectacles.<sup>68,69</sup> However, when the subjective performance of MFCLs with a similar design has been compared big differences have not been found.<sup>70-72</sup> Overall, most of the published studies agree on that simultaneous image MFCLs provide adequate and acceptable visual acuity at distance and near with preserved stereo acuity when worn by presbyopes.<sup>68-73</sup> Studies investigating the effect of the remaining accommodation, which may be used in addition to the add power conferred by the MFCLs correction worn by early presbyopes and young individuals, have been conducted. Significant differences in accommodative response at different accommodative levels have not been found when comparing different designs of simultaneous image MFCLs or when compared to monofocal designs.<sup>74-76</sup> Hence, it has been suggested that MFCLs do not provide important changes in the accommodative system of young subjects. Changes in the accommodative system of young subjects wearing MFCLs have only been assessed in terms of static accommodation. There are not studies that have looked into the interaction of simultaneous vision MFCLs with the accommodative fluctuations.

The evolution of the different solutions for presbyopia correction would not have been possible without the development of instrumentation. Far from the rudimentary pin-holes or optometers used by Scheiner<sup>3</sup> and Young<sup>5</sup>, the accessibility to new instruments is continuously renewing the interest and

extending the understanding in the mechanism of accommodation and the age-related changes. Therefore, various methods such as ultrasonography, Scheimpflug photography, partial coherence interferometry (PCI), OCT and MRI have been used to measure the dimensions of the lens *in-vivo*. Additionally, since the mid-1990's when aberrometry was introduced to the vision sciences field, ocular aberrations have been assessed in great detail.<sup>77-81</sup>

As a result of the considerable structural and optical changes that the eye undergoes during accommodation and ageing, a number of changes in ocular aberrations are induced and are described below.

### **1.3 Structural changes in the crystalline lens**

As indicated previously, the literature on the physiological and structural (particularly curvature and refractive index) changes in the eye as a result of ageing and accommodation that lead to the optical effects is reviewed in this section.

#### **1.3.1 Structural changes with accommodation**

Structural changes in the crystalline lens at different accommodative states can only be measured *in-vivo*. Recently, different methods such as Scheimpflug photography first used by Brown<sup>82</sup>, MRI, ultrasonography, OCT and PCI have been used.<sup>58, 60, 83-87</sup>

Scheimpflug photographs have shown excellent correlation with undistorted high resolution MRI data for the front surface but not for the posterior lens surface.<sup>87, 88</sup> Results for the maximal accommodation state produce greater agreement with *in-vitro* studies<sup>83, 88</sup> as the lens shape is the same due to the zonulae removal.<sup>60</sup> Overall the changes in the lens with accommodation are in good agreement between studies qualitatively<sup>60, 87, 88</sup> and they can be approximated by a linear function.<sup>83, 84</sup> Dubbelman<sup>83</sup> found anatomical changes per dioptre of accommodation (Table 1.1). An increase in lens thickness that leads to a decrease in anterior chamber depth (ACD) has been found<sup>58, 60, 83, 84, 87</sup> (Figure 1.4).

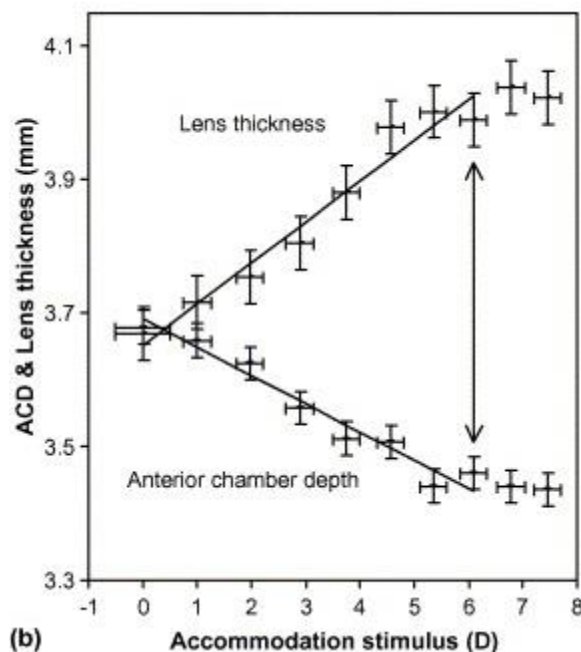


**Figure 1.4:** Change in anterior lens thickness and ACD during accommodation in a 29 year-old female. (Source: Dubbelman and Van der Heijde, 2005<sup>83</sup>)

Dubbelman et al.<sup>83</sup> detected that the decline in ACD is smaller than the rise in lens thickness. This indicates a backwards movement of the lens posterior surface and an anterior movement of the lens anterior surface, which was also found in a

number of other articles.<sup>84-86</sup> The anterior and posterior surfaces radii of curvature have also been measured in various studies, showing a decrease with accommodation.<sup>83, 87</sup> Kasthurirangan et al.<sup>58</sup> using MRI, observed a decrease in curvature and no change in the conic constant with accommodation.

**Table 1.1:** Anatomical changes (mean value and standard deviation) per dioptre of accommodation using Scheimpflug imaging. (Source: Dubbelman and Van der Heijde, 2005<sup>83</sup>)

<i>Parameter</i>		<i>Change with accommodation</i>
<b>Lens radius</b>	<b>Anterior</b>	-0.61 ± 0.15 mm/D
	<b>Posterior</b>	-0.13 ± 0.06 mm/D
<b>Lens surface curvature</b>	<b>Anterior</b>	0.0067 ± 0.0014 mm <sup>-1</sup> /D
	<b>Posterior</b>	0.0037 ± 0.0015 mm <sup>-1</sup> /D
<b>Lens thickness</b>		0.045 ± 0.012 mm/D
<b>k-value</b>		-0.5/D ± 0.3
<b>Anterior segment length</b>		0.0075 ± 0.014 mm/D
<b>Anterior chamber depth</b>		-0.038 mm/D

Both movement and changes in curvature are always greater for the anterior surface than for the posterior, accounting for 64% and 36% of the accommodative power respectively. This makes it harder to find changes in the posterior surface



with Scheimpflug imaging.<sup>83</sup> All these variations are in agreement with both the Helmholtz accommodation theory<sup>6, 7</sup> and the Gullstrand's<sup>10</sup> expansion of it, suggesting an intra-capsular mechanism.

### 1.3.2 Changes in refractive index

Accompanying the mentioned external changes of the lens, there are changes in the lens refractive index (intra-capsular mechanism). To explain the 'lens paradox'<sup>89</sup>, it has been suggested that these changes balance the effect of the increased curvature with age in order to maintain an emmetropic condition.

To assess this, some studies have assumed either a homogeneous index or equivalent refractive index to study its dependence on both accommodation and ageing, or a two-compartment (nucleus and cortex) lens model was used to simulate the accommodative process.<sup>90</sup> Despite these assumptions, it is widely accepted that the refractive index of the lens is neither uniform nor divided sharply into nuclear and cortical regions. Instead it increases from the surface inwards to the centre.<sup>91</sup> This means that there is a gradient of refractive index (GRIN) within the lens.

However, there is little consensus in the scientific community about the way this distribution changes from the nucleus to the capsule, which is due to measurement difficulties. The *in-vivo* GRIN measurements were provided by Kasthurirangan et al.<sup>92</sup> (Figure 1.5). They used MRI images which permit the changes in lens GRIN to be assessed not only with age but also with accommodation. They provided two-

dimensional maps<sup>92</sup> of the refractive index distribution, where they found a greater refractive index in the central region that steeply declines towards the periphery. However, this decrease becomes more gradual with accommodation in young subjects.

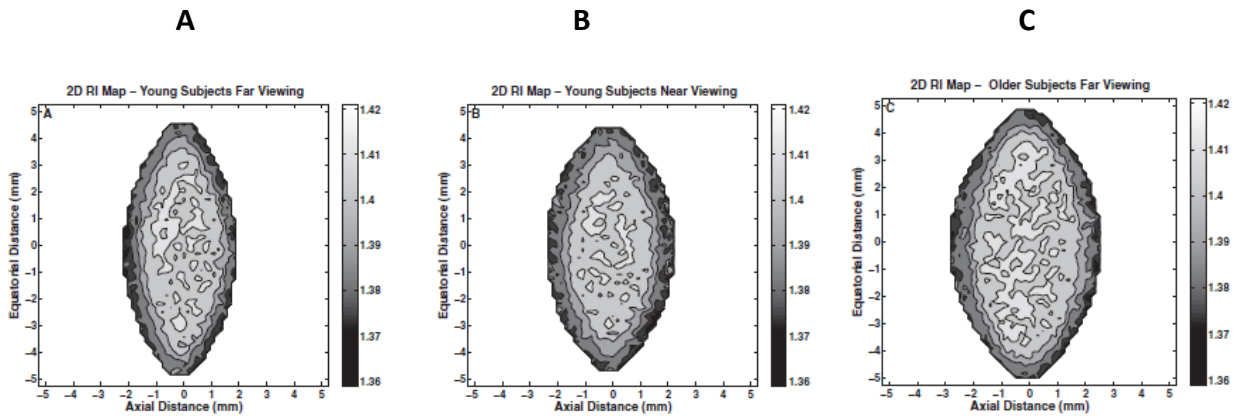


**Figure 1.5:** Contour plots of the refractive index distribution obtained in (A) young, unaccommodated; (B) young, accommodated, and (C) older crystalline lenses (Source: Kasthurirangan et al., 2008<sup>92</sup>).

Even though there were differences of refractive index distribution within the lens, the central and peripheral indices were found not to change either with age or with accommodation.<sup>92</sup> The study of Kasthurirangan et al.<sup>92</sup> is also in good agreement with previous studies both *in-vitro* and *in-vivo*.<sup>91, 93</sup> Despite this fact, much dispersion in published data is observed, probably because of the physical limitations of measurements, but it may also be due to the fact that this dispersion really exists within the population. Hence, further studies should be conducted in order to improve our understanding and also the development of eye models, which have been another way to study the contribution of the GRIN and the diverse changes that occur in the lens with age and accommodation. Eye models are used to predict the crystalline lens optical behaviour depending on different factors.

These studies propose to extract the structural data of the lens from experimental data of isolated lenses and many different types of models have been proposed. As an example, Navarro et al.<sup>94, 95</sup> developed a parametric, simple and concentric adaptive model of the GRIN structure of the lens, using Scheimpflug photography's data from Dubbelman et al.<sup>83</sup> to incorporate changes in surface and GRIN distributions with accommodation. Further development of these realistic optical models will allow us to establish the connection between anatomy and optical performance and more accurately predict the optical properties and their dependence on accommodation and age.

### 1.3.3 Structural changes with age

Anatomical changes in the crystalline lens that occur with advancing age have been widely evaluated both *in-vitro*<sup>96, 97</sup> and *in-vivo*.<sup>36, 58, 60, 83, 85, 86, 88</sup> *In-vivo* measurements can explain how the ocular environment adapts the lens in order to produce different optical properties, whilst *in-vitro* measurements provide information on the lens dimensions and how it grows. Again, despite the differences in methodologies and conditions the results are qualitatively in good concordance between maximally accommodated state *in-vivo* measurements and *in-vitro* zonulae removed measurements.<sup>58, 60, 83, 96, 97</sup> Considering these various factors, it is likely that ageing and accommodation result in similar changes of the shape of the lens.

*In-vitro* studies show a clearly linear increase with age of the anterior radius of curvature, but Glasser and Campbell<sup>96</sup> claim that this increase only occurs up to 65 years of age. Less of a consensus has been found regarding the posterior lens surface. While Glasser and Campbell<sup>96</sup> detected a tendency to flatten, Rosen et al.<sup>97</sup> determined that it remains constant between the ages of 20 and 99. Thus, suggesting an asymmetric growth of the lens, most likely explained by the compression of cells.<sup>97</sup> This independence from age for the posterior lens surface, as well as a significant increase of lens thickness and reduction of the ACD and anterior lens radius, has also been found in studies *in-vivo*.<sup>36, 58, 60, 83, 85, 86, 88</sup> However these changes with age typically show a large inter-individual variation.<sup>83</sup>

#### **1.3.4 Structural changes with accommodation and age**

Rosen et al.<sup>97</sup> in their *in-vitro* study detected that there isn't any change in lens shape with accommodative effort after around 55 and 60 years of age. Richdale et al.<sup>60</sup> and Dubbelman et al.<sup>83</sup> found a significant relationship between lens thickness with accommodation and age respectively, but this change was not significant when the interaction between age and accommodative response was considered. Also, Dubbelman et al.<sup>83</sup> found significant age-dependent changes in the ACD (per dioptre of accommodation) as a function of age, but this was not significant when it came to variations in anterior segment length.

## 1.4 Optical changes

The anatomical and physiological changes described above, have consequences on the optical quality of the eye. Therefore, changes in aberrations during accommodation have also been found with advancing age and accommodation and are reported below.

### 1.4.1 Optical changes with accommodation

It has been suggested that the accommodation-related changes in aberrations can be explained by the lens surface asphericities as well as the gradient refractive index structure.<sup>83, 98</sup> The decrease in lens surface curvature with accommodation makes the spherical aberration (SA) to rise. However, this rise is compensated by the internal refractive index gradients, which results in an overall negative shift of SA in the young accommodated eye.<sup>99</sup> Consequently, the crystalline lens has been identified as the main source of the changes in aberrations with accommodation. Li et al.<sup>100</sup> were the first to assess the corneal, internal and total aberrations in accommodative human eyes and they found no difference in corneal aberrations between accommodated and disaccommodated eyes. Recently, using a combined custom-built OCT and Hartmann-Shack aberrometer for static<sup>101</sup> and dynamic<sup>102</sup> measurements, it has been found that the changes in higher-order aberrations during accommodation are mainly a consequence of the increased convex curvature of the anterior lens surface.<sup>101, 102</sup> This attribution of the anterior surface of the lens to change aberrations was also predicted by the eye model developed

by Lopez-Gil and Fernandez-Sanchez.<sup>103</sup> They<sup>103</sup> determined that the change produced by the front surface in primary and secondary SA accounts for a 19% and 4% change, respectively for a 4 mm pupil diameter.

The tendency for SA towards negative values, which is linearly related to the amplitude of accommodation, has been generalised due to the number of studies that share this finding.<sup>99, 100, 103-106</sup> This general trend is accepted, although, a large dispersion indicating inter-subject variability, has been found.<sup>81, 99, 104, 105</sup> Additionally, there is little agreement between studies with regard to clinical methodology, pupil size, subject demographics or the evaluated accommodation range.

Although fourth-order SA is the Zernike coefficient that shows the largest change with accommodation, in some studies sixth-order SA also presents variations. Li et al.<sup>100</sup> found a decrease in secondary SA whilst Lopez-Gil and Fernandez-Sanchez<sup>103</sup>, using a Hartmann-Shack aberrometer that allowed rapid, accurate and objective aberration assessment, found an increase with accommodation. The latter<sup>103</sup> determined that despite the fact that secondary SA is lower than that of primary SA, it is not negligible. In addition, they found both fourth-order and sixth-order SA to influence the accommodative response by causing a decrease of approximately 1/7 D in accommodation.

Image quality is related to the overall wavefront error, thus root mean square (RMS) error is important; however, differences in results have been found among studies. Ninomiya<sup>106</sup> found that the RMS error is constant for up to 3 dioptres of accommodation. Cheng et al.<sup>104</sup> and He et al.<sup>81</sup> shared their finding but added that

it increases with accommodation greater than 3 dioptres. Also, Radhakrishnan and Charman<sup>99</sup> showed a maintenance of the RMS error with accommodation over a range of 0 to 4 D, but this could be due to the small pupil diameter (2.5 mm) used. This is why Lopez-Gil et al.<sup>105</sup> found an increase in RMS error with a fixed pupil diameter (4mm) but no difference with the natural one, attributing this reduction of RMS error impact in image quality, to accommodative miosis.

Assessing ocular aberrations provides essential information about the fundamentals of the visual system as well as in clinical applications. Such applications include pre and post-operative assessment in refractive surgery, some ocular conditions' diagnosis (e.g. keratoconus, dry eye, corneal dystrophies) and ophthalmic and IOLs design. This is because these techniques are more sensitive and accurate than traditional refraction and keratometry.<sup>107, 108</sup>

### **1.4.2 Optical changes with age**

The optical deterioration that occurs with human ageing is an effect of the systematic increase in higher-order aberrations found in many studies.<sup>99, 109-111</sup> This has been assessed by different authors using diverse methods, and a large inter-subject variability has been found in all of them.<sup>99, 109-111</sup> It is generally accepted that in young eyes, corneal aberrations are of positive value whilst lens aberrations tend to be more negative, thus compensating for one another. However, in older eyes, higher-order RMS error and also SA have been found to increase, hence breaking down the degree of compensation.<sup>99, 110, 111</sup> This decompensation, rather

than the changes in each individual component, is the attributed explanation by Artal et al.<sup>110</sup> to the worsening in the human eye optics with age. Artal et al.<sup>110</sup> measured the modulation transfer function (MTF) for the cornea and internal surfaces and found that they decreased minimally with age when measured separately, yet the total MTF was much lower for the older eyes. Despite this fact, the lens has been determined to be the greatest source of changes in aberrations with age.<sup>109</sup> This is in agreement with the findings of Radhakrishnan and Charman<sup>99</sup>, who attributed the age-related changes in aberrations to a reduction in the compensating effect of the refractive index gradient within the lens.

As previously reported, most studies show a significant increase in higher-order RMS error with age (Figure 1.6) but Artal et al.<sup>110</sup> and Lyall et al.<sup>111</sup> measured this metric at a fixed pupillary diameter suggesting that senile miosis will ameliorate the effect of ocular aberrations, thus having less impact on visual quality. This was confirmed by Radhakrishnan and Charman<sup>99</sup> who, measured them for a natural pupil diameter and found a constant level of higher-order RMS error with increasing age.



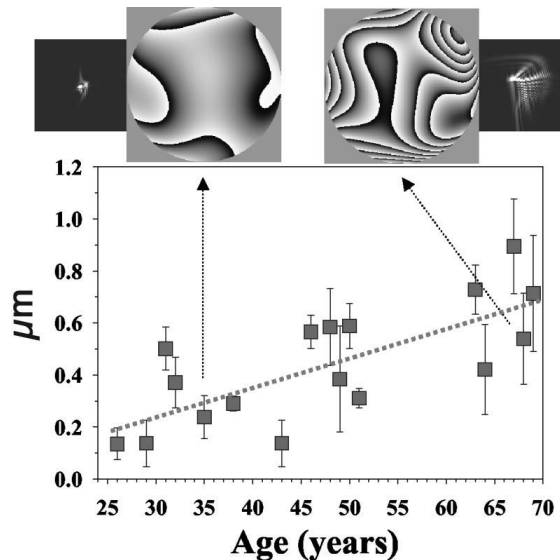


**Figure 1.6:** Higher-order RMS error of the eye expressed in micrometers ( $\mu\text{m}$ ) as a function of age for a 5.9 mm pupil diameter. The wavefront aberration and the associated point spread function (PSF) for one young and one older subject are also shown as an illustrative example. (Source: Artal et al., 2002<sup>110</sup>)

### 1.4.3 Optical changes with accommodation and age

There are two main studies that have investigated the relationship between the whole eye aberrations and accommodation as a function of age, so far<sup>99, 105</sup>. A considerable variability inter-subject in ocular aberrations was found in both studies. Their authors assess these changes using a natural pupil diameter and a fixed diameter, using the same aberrometer. López-Gil et al.<sup>105</sup> pointed out that subject comparison results difficult when using natural pupil data, but this was overcome by Radhakrishnan and Charman<sup>99</sup>, who used the equivalent defocus which is a metric that “specifies the vergence of a spherical wavefront that has the same total wavefront variance across the entire pupil”. Consequently, it has been suggested that not only accommodative miosis but also senile miosis are natural responses to mitigate the effects of optical blur caused by accommodation errors

and other higher-order aberrations.<sup>99, 112</sup> In order to measure changes with a fixed pupil diameter, López-Gil et al.<sup>105</sup> used a 4 mm diameter, but Radhakrishnan and Charman<sup>99</sup> used a 2.5mm one. Using this small diameter makes the system almost diffraction-limited and perhaps explains why Radhakrishnan and Charman<sup>99</sup> found no change in higher-order RMS error with accommodation. Meanwhile, López-Gil et al.<sup>105</sup> found an increase in higher-order RMS error with accommodation and age. This rise with age is more pronounced with higher accommodative demands, demonstrating an agreement between both studies when natural pupil results from Radhakrishnan and Charman<sup>99</sup> are taken into account. However, Radhakrishnan and Charman<sup>99</sup> found no change with age when analysis of variance was performed, and attributed this to the compensatory role of pupillary miosis.

Despite the fact that SA shows greater changes than any other Zernike coefficient term, changes in third-order coma have been also found. They just approached statistical significance<sup>99</sup> or were significant but with very low values.<sup>105</sup> This could be due to the differences in samples.

As previously described, when it comes to SA, there is complete agreement among researchers<sup>81, 99, 104, 105</sup> in that it declines from a positive value whilst viewing distance targets towards a more negative value when accommodating. Nonetheless, both Lopez-Gil et al.<sup>105</sup> and Radhakrishnan and Charman<sup>99</sup> oppose each other regarding the rate of change in SA per dioptre of accommodation. Radhakrishnan and Charman<sup>99</sup> state that SA becomes more constant with age. In contrast, López-Gil et al.<sup>105</sup> found a greater change per dioptre of accommodation with increasing age, attributing this as an assistance mechanism to increase the

amplitude of accommodation. This dissimilarity could be mainly due to the differences in the metrics used to obtain the aberrations. While Lopez-Gil et al.<sup>105</sup> calculated the Zernike coefficients for a 4mm fixed pupil size from the natural pupil data obtained, Radhakrishnan and Charman<sup>99</sup> used equivalent defocus, coma and spherical aberration as the metric to describe the aberrations. Equivalent defocus, coma and spherical aberration are calculated for full natural pupil diameters and allow comparison between subjects. Another source of differences between studies could be the large variability noted between individuals. Hence more studies should be performed in order to clarify this issue and improve our current understanding of this topic.

## **1.5 Dynamic changes**

A review on the short and long term stationary changes in the structure and optics of the eye has been conducted so far. However, it is interesting to take into account the effect of time and therefore gain more understanding of the visual system from a dynamic point of view.

A review of the literature on dynamic changes occurring in accommodation and aberrations and how ageing affects them is tackled below.

### 1.5.1 Dynamics of accommodation

Although usually accommodation is treated as such, it is not a static process. In 1959 based on the existent tremor in skeletal muscles, Campbell et al.<sup>113</sup> realized that during an accommodation response the refractive power undergoes microfluctuations. Thus, small amplitude fluctuations (0.3-0.5 D) are produced for different frequency components whose spectrum is typically classified into low (<0.5 Hz) and high (>0.5 - 2 Hz) frequency.<sup>114</sup>

With regard to the contribution of each of the dominant components in the accommodation control process, no consensus has been found. But usually, low-frequency microfluctuations have been found to be likely to play a role in the accommodation steady-state, maintaining focus and retinal contrast whilst fixating on a fixed target.<sup>116-119</sup> This is because they are in direct relationship with the stimulus conditions. Thus, when the pupil size and target luminance decrease, they increase their magnitude and frequency respectively.<sup>119-121</sup> Collins et al.<sup>122</sup>, found a substantial association between a peak in the low-frequency components of microfluctuations in accommodation and respiration. However, this peak was lower in amplitude than the one found in the high-frequency components when the subjects increased their breathing rate. For this reason, in some studies, such as those from Zhu et al.<sup>123, 124</sup>, two breathing rates are used in order to obtain more reliable regressions between the low-frequency component and instantaneous heart rate. Despite this fact, Winn et al.<sup>119</sup> suggested that the association between respiration and the low-frequency components of accommodative microfluctuations requires further investigation. This is because in order to improve

reliable identification of low-frequency signals, extended periods should be recorded. However, using a Canon Autorefractometer R-1, like Collins et al.<sup>122</sup>, this increase in the recording period could introduce additional artifacts.<sup>119</sup>

On the other hand, high-frequency microfluctuations have been often associated with factors such as lens elasticity, zonular tension, ciliary muscle pulse and thickness, intraocular pressure and arterial pulse.<sup>116, 117, 122</sup> In accordance, it has been suggested that they are unlikely to play an important role in the accommodation process.

Besides, there is a dependence of both high and low-frequency microfluctuations, with the stimulus vergence so that they increase when the accommodative demand rises<sup>116, 118</sup> whereas in some studies a peak is found in the middle of the accommodative range in the high-frequency band.<sup>116</sup> This analysis of the microfluctuations in the frequency domain provides information about the shape of the spectrum of the signal and thus the existence of the two frequency bands can be acknowledged. This kind of analysis assumes that the signal is stationary as it provides an average of spectra of the signal over time. Another method to analyse microfluctuations as a stationary signal is to calculate the RMS, which is equivalent to the standard deviation of the signal and can be expressed with a single value. Various studies have used this approach to assess the microfluctuations and other descriptive components of accommodation (i.e. latency and peak velocity) as a dynamic process.<sup>125-127</sup>

The relationship between ciliary muscle thickness (CMT) and high-frequency microfluctuations has been measured using OCT.<sup>117</sup> So far, only Schultz et al.<sup>117</sup> and Gamba et al.<sup>128</sup> have evaluated the effects of microfluctuations in accommodation

and CMT and lens shape, respectively. Thus, an OCT based device could provide novel wisdom on direct evaluation of the dynamic ciliary muscle and lens structural changes responsible for microfluctuations in accommodation. Gamba et al.<sup>128</sup> used a custom-developed 3D spectral OCT which corrected for optical distortion produced by the previous optical structures, to dynamically image the crystalline lens under steady-state conditions. They<sup>128</sup> found that microfluctuations increase with accommodation and that these microfluctuations are mainly dominated by changes in the radii of curvature, especially in the posterior lens surface. However, this device impedes from simultaneous imaging of the anterior and posterior lens surfaces. Besides, in this study the ciliary muscle was not considered and the accommodative response was obtained from an equation assuming a constant equivalent refractive index, for the 4 subjects of the sample. Like Schultz et al.<sup>117</sup>, Gamba et al.<sup>128</sup> didn't take measurements of the accommodative response and anatomical changes all at once. Hence, more studies are needed in a bigger sample but their extent is limited by the technological constraints. This is because the OCT axial and instantaneous linewidth range is limited and the acquisition times are relatively slow, thus preventing real time imaging of the structures of the eye.

### **1.5.2 Dynamics of aberrations**

Aberrations have traditionally been dynamically (e.g., changes with accommodation) or statically measured, but not at high sampling frequencies which allow their analysis to within one-hundredth of a second (i.e. microfluctuations with accommodation). In 2001, Hofer et al.<sup>129</sup> were the first who attempted to assess the

microfluctuations exhibited not just in defocus but also in other higher-order aberrations.<sup>129</sup> Neither rotational nor translational eye movements have been found to be significant.<sup>129</sup> In spite of this fact, to date the cause of microfluctuations in aberrations is still unknown. Although according to other subsequent articles it has been suggested that the origin could be its association with the cardiopulmonary system (similar to that reported for accommodation), since a significant relationship between high-frequency components, Zernike coefficients and the pulse frequency and instantaneous heart rate has been found.<sup>123</sup> It is likely that there could be a direct association through the pulsatile ocular blood flow in the ciliary muscle or the intraocular pressure. Hence, when the eye is in an accommodated state and the muscle is constricted, the structures of the eye are more sensitive to the ciliary muscle pulse, thus increasing the microfluctuations in aberrations.<sup>124</sup>

There are only a few studies that assess the microfluctuations in aberrations<sup>123,124,129</sup>, each using a Hartman-Shack; however they each analyse their data at different sampling frequencies. Whilst Hofer et al.<sup>129</sup> quantify the temporal power spectra by using a discrete Fourier transform algorithm for one frequency band; Zhu et al.<sup>124</sup> estimated the power for two frequency bands (low and high regions). These bands are more similar to the ones which the spectrum of accommodation microfluctuations are typically classified too.<sup>118</sup> Zhu et al.<sup>124</sup> also used the auto-regressive process suggested by Iskander et al.<sup>130</sup> and found that the bigger the accommodative demand is (i.e. the more accommodation is required), the greater the increase (with statistical significance) in defocus at both the low and

high-frequency regions. This is consistent with other reports investigating microfluctuations in accommodation measured with different instruments other than aberrometers.<sup>114, 116, 118, 125</sup> When it comes to higher-order aberrations, for a greater stimulus, Zhu et al.<sup>124</sup> reported an increase in different Zernike coefficients dependant on the frequency evaluated. Despite these results, further investigations (perhaps in an older cohort of subjects) are needed to explore how ageing affects microfluctuations in aberrations.

### 1.5.3 Dynamics of accommodation with age

The effect of age on accommodative microfluctuations hasn't been widely studied, but there are some articles in which both low and high-frequency microfluctuations decrease with increasing age.<sup>115, 116</sup> Toshida et al.<sup>116</sup> noted that the peak usually found in high-frequencies in the middle of the accommodative range disappeared with age showing almost no changes. This is in contrast with the findings of Anderson et al.<sup>114</sup> They found the relationship between age and RMS deviation, which quantifies the magnitude of the accommodative microfluctuations, as a quadratic function that declines with increasing age in the 20's but then rises by the third decade of life. The same authors<sup>114</sup> found that with increasing age there are also changes in other descriptive components of accommodation dynamics, such as latency and peak velocity. Thus, an increase in the disaccommodation latency as well as a maintenance in its velocity but a reduction in accommodation velocity has



been reported.<sup>114</sup> Nevertheless, this has only been assessed in a relatively young cohort with no patients older than 48 years of age.

## **1.6 Rationale and general aims**

After having done a comprehensive review of the scientific peer-reviewed literature, it is evident that the crystalline lens is a very important element for vision. The lens undergoes long-term changes as a consequence of ageing, and short-term changes through its ability to change the shape during accommodation. As human accommodation has been studied since the 17th century, very different methods have been used to assess it. The most accepted theory of accommodation is the Helmholtzian one.<sup>6</sup> Despite this fact, other structures aside from the crystalline lens have been suggested to play a role in accommodation and in Chapter 2 of this thesis further investigations are carried out to clarify how accommodation affects the cornea.

Accommodation ability is progressively lost throughout life, leading to presbyopia. Different theories of presbyopia evolution have been proposed but no single theory has attained general support from the vision research community although the more relevant ones are described as lenticular and extralenticular theories. Presbyopia is an increasing condition due to the ageing and longevity of nowadays population.<sup>131</sup> Therefore, currently several solutions for presbyopia correction are commercially available. Some of these methods are static but others rely on the ciliary muscle functionality. Accordingly, Chapter 3 of this thesis intends to extend the understanding of the changes in ciliary muscle with age at different

accommodative states including people over 50 years of age. Besides, in order to investigate further if changes in accommodation and ocular aberrations exist and are different between two generations of MFCLs, Chapter 5 of this thesis has been produced.

Assessment of structural changes that occur with accommodation and age has been achieved through many different methods. Overall, the results are in a good qualitative agreement, showing that ageing and accommodation lead to similar changes of the lens shape. Also, it is known that the refractive index of the lens is not uniform but there is a gradient (GRIN) within the lens whose variations are still poorly understood. Hence eye models have been developed to predict optical behaviour of the crystalline lens. These anatomical changes are linked with the optical quality of the eye and can be assessed through aberration measurements. Aberrations are mainly attributable to variations in the lens and vary with age and accommodation, which is usually treated as a static process but is a dynamic one as microfluctuations are produced. Therefore, the study presented in Chapter 4 of this thesis including a large age range of patients is warranted to understand the microfluctuations in the eye further and assess the accommodative and disaccommodative performance in both static and dynamic conditions in a young cohort fitted with different designs of MFCLs.

Consequently, the prime objective of this thesis is to advance our understanding on the human eye accommodative system, the variations which occur in it as a

function of accommodation and ageing and in consequence how the different options of presbyopia correction could interfere in the accommodative system.

### **1.6.1 Specific objectives**

- Clarifying how accommodation affects the cornea (including the peripheral area) and its aberrations.
- Looking into the relationship between the accommodative response and evaluate the changes in the ciliary muscle characteristics in an age divided cohort at different accommodative levels.
- Knowing the extent of microfluctuations for distance and near to understand the changes in microfluctuations with age by extending the age range to 70 years.
- Assessing the accommodative and disaccommodative performance in both static and dynamic conditions in young subjects fitted with MFCLs.
- Investigating if changes are produced in accommodation and ocular aberrations while wearing two generations of simultaneous vision MFCLs.

All in all, this work aims to explore further what are the changes produced during accommodation and ageing that affect vision. This may potentially contribute to improve the design of contact lenses for presbyopia, the cataract surgery customization level and to advance in the development of dynamic corrections that aim to restore accommodation such as accommodating IOLs, regeneration of the

lens, lens refilling or photodisruption. The development and improvement of these therapeutic, external and surgical solutions will possibly allow restoring the visual function in an adult eye.

## 1.7 References

1. Augusteyn RC. On the growth and internal structure of the human lens. *Exp Eye Res* 2010;90:643-654.
2. Koretz JF, Handelman GH. How the human eye focuses. 1988:92-99.
3. Scheiner C. *Oculus, hoc est: Fundamentum opticum*. Londini: Londini : Excudebat J. Flesher, & prostant apud Cornelium Bee; 1652.
4. Daxecker F. Christoph scheiner's eye studies. *Doc Ophthalmol* 1992;81:27-35.
5. Young T. The Bakerian Lecture: on the mechanism of the eye. *Philos Trans R Soc Lond B Biol Sci* 1801;91:23-88.
6. Helmholtz H. Ueber die Accommodation des Auges. *Archiv für Ophthalmologie* 1855;2:1-74.
7. Hartridge H. Helmholtz's theory of accommodation. *Br J Ophthalmol* 1925;9:521-523.
8. Rohen JW. Scanning electron microscopic studies of the zonular apparatus in human and monkey eyes. *Invest Ophthalmol Vis Sci* 1979;18:133-144.
9. Nobel Foundation. Nobel lectures in physiology or medicine 1901-1921. *Amsterdam: Elsevier Publishing Company; 1967:409-433.*
10. Timoney PJ, Breathnach CS. Allvar Gullstrand and the slit lamp 1911. *Ir J Med Sci* 2013;182:301-305.
11. Schachar RA, Bax AJ. Mechanism of accommodation. *Int Ophthalmol Clin* 2001;41:17-32.

12. Tscherning MHE. The development of the science of physiological optics in the nineteenth century. *TROS* 1907;9:1-21.
13. Strenk SA, Strenk LM, Koretz JF. The mechanism of presbyopia. *Prog Retin Eye Res* 2005;24:379-393.
14. Burd HJ, Judge SJ, Flavell MJ. Mechanics of accommodation of the human eye. *Vision Res* 1999;39:1591-1595.
15. Burd HJ. A structural constitutive model for the human lens capsule. *Biomech Model Mechanobiol* 2009;8:217-231.
16. Croft MA, Heatley G, McDonald JP, Katz A, Kaufman PL. Accommodative movements of the lens/capsule and the strand that extends between the posterior vitreous zonule insertion zone & the lens equator, in relation to the vitreous face and aging. *Ophthalmic Physiol Opt* 2016;36:21-32.
17. Croft MA, McDonald JP, Katz A, Lin TL, Lutjen-Drecoll E, Kaufman PL. Extralenticular and lenticular aspects of accommodation and presbyopia in human versus monkey eyes. *Invest Ophthalmol Vis Sci* 2013;54:5035-5048.
18. Croft MA, Nork TM, McDonald JP, Katz A, Lutjen-Drecoll E, Kaufman PL. Accommodative movements of the vitreous membrane, choroid, and sclera in young and presbyopic human and nonhuman primate eyes. *Invest Ophthalmol Vis Sci* 2013;54:5049-5058.
19. Ljublimova D, Eriksson A, Bauer S. Numerical study of the effect of vitreous support on eye accommodation. *Acta Bioeng Biomech* 2005;7:1-14.
20. Fisher RF. Is the vitreous necessary for accommodation in man? *Br J Ophthalmol* 1983;67:206.

21. Beauchamp R, Mitchell B. Ultrasound measures of vitreous chamber depth during ocular accommodation. *Am J Optom Physiol Opt* 1985;62:523-532.
22. Hollins M. Does the central human retina stretch during accommodation? *Nature* 1974;251:729-730.
23. Woodman EC, Read SA, Collins MJ. Axial length and choroidal thickness changes accompanying prolonged accommodation in myopes and emmetropes. *Vision Res* 2012;72:34-41.
24. Woodman-Pieterse EC, Read SA, Collins MJ, Alonso-Caneiro D. Regional Changes in Choroidal Thickness Associated With Accommodation. *Invest Ophthalmol Vis Sci* 2015;56:6414-6422.
25. Ni Y, Liu X, Lin Y, Guo X, Wang X, Liu Y. Evaluation of corneal changes with accommodation in young and presbyopic populations using Pentacam High Resolution Scheimpflug system. *Clinical & experimental ophthalmology* 2013;41:244-250.
26. Yasuda A, Yamaguchi T, Ohkoshi K. Changes in corneal curvature in accommodation. *J Cataract Refract Surg* 2003;29:1297-1301.
27. Read SA, Buehren T, Collins MJ. Influence of accommodation on the anterior and posterior cornea. *J Cataract Refract Surg* 2007;33:1877-1885.
28. Buehren T, Collins MJ, Loughridge J, Carney LG, Iskander DR. Corneal topography and accommodation. *Cornea* 2003;22:311-316.
29. Bayramlar H, Sadigov F, Yildirim A. Effect of accommodation on corneal topography. *Cornea* 2013;32:1251-1254.
30. Donders F, Moore W. On the anomalies of accommodation and refraction of the eye. *London: The Sydenham Society; 1864.*

31. Duane A. Normal values of the accommodation at all ages. *JAMA* 1912;LIX:1010.
32. Turner MJ. Observations on the normal subjective amplitude of accommodation. *Br J Physiol Opt* 1958;15:70.
33. Ramsdale C, Charman WN. A longitudinal study of the changes in the static accommodation response. *Ophthalmic Physiol Opt* 1989;9:255-263.
34. Kalsi M, Heron G, Charman WN. Changes in the static accommodation response with age. *Ophthalmic Physiol Opt* 2001;21:77-84.
35. Atchison DA. Accommodation and presbyopia. *Ophthalmic Physiol Opt* 1995;15:255-272.
36. Koretz JF, Cook CA, Kaufman PL. Aging of the human lens: changes in lens shape at zero-diopter accommodation. *J Opt Soc Am A Opt Image Sci Vis* 2001;18:265-272.
37. Bron AJ, Vrensen G, Koretz J, Maraini G, Harding JJ. The ageing lens. *Ophthalmologica*; 2000:86-104.
38. Hess C. Arbeiten aus dem Gebiete der Accommodationslehre. *Albrecht von Graefes Archiv für Ophthalmologie* 1901;52:143-174.
39. Gullstrand A. Mechanism of accommodation. In: Helmholtz Hv (ed), Helmholtz's treatise on physiological optics / translated from the 3d German ed. edited by James PC Southall Vol 1 Rochester, N.Y.: *Rochester, Optical Society of America*; 1924.
40. Duane A. Are the current theories of accommodation correct? *Am J Ophthalmol* 1925;196-202.
41. Fincham E. The mechanism of accommodation. *Br J Ophthalmol*; 1937:5-80.



42. Charman WN. The eye in focus: accommodation and presbyopia. *Clin Exp Optom* 2008;91:207-225.
43. Gilmartin B. The aetiology of presbyopia: a summary of the role of lenticular and extralenticular structures. *Ophthalmic Physiol Opt* 1995;15:431-437.
44. Schachar RA. The mechanism of accommodation and presbyopia. *Int Ophthalmol Clin* 2006;46:39-61.
45. Fisher RF. The force of contraction of the human ciliary muscle during accommodation. *J Physiol* 1977;270:51-74.
46. Duane A. Studies in Monocular and Binocular Accommodation, with Their Clinical Application. *Trans Am Ophthalmol Soc* 1922;20:132-157.
47. Fincham EF. The proportion of ciliary muscular force required for accommodation. *J Physiol* 1955;128:99-112.
48. Shao Y, Tao A, Jiang H, et al. Age-related changes in the anterior segment biometry during accommodation. *Invest Ophthalmol Vis Sci* 2015;56:3522-3530.
49. Farnsworth PN, Shyne SE. Anterior zonular shifts with age. *Exp Eye Res* 1979;28:291-297.
50. Koretz JF, Handelman GH, Brown NP. Analysis of human crystalline lens curvature as a function of accommodative state and age. *Vision Res* 1984;24:1141-1151.
51. Koretz JF, Handelman GH. Modeling age-related accommodative loss in the human eye. *Mathematical Modelling* 1986;7:1003-1014.
52. Strenk SA, Semmlow JL, Strenk LM, Munoz P, Gronlund-Jacob J, DeMarco JK. Age-related changes in human ciliary muscle and lens: a magnetic resonance imaging study. *Invest Ophthalmol Vis Sci* 1999;40:1162-1169.

53. Strenk SA, Strenk LM, Guo S. Magnetic resonance imaging of the anteroposterior position and thickness of the aging, accommodating, phakic, and pseudophakic ciliary muscle. *J Cataract Refrac Surg* 2010;36:235-241.
54. Strenk SA, Strenk LM, Semmlow JL. High resolution MRI study of circumlental space in the aging eye. *J Refractive Surg* 2000;16:S659-S660.
55. Strenk SA, Strenk LM, Semmlow JL, DeMarco JK. Magnetic resonance imaging study of the effects of age and accommodation on the human lens cross-sectional area. *Invest Ophthalmol Vis Sci* 2004;45:539-45.
56. Strenk SA, Strenk LM, Semmlow JL. MRI study of the effect of age and accommodation on ciliary muscle location. *Invest Ophthalmol Vis Sci* 2004;45:U931-U931.
57. Strenk SA, Strenk LM, Guo S. Magnetic resonance imaging of aging, accommodating, phakic, and pseudophakic ciliary muscle diameters. *J Cataract Refrac Surg* 2006;32:1792-1798.
58. Kasthurirangan S, Markwell EL, Atchison DA, Pope JM. MRI study of the changes in crystalline lens shape with accommodation and aging in humans. *J Vis* 2011;11.
59. Sheppard AL, Davies LN. The effect of ageing on in vivo human ciliary muscle morphology and contractility. *Invest Ophthalmol Vis Sci* 2011;52:1809-1816.
60. Richdale K, Sinnott LT, Bullimore MA, et al. Quantification of age-related and per diopter accommodative changes of the lens and ciliary muscle in the emmetropic human eye. *Invest Ophthalmol Vis Sci* 2013;54:1095-1105.

61. Weale R. Presbyopia toward the end of the 20th century. *Surv Ophthalmol*; 1989;15-30.
62. Weale RA. On potential causes of presbyopia. *Vision Res* 1999;39:1263-1265.
63. Charman WN. Developments in the correction of presbyopia II: surgical approaches. *Ophthalmic Physiol Opt* 2014;34:397-426.
64. Gil-Cazorla R, Shah S, Naroo SA. A review of the surgical options for the correction of presbyopia. *Br J Ophthalmol* 2016;100:62-70.
65. Javitt JC, Steinert RF. Cataract extraction with multifocal intraocular lens implantation: a multinational clinical trial evaluating clinical, functional, and quality-of-life outcomes. *Ophthalmology* 2000;107:2040-2048.
66. Charman WN. Developments in the correction of presbyopia I: spectacle and contact lenses. *Ophthalmic Physiol Opt* 2014;34:8-29.
67. Morgan PB, Efron N, Woods CA. An international survey of contact lens prescribing for presbyopia. *Clin Exp Optom* 2011;94:87-92.
68. Llorente-Guillemot A, Garcia-Lazaro S, Ferrer-Blasco T, Perez-Cambrodi RJ, Cervino A. Visual performance with simultaneous vision multifocal contact lenses. *Clin Exp Optom* 2012;95:54-59.
69. Madrid-Costa D, Tomas E, Ferrer-Blasco T, Garcia-Lazaro S, Montes-Mico R. Visual performance of a multifocal toric soft contact lens. *Optom Vis Sci* 2012;89:1627-1635.
70. Ferrer-Blasco T, Madrid-Costa D. Stereoacuity with simultaneous vision multifocal contact lenses. *Optom Vis Sci* 2010;87:E663-668.

71. Madrid-Costa D, Garcia-Lazaro S, Albarran-Diego C, Ferrer-Blasco T, Montes-Mico R. Visual performance of two simultaneous vision multifocal contact lenses. *Ophthalmic Physiol Opt* 2013;33:51-56.
72. Vasudevan B, Flores M, Gaib S. Objective and subjective visual performance of multifocal contact lenses: pilot study. *Cont Lens Anterior Eye* 2014;37:168-174.
73. Ferrer-Blasco T, Madrid-Costa D. Stereoacuity with balanced presbyopic contact lenses. *Clin Exp Optom* 2011;94:76-81.
74. Madrid-Costa D, Ruiz-Alcocer J, Radhakrishnan H, Ferrer-Blasco T, Montes-Mico R. Changes in accommodative responses with multifocal contact lenses: a pilot study. *Optom Vis Sci* 2011;88:1309-1316.
75. Montes-Mico R, Madrid-Costa D, Radhakrishnan H, Charman WN, Ferrer-Blasco T. Accommodative functions with multifocal contact lenses: a pilot study. *Optom Vis Sci* 2011;88:998-1004.
76. Ruiz-Alcocer J, Madrid-Costa D, Radhakrishnan H, Ferrer-Blasco T, Montes-Mico R. Changes in accommodation and ocular aberration with simultaneous vision multifocal contact lenses. *Eye Contact Lens* 2012;38:288-294.
77. Liang J, Grimm B, Goelz S, Bille JF. Objective measurement of wave aberrations of the human eye with the use of a Hartmann-Shack wave-front sensor. *J Opt Soc Am A Opt Image Sci Vis* 1994;11:1949-1957.
78. Liang J, Williams DR. Aberrations and retinal image quality of the normal human eye. *J Opt Soc Am A Opt Image Sci Vis* 1997;14:2873-2883.
79. López-Gil N, Iglesias I, Artal P. Retinal image quality in the human eye as a function of the accommodation. *Vision Res* 1998;38:2897-2907.

80. Atchison DA, Collins MJ, Wildsoet CF, Christensen J, Waterworth MD. Measurement of monochromatic ocular aberrations of human eyes as a function of accommodation by the Howland aberroscope technique. *Vision Res* 1995;35:313-323.
81. He JC, Burns SA, Marcos S. Monochromatic aberrations in the accommodated human eye. *Vision Res* 2000;40:41-48.
82. Brown N. The change in lens curvature with age. *Exp Eye Res* 1974;19:175-183.
83. Dubbelman M, Van der Heijde GL, Weeber HA. Change in shape of the aging human crystalline lens with accommodation. *Vision Res* 2005;45:117-132.
84. Ostrin L, Kasthurirangan S, Win-Hall D, Glasser A. Simultaneous measurements of refraction and A-scan biometry during accommodation in humans. *Optom Vis Sci* 2006;83:657-665.
85. Tsorbatzoglou A, Nemeth G, Szell N, Biro Z, Berta A. Anterior segment changes with age and during accommodation measured with partial coherence interferometry. *J Cataract Refrac Surg* 2007;33:1597-1601.
86. Koretz JF, Cook CA, Kaufman PL. Aging of the human lens: changes in lens shape upon accommodation and with accommodative loss. *J Opt Soc Am A Opt Image Sci Vis* 2002;19:144-151.
87. Hermans EA, Pouwels PJW, Dubbelman M, Kuijjer JPA, van der Heijde RGL, Heethaar RM. Constant Volume of the Human Lens and Decrease in Surface Area of the Capsular Bag during Accommodation: An MRI and Scheimpflug Study. *Invest Ophthalmol Vis Sci* 2009;50:281-289.

88. Koretz JE, Strenk SA, Strenk LM, Semmlow JL. Scheimpflug and high-resolution magnetic resonance imaging of the anterior segment: a comparative study. *J Opt Soc Am A Opt Image Sci Vis* 2004;21:346-354.
89. Brown NP, Koretz JF, Bron AJ. The development and maintenance of emmetropia. *Eye (Lond)* 1999;13(Pt 1):83-92.
90. Hermans EA, Dubbelman M, Van der Heijde R, Heethaar RM. Equivalent refractive index of the human lens upon accommodative response. *Optom Vis Sci* 2008;85:1179-1184.
91. Jones CE, Atchison DA, Meder R, Pope JM. Refractive index distribution and optical properties of the isolated human lens measured using magnetic resonance imaging (MRI). *Vision Res* 2005;45:2352-2366.
92. Kasthurirangan S, Markwell EL, Atchison DA, Pope JM. In vivo study of changes in refractive index distribution in the human crystalline lens with age and accommodation. *Invest Ophthalmol Vis Sci* 2008;49:2531-2540.
93. Jones CE, Atchison DA, Pope JM. Changes in lens dimensions and refractive index with age and accommodation. *Optom Vis Sci* 2007;84:990-995.
94. Navarro R, Palos F, Gonzalez L. Adaptive model of the gradient index of the human lens. I. Formulation and model of aging ex vivo lenses. *J Opt Soc Am A Opt Image Sci Vis* 2007;24:2175-2185.
95. Navarro R, Palos F, Gonzalez LM. Adaptive model of the gradient index of the human lens. II. Optics of the accommodating aging lens. *J Opt Soc Am A Opt Image Sci Vis* 2007;24:2911-2920.

96. Glasser A, Campbell MC. Biometric, optical and physical changes in the isolated human crystalline lens with age in relation to presbyopia. *Vision Res* 1999;39:1991-2015.
97. Rosen AM, Denham DB, Fernandez V, et al. In vitro dimensions and curvatures of human lenses. *Vision Res* 2006;46:1002-1009.
98. Diaz JA, Fernandez-Dorado J, Sorroche F. Role of the human lens gradient-index profile in the compensation of third-order ocular aberrations. *J Biomed Opt* 2012;17.
99. Radhakrishnan H, Charman WN. Age-related changes in ocular aberrations with accommodation. *J Vis* 2007;7:11.11-21.
100. Li YJ, Choi JA, Kim H, Yu SY, Joo CK. Changes in ocular wavefront aberrations and retinal image quality with objective accommodation. *J Cataract Refrac Surg* 2011;37:835-841.
101. Yuan Y, Shao Y, Tao A, et al. Ocular anterior segment biometry and high-order wavefront aberrations during accommodation. *Invest Ophthalmol Vis Sci* 2013;54:7028-7037.
102. Zhu D, Shao Y, Peng Y, et al. Real-Time Measurement of Dynamic Changes of Anterior Segment Biometry and Wavefront Aberrations During Accommodation. *Eye Contact Lens* 2016;42:322-327.
103. Lopez-Gil N, Fernandez-Sanchez V. The change of spherical aberration during accommodation and its effect on the accommodation response. *J Vis* 2010;10:12.
104. Cheng H, Barnett JK, Vilupuru AS, et al. A population study on changes in wave aberrations with accommodation. *J Vis* 2004;4:272-280.

105. Lopez-Gil N, Fernandez-Sanchez V, Legras R, Montes-Mico R, Lara F, Nguyen-Khoa JL. Accommodation-related changes in monochromatic aberrations of the human eye as a function of age. *Invest Ophthalmol Vis Sci* 2008;49:1736-1743.
106. Ninomiya S, Fujikado T, Kuroda T, et al. Changes of ocular aberration with accommodation. *Am J Ophthalmol* 2002;134:924-926.
107. Macrae SM, Schwiegerling J, Snyder R. Customized corneal ablation and super vision. *J Refract Surg* 2000;16:S230-235.
108. Bruce AS, Catania LJ. Clinical applications of wavefront refraction. *Optom Vis Sci* 2014;91:1278-1286.
109. Amano S, Amano Y, Yamagami S, et al. Age-related changes in corneal and ocular higher-order wavefront aberrations. *Am J Ophthalmol* 2004;137:988-992.
110. Artal P, Berrio E, Guirao A, Piers P. Contribution of the cornea and internal surfaces to the change of ocular aberrations with age. *J Opt Soc Am A Opt Image Sci Vis* 2002;19:137-143.
111. Lyall DA, Srinivasan S, Gray LS. Changes in ocular monochromatic higher-order aberrations in the aging eye. *Optom Vis Sci* 2013;90:996-1003.
112. Lopez-Gil N, Martin J, Liu T, Bradley A, Diaz-Munoz D, Thibos LN. Retinal image quality during accommodation. *Ophthalmic Physiol Opt* 2013;33:497-507.
113. Campbell FW, Robson JG, Westheimer G. Fluctuations of accommodation under steady viewing conditions. *J Physiol* 1959;145:579-594.
114. Anderson HA, Glasser A, Manny RE, Stuebing KK. Age-Related Changes in Accommodative Dynamics from Preschool to Adulthood. *Invest Ophthalmol Vis Sci* 2010;51:614-622.



115. Heron G, Schor C. The fluctuations of accommodation and ageing. *Ophthalmic Physiol Opt* 1995;15:445-449.
116. Toshida K, Okuyama F, Tokoro T. Influences of the accommodative stimulus and aging on the accommodative microfluctuations. *Optom Vis Sci* 1998;75:221-226.
117. Schultz KE, Sinnott LT, Mutti DO, Bailey MD. Accommodative fluctuations, lens tension, and ciliary body thickness in children. *Optom Vis Sci* 2009;86:677-684.
118. Charman WN, Heron G. Fluctuations in accommodation: a review. *Ophthalmic Physiol Opt* 1988;8:153-164.
119. Winn B. Accommodative microfluctuations: a mechanism for steady-state control of accommodation. In: Frantzen O, Richter H, Stark L (eds), *Accommodation and Vergence Mechanisms in the Visual System*. Boston, Mass: Boston, Mass : Birkhäuser Verlag; 2000:129-140.
120. Gray LS, Winn B, Gilmartin B. Accommodative microfluctuations and pupil diameter. *Vision Res* 1993;33:2083-2090.
121. Gray LS, Winn B, Gilmartin B. Effect of target luminance on microfluctuations of accommodation. *Ophthalmic Physiol Opt* 1993;13:258-265.
122. Collins M, Davis B, Wood J. Microfluctuations of steady-state accommodation and the cardiopulmonary system. *Vision Res* 1995;35:2491-2502.
123. Zhu M, Collins MJ, Robert Iskander D. Microfluctuations of wavefront aberrations of the eye. *Ophthalmic Physiol Opt* 2004;24:562-571.
124. Zhu M, Collins MJ, Iskander DR. The contribution of accommodation and the ocular surface to the microfluctuations of wavefront aberrations of the eye. *Ophthalmic Physiol Opt* 2006;26:439-446.

125. Kasthurirangan S, Glasser A. Age related changes in accommodative dynamics in humans. *Vision Res* 2006;46:1507-1519.
126. Anderson HA, Glasser A, Manny RE, Stuebing KK. Age-related changes in accommodative dynamics from preschool to adulthood. *Invest Ophthalmol Vis Sci* 2010;51:614-622.
127. Candy TR, Bharadwaj SR. The stability of steady state accommodation in human infants. *J Vis* 2007;7:4.1-16.
128. Gamba E, Ortiz S, Perez-Merino P, Gora M, Wojtkowski M, Marcos S. Static and dynamic crystalline lens accommodation evaluated using quantitative 3-D OCT. *Biomed Opt Express* 2013;4:1595-1609.
129. Hofer H, Artal P, Singer B, Aragón JL, Williams DR. Dynamics of the eye's wave aberration. *J Opt Soc Am A Opt Image Sci Vis* 2001;18:497-506.
130. Iskander DR, Collins MJ, Morelande MR, Zhu M. Analyzing the dynamic wavefront aberrations in the human eye. *IEEE Trans Biomed Eng* 2004;51:1969-1980.
131. United Nations. Department of Economic and Social Affairs, Population Division (2015). World Population Ageing 2015. (ST/ESA/SERA/390).

## 2 CORNEAL CHANGES WITH ACCOMMODATION

### USING DUAL SCHEIMPFLUG PHOTOGRAPHY

#### CONTRIBUTIONS

The study was designed by me and my supervisors during my placement at the University of Valencia (Spain), Robert Montes-Mico and Teresa Ferrer-Blasco. The data collection was done by Antonio del Aguila-Carrasco and Alberto Dominguez-Vicent. I performed the data analysis and wrote the manuscript and the final version was reviewed by the co-authors.

#### PUBLISHING OF THE PAPER

Sisó-Fuertes I, Domínguez-Vicent A, del Águila-Carrasco A, Ferrer-Blasco T, Montés-Micó R. Corneal changes with accommodation using dual Scheimpflug photography. *J Cataract Refract Surg.* 2015 May;41(5):981-9.

#### PRESENTATION AT CONFERENCE

A talk was delivered about the contents of this research under the title of: “Age related changes in the human eye with accommodation” at the International conference of Optometry and Contactology, OC’15 held in Valencia (Spain) in March 2015.

## 2.1 ABSTRACT

**PURPOSE:** To assess whether corneal parameters and aberrations are affected by accommodation.

**METHODS:** The Galilei G4 dual Scheimpflug device was used to obtain data on the anterior and posterior axial curvatures, total corneal power (TCP), and corneal pachymetry from 3 corneal zones (central: 0.0 up to 4.0 mm; paracentral or mid: 4.0 up to 7.0 mm; peripheral: 7.0 up to 10.0 mm) in young emmetropic eyes in the unaccommodated and 4 accommodated states (from -1.0 to -4.0 diopters [D] in 1.0 D steps). The 2nd-, 3rd-, and 4th-order aberrations as well as the root mean square (RMS) were also determined for the entire cornea at the same accommodative demands.

**RESULTS:** The study evaluated 7 subjects (12 eyes). No significant changes in any measured parameter were found during accommodation for any corneal zone ( $P > .05$ ). Statistically significant differences were found in the various corneal zones when it was assumed they were constant with accommodation ( $P < .01$ ). A stable lineal trend with accommodation was also found for corneal aberrations, although individual variations existed because of the high standard deviation values.

**CONCLUSION:** Different parameters in various zones of the cornea as well as corneal aberrations were stable during accommodation.

## **2.2 INTRODUCTION**

In 1795, Home<sup>1</sup> attributed accommodative capacity to 3 changes in the eye as follows: “an increase of curvature in the cornea, an elongation of the axis of vision, and a motion of the crystalline lens.” This was considered but finally rejected by Young,<sup>2</sup> who stated that the mechanism of accommodation mostly accounts for changes in the crystalline lens. Subsequently, and according to the widely accepted Helmholtz<sup>3</sup> theory of accommodation, it is known that the rise in optical power during accommodation is a consequence of a contraction of the annular ciliary muscle, which increases the thickness and curvature of the crystalline lens. This muscle pulls the ciliary body forward and reduces tension in the zonular fibers attached on either side of the lens equator.<sup>3</sup> However, even though today it is known that the lens is the ocular structure that undergoes the principal anatomic changes during accommodation, the cornea is known to be very malleable entity, and the corneal changes that occur during accommodating remain uncertain.

Farmaid<sup>4</sup> and Löpping and Weale<sup>5</sup> were first to study whether corneal changes occur during accommodation using an ophthalmometer and photokeratometer, respectively. Since then, and as a result of technological evolution, there have been controversy and a diversity of measurement methods reported in the published literature. The possible corneal changes occurring during accommodation have been mostly assessed using corneal topography, including keratometers,<sup>6</sup> videokeratoscopes,<sup>7,8</sup> and Placido disk-based topographers.<sup>9,10</sup> Recently, new instruments based on Scheimpflug photography have been used to obtain images not only of corneal topography but also of other parameters and structures in the

anterior eye segment. The Pentacam HR (Oculus) and Galilei (Ziemer) are 2 devices that use Scheimpflug technology. The former has been used by Read et al.<sup>11</sup> and Ni et al.<sup>12</sup> to study the influence of accommodation in the cornea. The Pentacam HR system uses a rotating Scheimpflug camera (180 degrees), while Galilei system uses a dual rotating Scheimpflug camera integrated with a Placido disk. The Galilei G4 is the latest version of this system, which enables fast acquisition of thousands of data points per scan. This allows one to calculate a 3-dimensional model of the anterior segment. To our knowledge, this system has never been used to assess corneal changes during accommodation.

The idea that the cornea plays a role in accommodation comes from the assumption that the ciliary muscle affects the cornea. It has been suggested that this effect occurs mainly in the corneal periphery because of the anatomic proximity of the ciliary muscle to the limbus.<sup>7,10,12</sup> Therefore, assessments of the corneal periphery ( $\geq 7.0$  mm) have shown steepening of the corneal topography in the maximum and minimum keratometry (K) values,<sup>7,10</sup> an increase in refraction,<sup>10</sup> a rise in corneal volume,<sup>12</sup> and a change in corneal aberrations with accommodation.<sup>8,12</sup> Other studies<sup>11,13</sup> suggest that the origin of corneal changes with accommodation is the significant cyclotorsion produced in the corneal topography when changing focus. When this rotation is corrected, the corneal changes decrease considerably and are not statistically significant.<sup>11,13</sup> On the other hand, using corneal topographic images and analyzing the mean K and astigmatic readings, Bayramlar et al.<sup>9</sup> found neither corneal changes nor corneal cyclotorsion during accommodation. This is in agreement with previous assumptions of Schachar

et al.,<sup>14</sup> who used the cornea and sclera as invariant positional references to align anterior segment ultrasound biomicroscopy images in different accommodated states. These findings were in agreement with findings by Drexler et al.,<sup>15</sup> who addressed corneal changes during accommodation using central pachymetry only.

Thus, this study sought to clarify how accommodation affects the cornea and its aberrations, assessing it in a more peripheral corneal area (7.0 to 10.0 mm) than in previous studies using dual rotating Scheimpflug–Placido disk technology.

## **2.3 METHODS**

### **2.3.1 Subjects**

This retrospective study comprised 7 healthy emmetropic volunteers from the University of Valencia staff who were not using topical or systemic medication that could affect accommodation. In addition, none of them had corneal refractive surgery or any other surgery that could distort the measurements in both eyes. All participants were informed about the details of this study and provided written informed consent in accordance with the tenets of the Declaration of Helsinki.

### **2.3.2 Measurement System**

The Galilei G4 was used for the measurements in all cases. This noninvasive noncontact optical diagnostic system is based on processed optical images from an integrated rotating dual-Scheimpflug and a 20-ring Placido disk capable of measuring up to 100,000 points. It incorporates a patented iris-based eye-motion compensation feature that monitors corneal changes. The system has a red light-emitting diode that serves as a fixation target and can be moved in 0.25 diopter (D) steps from  $-20.0$  to  $+20.0$  D.

### **2.3.3 Measurement Procedure**

Data were obtained from several reports from the dual rotating Scheimpflug–Placido disk system to obtain a comprehensive overview of the cornea. Different corneal zone data with various diameters, which in the system are called central (0.0 up to 4.0 mm), paracentral or mid (4.0 up to 7.0 mm), and peripheral (7.0 up to 10.0 mm) were collected for the anterior and posterior axial curvatures, total corneal power (TCP), and corneal pachymetry. The latter is the corneal thickness calculated across the 3 zones. The TCP is the power of the cornea in diopters; it is calculated by ray tracing using Snell's law and pachymetry data with the reference plane in the posterior corneal surface. The dual rotating Scheimpflug–Placido disk system also displays wavefront maps of the total cornea (front and back surfaces) in microns for a region of interest 6.0 mm in diameter and provides a pyramid of Zernike polynomials from which the factors of the 2nd-order, 3rd-order, and 4th-



order polynomials are taken. The internal software reconstructs the corneal topography from every point height data and provides analysis of corneal wavefront aberrations without limitation to the pupillary area. Therefore, in this study subject's pupil size was not measured. All measurements were taken during the same session. To facilitate natural pupil dilation, measurements were taken in a dark room. Before each measurement, central Placido rings were focused, after which the instrument was aligned. Next, the subject was asked to blink and look at the fixation target, ensuring he or she could clearly see the accommodation stimulus for all conditions. The subjects were asked to stare at it for 2 seconds to obtain an appropriate accommodation response<sup>16</sup> and a homogeneous tear film along the cornea. This allowed the person taking the measurements to obtain good-quality images and to avoid changes in corneal aberrations with time after blink.<sup>17</sup> After, the subject was asked not to blink during the measurement. Every measurement was taken monocularly. The examined eye was fixated on the optical target and the contralateral one covered with a patch to restrict the examined eye from adduction in convergence. The possible corneal changes were measured at different accommodation states, from unaccommodated up to 4.0 D. To make sure the subjects were not accommodating, the different parameters were measured at +1.0 D. Then, the stimulus was progressively changed up to -4.0 D in 1.0 D steps. To ensure that all the subjects were accommodating, the aqueous humor depth and central corneal thickness (CCT) data were recorded in all cases. Both parameters are related to the anterior chamber depth (ACD) through this expression:  $ACD = \text{aqueous humor depth} + CCT$ .

### **2.3.4 Statistical Analysis**

Because of the small sample in this study and the likely effect of random errors, all findings were first analyzed in graph form and then confirmed statistically. Statistical analysis was performed using SPSS for Windows software (version 20, SPSS, Inc.). Linearity of corneal parameters was tested using graphs, and 2-way repeated measures analysis of variance (ANOVA) was performed to determine whether corneal parameters changed under different accommodative states and corneal zones and to determine whether there was an interaction between these 2 factors on the various dependent variables.

Regarding corneal aberrations, 2nd-, 3rd-, and 4th-order Zernike polynomials and root mean square (RMS) for every participant were assessed using graphs.

To statistically test whether significant changes in corneal aberrations existed with accommodation, the repeated-measures ANOVA was used. All these tests were calculated for a significance level of 0.05.

## **2.4 RESULTS**

This study comprised 12 eyes of 7 subjects. Measurements from the right eye of one participant and left eye from another participant were discarded from the data analysis due to errors during the acquisition. The mean age was 30 years  $\pm$  5.83 (SD) (range 23 to 37 years).

There were no significant changes in anterior or posterior corneal keratometry, TCP, or pachymetry during accommodation for the mean of the sample (Figure 2.1). The best-fit linear trend line shows minimal slope, which means that the variation of corneal parameters with different accommodative demands was almost negligible because it was smaller than the possible measurement error. This observation was true for all 3 zones (central, mid, and peripheral) and is indicated by the linear trend found for all the parameters and different levels of accommodation (Figure 2.1). Thus, accommodation and anterior and posterior corneal keratometry, TCP, and pachymetry were independent variables.

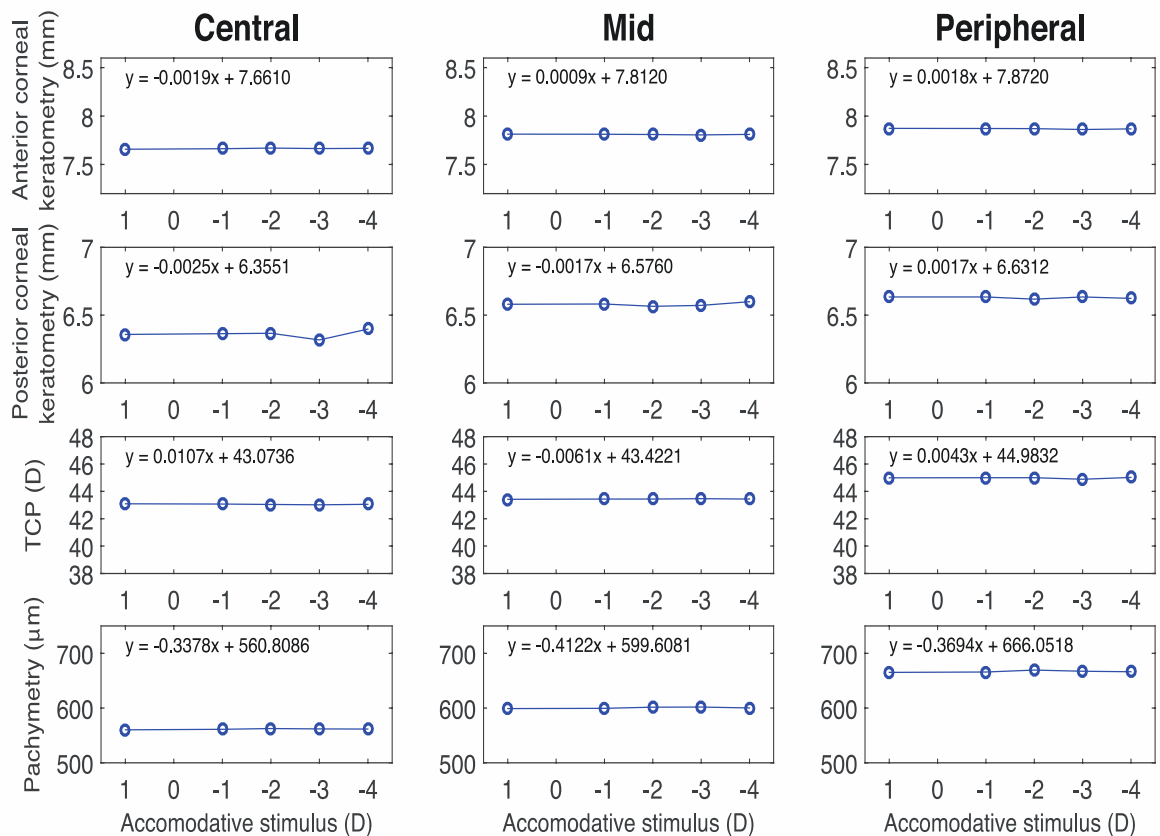


**Figure 2.1:** The mean anterior and posterior corneal curvature keratometry, mean total corneal power, and mean pachymetry at different accommodative demands for the 3 corneal zones (central, mid, and peripheral).

Table 2.1 shows the mean anterior and posterior corneal surface keratometry, TCP, and pachymetry for different accommodative demands. There were no statistically significant differences in any of measured parameters during accommodating with different stimuli ( $P > .05$ ).

**Table 2.1:** Mean anterior and posterior corneal surface keratometry, TCP, and pachymetry for the different accommodative demands. Two-way repeated ANOVA results statistical significance (*P Value*) and substantive significance (*Partial Eta Squared*).

<b>Parameter</b>	<b>Accommodative Demand</b>					<b>F Test</b>	<b>P Value</b>	<b>Partial Eta Squared</b>
	<b>+1.0 D</b>	<b>-1.0 D</b>	<b>-2.0 D</b>	<b>-3.0 D</b>	<b>-4.0 D</b>			
<b>Mean Kant (mm)</b>	7.781 ± 0.348	7.782 ± 0.348	7.783 ± 0.354	7.777 ± 0.346	7.782 ± 0.358	0.558	.694	0.048
<b>Mean Kpost (mm)</b>	6.523 ± 0.189	6.526 ± 0.190	6.516 ± 0.175	6.507 ± 0.200	6.539 ± 0.195	0.708	.591	0.060
<b>Mean TCP (D)</b>	43.828 ± 2.299	43.833 ± 2.303	43.825 ± 2.368	43.789 ± 2.329	43.831 ± 2.352	0.386	.817	0.034
<b>Mean pachymetry (μm)</b>	608 ± 62	609 ± 62	611 ± 67	610 ± 65	609 ± 63	0.871	.489	0.073

Means ± SD

Kant = anterior corneal surface keratometry; Kpost = posterior corneal surface keratometry; TCP = total corneal power

Based on the above, it can be assumed that the different corneal parameters were constant with accommodation. Figure 2.2 shows the significant differences between the corneal zones for the 4 corneal parameters evaluated. These findings were confirmed on statistical analysis. When accommodation was ignored, there were statistically significant differences between corneal zones for anterior ( $F[2.22] = 104.232$ ;  $P = .000$ ) and posterior ( $F[2.22] = 76.604$ ;  $P = .000$ ) corneal surface keratometry, TCP ( $F[2.22] = 82.299$ ;  $P = .000$ ); and pachymetry ( $F[2.22] = 402.265$ ,  $P = .000$ ). In addition, the Bonferroni post hoc test showed that differences were statistically significant between each zone for all parameters ( $P < .05$ ).

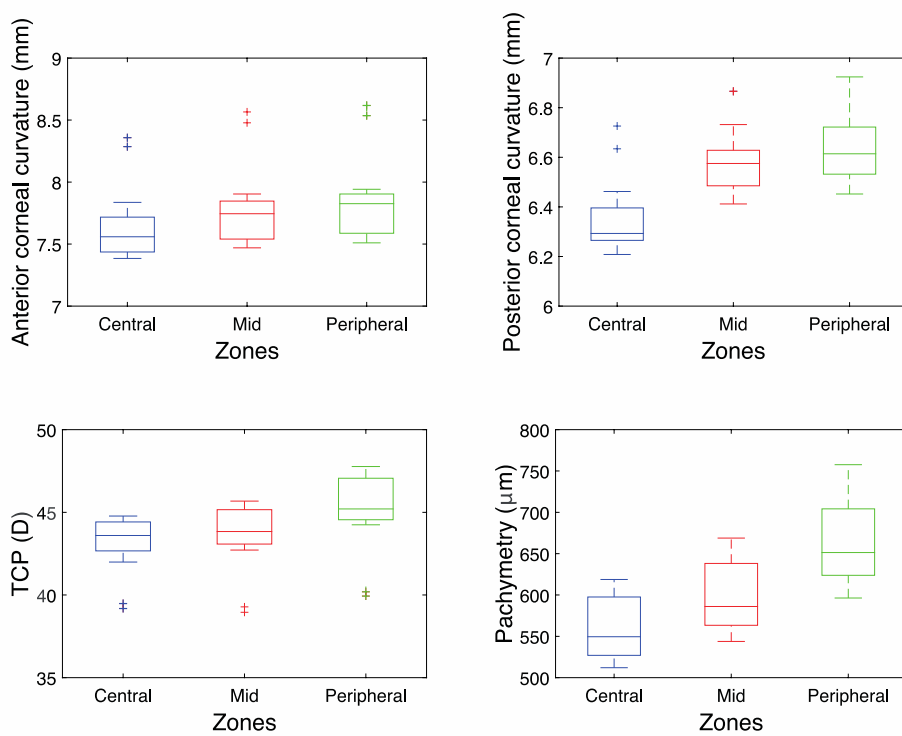


**Figure 2.2:** Anterior and posterior corneal keratometry, TCP, and pachymetry for the 3 corneal zones (central, mid, and peripheral) with the assumption that they are constant with accommodation. Boxplots with medians (lines), 25% to 75% quartiles (boxes), ranges (whiskers), and outliers (+).

Two-way repeated measures ANOVA of the effect of accommodation and the 3 corneal zones on anterior and posterior corneal surface keratometry, TCP, and pachymetry showed no statistically significant interaction between accommodation and corneal zones for any parameter as follows: anterior keratometry,  $F(8.88)=1.285$  and  $P=0.262$ ; posterior keratometry,  $F(8.88)=1.882$  and  $P=0.073$ ; TCP,  $F(8.88)=0.569$  and  $P=0.801$ ; pachymetry,  $F(8.88)=0.272$  and  $P=.974$ . Figure 2.3 shows this lack of interaction.

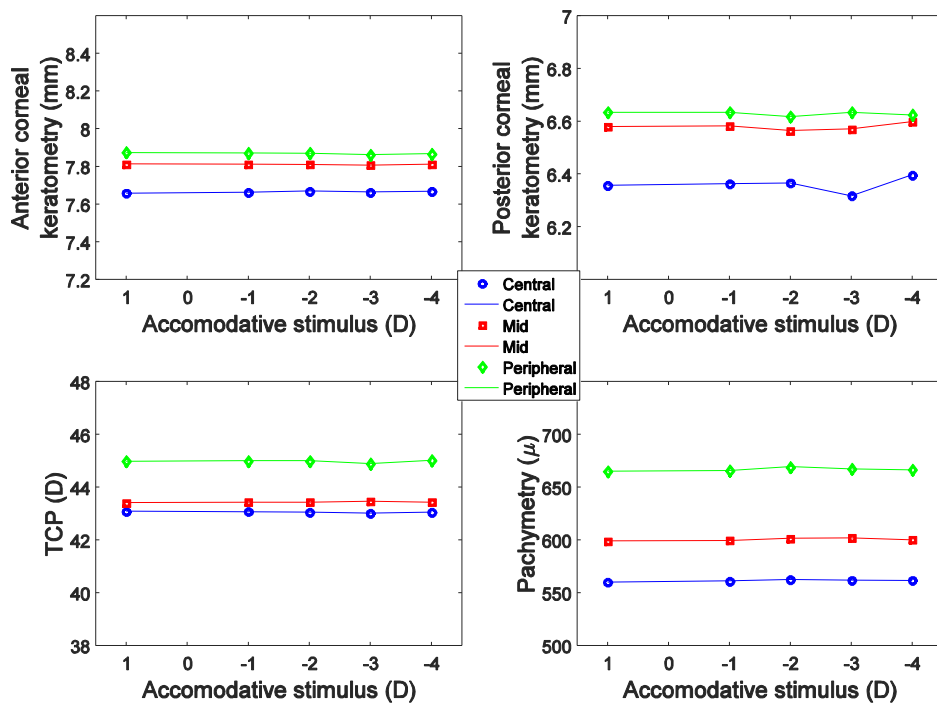


**Figure 2.3:** The mean anterior and posterior corneal keratometry, TCP, and pachymetry for the 3 corneal zones (central, mid, and peripheral) with accommodation.

Repeated-measures ANOVA of the ACD showed a statistically significant difference between different accommodated states ( $F[4.44] = 24.603$ ;  $P = .000$ ), while CCT differences were not statistically significant ( $F[4.44] = 1.384$ ;  $P = .255$ ).

Figure 2.4 shows mean defocus  $Z(2,0)$  and spherical aberration  $Z(4,0)$  of the sample. These 2 coefficients were more stable between individuals at different accommodative demands. On the graph, both show a linear plain trend line, indicating both Zernike coefficients were independent of accommodation. This behaviour was the same for all aberrations in this study. Repeated-measures ANOVA showed no statistically significant differences in any Zernike polynomial between the accommodative states ( $P > .05$ ). Despite this, high standard deviation (SD) values showed great variability between subjects. Table 2.2 shows the mean coefficient for each Zernike and for the different accommodative demands.

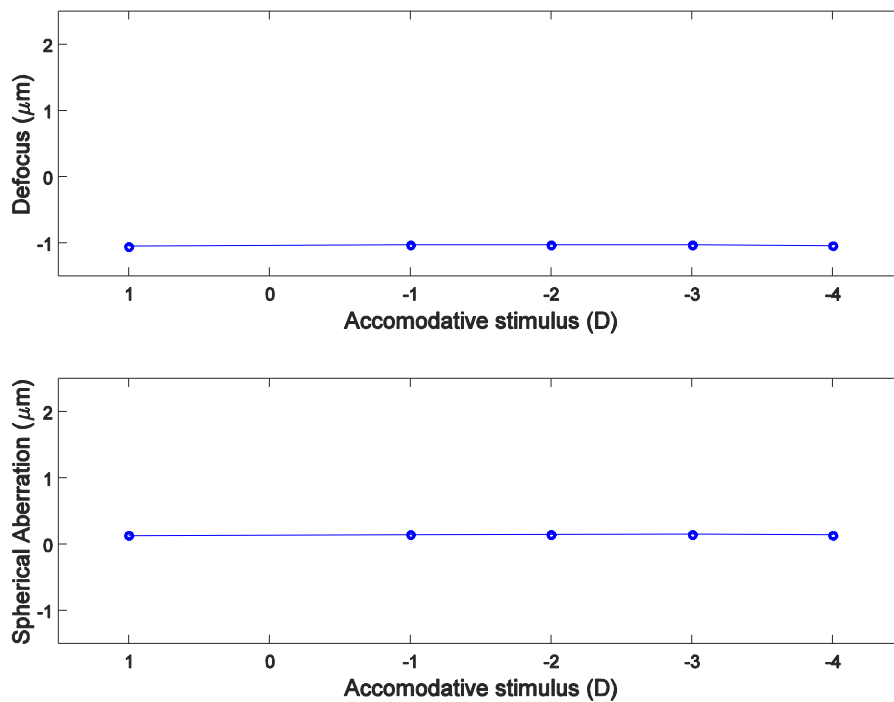


**Figure 2.4** Mean defocus  $Z(2,0)$  and spherical aberration  $Z(4,0)$  at different accommodative demand



**Table 2.2:** Mean of Zernike polynomials for the different accommodative states. Repeated ANOVA results and significance.

Value ( $\mu\text{m}$ )	Accommodative Demand					F Test	P Value
	+1.0 D	-1.0 D	-2.0 D	-3.0 D	-4.0 D		
<b>Mean Z(2,-2)</b>	0.092 ± 0.268	0.077 ± 0.259	0.058 ± 0.290	-0.006 ± 0.251	0.021 ± 0.290	0.912	.465
<b>Mean Z(2,0)</b>	-1.050 ± 0.171	-1.028 ± 0.177	-1.028 ± 0.188	-1.028 ± 0.184	-1.042 ± 0.179	0.869	.490
<b>Mean Z(2,2)</b>	-0.672 ± 0.338	-0.666 ± 0.348	-0.619 ± 0.331	-0.649 ± 0.309	-0.637 ± 0.366	0.252	.907
<b>Mean Z(3,-3)</b>	-0.055 ± 0.132	-0.171 ± 0.321	-0.048 ± 0.174	-0.057 ± 0.113	-0.043 ± 0.175	1.973	.114
<b>Mean Z(3,-1)</b>	-0.052 ± 0.307	0.031 ± 0.315	-0.064 ± 0.236	-0.018 ± 0.227	-0.035 ± 0.270	1.633	.181
<b>Mean Z(3,1)</b>	-0.013 ± 0.315	-0.059 ± 0.338	0.037 ± 0.363	-0.074 ± 0.346	-0.028 ± 0.301	1.347	.266
<b>Mean Z(3,3)</b>	-0.065 ± 0.354	0.067 ± 0.223	-0.035 ± 0.144	0.058 ± 0.162	0.032 ± 0.097	1.050	.391
<b>Mean Z(4,-4)</b>	0.000 ± 0.087	0.012 ± 0.046	0.003 ± 0.029	0.007 ± 0.021	0.006 ± 0.018	0.096	.983
<b>Mean Z(4,-2)</b>	-0.014 ± 0.084	-0.002 ± 0.052	0.005 ± 0.070	0.015 ± 0.089	0.001 ± 0.090	0.384	.844
<b>Mean Z(4,0)</b>	0.127 ± 0.085	0.142 ± 0.087	0.144 ± 0.078	0.148 ± 0.076	0.138 ± 0.076	2.179	.085
<b>Mean Z(4,2)</b>	-0.013 ± 0.115	0.016 ± 0.123	-0.025 ± 0.075	0.015 ± 0.066	-0.025 ± 0.090	0.728	.577
<b>Mean Z(4,4)</b>	-0.125 ± 0.356	-0.025 ± 0.075	0.005 ± 0.085	-0.017 ± 0.069	0.018 ± 0.072	1.621	.184
<b>Mean RMS</b>	1.455 ± 0.312	1.435 ± 0.325	1.368 ± 0.253	1.367 ± 0.247	1.385 ± 0.217	0.926	.457

Means ± SD  
RMS = root mean square

## **2.5 DISCUSSION**

To our knowledge, the only studies in the literature that assessed corneal changes at different accommodation ranges were by Buehren et al.<sup>13</sup> and Yasuda et al.<sup>10</sup> All other studies<sup>8-12</sup> assessed the changes for the unaccommodated state and for 5.0 D of accommodation. Hence, our study provides new information by assessing the changes at different accommodative states from unaccommodated up to 4.0 D, which is the most common practical near working distance.

The differences we found between corneal zones were not a surprising finding because of the generally accepted knowledge that the anterior and posterior corneal shapes can be described as aspheric surfaces whose asphericity increases toward the periphery. Both the anterior and posterior corneal surface are prolate ellipses whose conic constants are different, with the posterior being more negative than the anterior.<sup>18,19</sup> This means that the cornea is thicker in the periphery. This agrees with the differences we found in each parameter between corneal zones.

Moreover, effective accommodation has been proven objectively with ACD measurement despite having included potential pre-presbyopes in our sample (age range 23 to 37 years) Our results agree with those in many studies<sup>20-23</sup> that found an increase in lens thickness that led to a decrease in the ACD with accommodation. It also objectively proves that all the subjects were correctly accommodating during the data collection and that the central cornea did not undergo changes. Therefore, the global description provided by the axial curvature data as well as the TCP and pachymetry data show a constant linear trend with accommodation, indicating that no changes were produced in the cornea during accommodation.

Because some studies attribute the origin of corneal changes with accommodation to significant cyclotorsion produced in the corneal topography when changing focus,<sup>11,13</sup> we avoided any eye movement during the acquisition process to obtain motion-corrected data. In addition, with the Galilei G4 system, eye motion during a measurement can affect the “apparent image” or elevation measured from the posterior surface (which also affects pachymetry). However, this is overcome by combining the 2 camera views using the patented dual-Scheimpflug feature. The systematic error is automatically corrected, and it removes decentration error caused by eye motion or misalignment. This prevents the acquired images from possible cyclotorsion, and this movement is also avoided because of the measurement procedure. While the measurements were being taken, convergence eye movements and misalignments between the eye and the measurement system were prevented by covering the contralateral eye.<sup>24</sup> Hence, our results were not affected by significant torsional movement and thus agree with the findings of Read et al.<sup>11</sup> and Buehren et al.,<sup>13</sup> both of whom found no consistent significant changes when data were recentered and cyclotorsion was corrected.

Furthermore, it has been suggested that because the ciliary muscle is close to the cornea, it is the peripheral cornea that might change more when accommodating.<sup>6,11</sup> This is the reason we took data from 3 corneal zones. We found the expected differences between zones because of the aspheric configuration of the cornea; however, we did not find a significant change in any of them during accommodation. This is in agreement results of Yasuda et al.<sup>10</sup> and Read et al.<sup>11</sup> who, despite having found contradictory results regarding corneal changes with

accommodation, stated that these changes with accommodation were equal at all measured points. Nevertheless 1 subject in the study by Read et al.<sup>11</sup> had changes in the posterior peripheral corneal surface. Conversely, Ni et al.<sup>12</sup> reported differences in corneal zones in terms of the magnitude of change and corneal volume with accommodation; however, they did not statistically analyze the differences.

On the other hand, the invariability in total corneal aberrations with accommodation in our study is in agreement with that in the study by Li et al.,<sup>25</sup> who assessed the corneal, internal, and total aberrations in accommodated human eyes. Since corneal aberrations are directly calculated from height data of the corneal surface and the rest of our results point to a stability of the cornea during accommodation, no change in defocus term was expected. Similarly, Li et al.<sup>25</sup> found no difference in corneal aberrations between accommodated eyes and unaccommodated eyes. Thus, the crystalline lens is thought to be the main source of changes in aberrations with accommodation, even though the cornea is the major refracting surface of the eye. This confirms the suggestions of Dubbelman et al.<sup>23</sup> and Díaz et al.,<sup>26</sup> who stated that the accommodation-related changes in aberrations are explained by lens surface asphericities as well as the gradient refractive index structure. He et al.<sup>8</sup> and Ni et al.<sup>12</sup> also studied corneal aberrations during accommodation. Our results agree with those of He et al.,<sup>8</sup> who found no general changes in RMS or 2nd-order astigmatism  $Z(2,-2)$  and  $Z(2,2)$  in the anterior corneal surface with accommodation. This was the general trend, although the authors did find changes in some individuals. Our high SD values also indicate that

great variations exist between subjects. However, He et al.<sup>8</sup> found changes in horizontal coma  $Z(3,1)$  and spherical aberration  $Z(4,0)$ , while we did not. Ni et al.<sup>12</sup> measured corneal aberrations from the anterior, posterior, and entire cornea with a single Scheimpflug device. They found changes in vertical coma  $Z(3,-1)$  and spherical aberration  $Z(4,0)$  and a decrease in higher-order aberrations (3rd- to 8th-order) for the anterior and entire cornea. These outcomes do not match our findings and might be the result of ethnic differences between the samples. The study by Ni et al.<sup>12</sup> was of Asian subjects, while our study evaluated a sample of Caucasian participants. Demographic data on refractive error show higher average levels of astigmatism in Asian eyes than in non-Asians eyes, a difference that has been attributed to greater tightness of Asian eyelids and narrower palpebral apertures, which cause pressure that produces changes in corneal topography.<sup>27-29</sup> Given that corneal aberrations are directly extracted from topography, this could be the reason for the difference in findings between the study of Ni et al.<sup>12</sup> and our study.

This study has limitations that led to our results being different from those in previous studies. A possible source of disagreement in results between studies is the difference in devices used. The devices used to assess corneal changes during accommodation before Scheimpflug photography was available could not monitor accommodation during data collection and required visual or manual fixation control. In addition, keratometers, videokeratoscopes, and Placido disk-based topographers consider the anterior surface of the cornea as a convex mirror. They obtain the curvature by deriving the slope data from the reflection of the

concentric rings of light rather than by reconstructing the corneal surface by splines (piecewise defined curve by polynomials), which is what the Galilei G4 system does. Moreover, depending on the size and curvature of the Placido disk or the device's constraints, corneal topography cannot be acquired in the total cornea while the Galilei G4 system obtains data from a 10.0 mm diameter area. Thus, the equipment used in this study provides trustworthy results because of the duality; dual Scheimpflug systems are reported to have reported good repeatability and more reliable and accurate detection of pachymetry data and corneal posterior surface data than single Scheimpflug devices.<sup>30-32</sup>

The main limitation of this study is the small sample. Although the results allow us to accurately describe our sample, extrapolation to the rest of the population should be carefully considered. This is because the effect size of the corneal changes with accommodation given by the values of partial Eta squared (Table 2.1), is small and therefore a larger sample size would be required in order to avoid a possible Type II error. Moreover, similar to other studies,<sup>9,11,12</sup> we assessed corneal changes with accommodation in emmetropic subjects only. However, studies of corneal biomechanical properties<sup>33</sup> have found that lower corneal hysteresis values indicate a soft and flexible cornea and are associated with high myopia. Thus, this might be why the results of Yasuda et al.,<sup>10</sup> who included participants with refractive ranging from -8.50 to +0.50 D, showed the greatest significant corneal changes between the unaccommodated state and the accommodated state. Nevertheless, based on the same proven assumption that ocular rigidity is lower in keratoconic eyes<sup>34</sup> and therefore these eyes are more susceptible to changes,

Buehren et al.<sup>13</sup> did not find greater corneal changes with accommodation in keratoconic corneas than in normal corneas. Hence, studies with a larger sample that includes ametropic subjects should be performed to clarify this.

A decline in the corneal resistance factor has also been found with increasing age. However, when changes in corneal parameters with accommodation were assessed in elderly people,<sup>10,12</sup> significant differences were not found between young people and presbyopic people. Similarly, total corneal aberrations increase with age, with spherical aberration being the main contributor.<sup>19</sup> As a result of the misalignment between surfaces, coma-like aberrations also increase with age.<sup>19</sup> This encourages a reduction in accommodation capacity with age and thus accounts for the accommodation that is not explainable by lens changes, which is called pseudoaccommodation. It is key to understand pseudoaccommodation to advance our knowledge and achieve the goal of restoring accommodation. Hence, aging affects corneal biomechanical properties and aberrations and the baseline for a study like this one would be different. Thus, a study using the last technology of Galilei G4 system in a larger cohort including subjects with different refraction conditions and in different age groups would provide more robust results and would answer unresolved questions that might be relevant in the clinical practice. There are multiple applications as for instance, corneal topography measurements are essential not only in refractive but also in premium intraocular lens (IOL) surgery. The so-called premium IOLs are those that have advanced features beyond those found in basic single vision IOLs that are covered by some types of health

insurance. These include accommodating IOLs for which implantation would be crucial to understand fully the contribution of the cornea to accommodation.

In summary, central, paracentral, and peripheral anterior and posterior corneal keratometry, TCP, and pachymetry unaffected by cyclotorsional effects were stable during accommodation. Similarly, total corneal aberrations were constant at different accommodated states. This reaffirms the classic statements by Young.<sup>2</sup> However, a more robust study with a more diverse and larger sample is needed to improve our understanding and contribute to the development and improvement of therapeutic and surgical solutions.



## 2.6 REFERENCES

1. Home E. The Croonian lecture on muscular motion. *Phil Trans R Soc Lond* 1795; 85:202–220. Available at: <http://rstl.royalsocietypublishing.org/content/85/202.full.pdf>. Accessed January 11, 2015
2. Young T. The Bakerian lecture: on the mechanism of the eye. *Phil Trans R Soc Lond* 1801; 91:23–88. Available at: <http://rstl.royalsocietypublishing.org/content/91/23.full.pdf>. Accessed January 11, 2015
3. Helmholtz H. Ueber die Accommodation des Auges [About accommodation of the eyes]. *Albrecht von Graefes Arch Ophthalmol* 1855; 1(2):1–74
4. Fairmaid JA. The constancy of corneal curvature; an examination of corneal response to changes in accommodation and convergence. *Br J Physiol Opt* 1959;16:2–23
5. Löpping B, Weale RA. Changes in corneal curvature following ocular convergence. *Vision Res* 1965; 5:207–215
6. Pierścionek BK, Popiołek-Masajada A, Kasprzak H: Corneal shape change during accommodation. *Eye* 2001; 15:766–769. Available at: <http://www.nature.com/eye/journal/v15/n6/pdf/eye2001246a.pdf>. Accessed January 11, 2015

7. Yasuda A, Yamaguchi T. Steepening of corneal curvature with contraction of the ciliary muscle. *J Cataract Refract Surg* 2005; 31:1177–1181
8. He JC, Gwiazda J, Thorn F, Held R, Huang W. Change in corneal shape and corneal wave-front aberrations with accommodation. *J Vis* 2003; 3:456–463. Available at: <http://www.journalofvision.org/content/3/7/1.full.pdf>. Accessed January 11, 2015
9. Bayramlar H, Sadigov F, Yildirim A. Effect of accommodation on corneal topography. *Cornea* 2013; 32:1251–1254
10. Yasuda A, Yamaguchi T, Ohkoshi K. Changes in corneal curvature in accommodation. *J Cataract Refract Surg* 2003; 29:1297–1301
11. Read SA, Buehren T, Collins MJ. Influence of accommodation on the anterior and posterior cornea. *J Cataract Refract Surg* 2007; 33:1877–1885
12. Ni Y, Liu X, Lin Y, Guo X, Wang X, Liu Y. Evaluation of corneal changes with accommodation in young and presbyopic populations using Pentacam high resolution Scheimpflug system. *Clin Exp Ophthalmol* 2013; 41:244–250
13. Buehren T, Collins MJ, Loughridge J, Carney LG, Iskander DR. Corneal topography and accommodation. *Cornea* 2003; 22:311–316
14. Schachar RA, Tello C, Cudmore DP, Liebmann JM, Black TD, Ritch R. In vivo increase of the human lens equatorial diameter during accommodation. *Am J Physiol* 1996; 271:R670–R676

15. Drexler W, Baumgartner A, Findl O, Hitzenberger CK, Fercher AF. Biometric investigation of changes in the anterior eye segment during accommodation. *Vision Res* 1997; 37:2789–2800
16. López-Gil N, Fernández-Sánchez V, Legras R, Montés-Micó R, Lara F, Nguyen-Khoa JL. Accommodation-related changes in monochromatic aberrations of the human eye as a function of age. *Invest Ophthalmol Vis Sci* 2008; 49:1736–1743. Available at: <http://www.iovs.org/cgi/reprint/49/4/1736>. Accessed January 12, 2015
17. Montés-Micó R. Role of the tear film in the optical quality of the human eye. *J Cataract Refract Surg* 2007; 33:1631–1635
18. Kiely PM, Smith G, Carney LG. The mean shape of the human cornea. *Optica Acta* 1982; 29:1027–1040
19. Navarro R, Rozema JJ, Tassignon M-J. Optical changes of the human cornea as a function of age. *Optom Vis Sci* 2013; 90:587–598. Available at: [http://journals.lww.com/optvissci/Fulltext/2013/06000/Optical\\_Changes\\_of\\_the\\_Human\\_Cornea\\_as\\_a\\_Function.10.aspx](http://journals.lww.com/optvissci/Fulltext/2013/06000/Optical_Changes_of_the_Human_Cornea_as_a_Function.10.aspx). Accessed January 12, 2015
20. Richdale K, Sinnott LT, Bullimore MA, Wassenaar PA, Schmalbrock P, Kao C-Y, Patz S, Mutti DO, Glasser A, Zadnik K. Quantification of age-related and per diopter accommodative changes of the lens and ciliary muscle in the emmetropic human eye. *Invest Ophthalmol Vis Sci* 2013; 54:1095–1105. Available at: <http://www.iovs.org/content/54/2/1095.full.pdf>. Accessed January 12, 2015

21. Kasthurirangan S, Markwell EL, Atchison DA, Pope JM. MRI study of the changes in crystalline lens shape with accommodation and aging in humans. *J Vis* 2011; 11(3):19,1–16. Available at: <http://www.journalofvision.org/content/11/3/19.full.pdf>. Accessed January 12, 2015
22. Ostrin L, Kasthurirangan S, Win-Hall D, Glasser A. Simultaneous measurements of refraction and A-scan biometry during accommodation in humans. *Optom Vis Sci* 2006; 83:657–665. Available at: [http://journals.lww.com/optvissci/Fulltext/2006/09000/Simultaneous\\_Measurements\\_of\\_Refraction\\_and\\_A\\_Scan.10.aspx](http://journals.lww.com/optvissci/Fulltext/2006/09000/Simultaneous_Measurements_of_Refraction_and_A_Scan.10.aspx). Accessed January 12, 2015
23. Dubbelman M, van der Heijde GL, Weeber HA. Change in shape of the aging human crystalline lens with accommodation. *Vision Res* 2005; 45:117–132
24. Bolz M, Prinz A, Drexler W, Findl O. Linear relationship of refractive and biometric lenticular changes during accommodation in emmetropic and myopic eyes. *Br J Ophthalmol* 2007; 91:360–365. Available at: <http://www.ncbi.nlm.nih.gov/pmc/articles/PMC1857649/pdf/360.pdf>. Accessed January 12, 2015
25. Li Y-J, Choi JA, Kim H, Yu S-Y, Joo C-K. Changes in ocular wavefront aberrations and retinal image quality with objective accommodation. *J Cataract Refract Surg* 2011; 37:835–841

26. Díaz JA, Fernández-Dorado J, Sorroche F. Role of the human lens gradient-index profile in the compensation of third-order ocular aberrations. *J Biomed Opt* 2012; 17:075003
27. Kame RT, Jue TS, Shigekuni DM. A longitudinal study of corneal astigmatism changes in Asian eyes. *J Am Optom Assoc* 1993; 64:215–219
28. Shaw AJ, Collins MJ, Davis BA, Carney LG. Eyelid pressure: inferences from corneal topographic changes. *Cornea* 2009; 28:181–188
29. Read SA, Collins MJ, Carney LG. A review of astigmatism and its possible genesis. *Clin Exp Optom* 2007; 90:5–19. Available at: <http://onlinelibrary.wiley.com/doi/10.1111/j.1444-0938.2007.00112.x/pdf>. Accessed January 12, 2015
30. Crawford AZ, Patel DV, McGhee CNJ. Comparison and repeatability of keratometric and corneal power measurements obtained by Orbscan II, Pentacam, and Galilei corneal tomography systems. *Am J Ophthalmol* 2013; 156:53–60
31. Aramberri J, Araiz L, Garcia A, Illarramendi I, Olmos J, Oyanarte I, Romay A, Vigara I. Dual versus single Scheimpflug camera for anterior segment analysis: precision and agreement. *J Cataract Refract Surg* 2012; 38:1934–1949
32. Salouti R, Nowroozzadeh MH, Zamani M, Fard AH, Niknam S. Comparison of anterior and posterior elevation map measurements between 2 Scheimpflug imaging systems. *J Cataract Refract Surg* 2009; 35:856–862

33. del Buey MA, Lavilla L, Ascaso FJ, Lanchares E, Huerva V, Cristóbal JA. Assessment of corneal biomechanical properties and intraocular pressure in myopic Spanish healthy population. *J Ophthalmol* 2014; Article ID:905129. Available at: <http://www.ncbi.nlm.nih.gov/pmc/articles/PMC3955599/pdf/JOPH2014-905129.pdf>. Accessed January 12, 2015

34. Shah S, Laiquzzaman M, Bhojwani R, Mantry S, Cunliffe I. Assessment of the biomechanical properties of the cornea with the Ocular Response Analyzer in normal and keratoconic eyes. *Invest Ophthalmol Vis Sci* 2007; 48:3026–3031. Available at: <http://www.iovs.org/cgi/reprint/48/7/3026>. Accessed January 12, 2015

### **3 RELATIONSHIP BETWEEN ACCOMMODATIVE RESPONSE FUNCTION AND CILIARY MUSCLE CHARACTERISTICS**

#### **CONTRIBUTIONS**

The study was designed by me and my supervisor, Hema Radhakrishnan and we obtained ethics approval for the study. The data collection was done by me along with the image analysis using a MATLAB code written by my co-author and supportive colleague Danilo Andrade de Jesus. I wrote the first draft of the manuscript which was revised and finalised with support from the co-authors.

#### **PUBLISHING OF THE PAPER**

Authors for this study are Irene Siso-Fuertes, Danilo Andrade de Jesus and Hema Radhakrishnan. This paper will be submitted with the title: "Age-related relationship between accommodative response function and ciliary muscle". Target journal: *Ophthalmic and Physiological Optics (OPO)*. To be submitted.

#### **PRESENTATION AT CONFERENCE**

A talk was delivered about the contents of this research:

Siso-Fuertes, I., Jesus, D. & Radhakrishnan. 2017. Relationship between ciliary muscle and accommodative response across age groups. *Investigative Ophthalmology & Visual Science (IOVS)*, Proceedings of Association for Research in Vision and Ophthalmology (ARVO) Annual Meeting, 2017, Abstract.

### 3.1 ABSTRACT

**PURPOSE:** Presbyopia is an ageing condition that affects millions of people worldwide. Understanding the accommodative ability in older subjects has been a major challenge and of major importance to advance in the design of methods for presbyopia correction. We conducted a cross-sectional study in order to investigate the age-related changes in the ciliary muscle dimensions with the accommodative function.

**METHODS:** Subjects aged between 18 to 75 years were included and divided into 3 age groups. Ciliary muscle images at three different accommodative demands (0, 2.5 and 4D) were taken with a Visante Anterior-Segment Optical Coherence Tomographer (AS-OCT). A customised MATLAB code was developed to measure the ciliary muscle thickness (CMT) from the OCT images at 2 (CMT2), 2.5 (CMT25) and 3 (CMT3) mm from the scleral spur in a semi-automated way. Accommodative response of the eye was measured using a Hartman-Shack aberrometer (irx3).

**RESULTS:** Linear regressions showed that the correlation between age and CMT2, CMT25 and CMT3 was not statistically significant ( $p > 0.05$ ). However, Friedman test revealed statistically significant ( $p < 0.05$ ) CMT changes with accommodation in age group 2 for CMT2 and CMT25 and in age group 3 for CMT3. The slope of the accommodative response and the absolute value of the CMT slope negatively correlated in age group 1 while a positive correlation was found for age groups 2 and 3.

**CONCLUSIONS:** Ciliary muscle is invariant with age but does reduce its thickness in the posterior part with accommodation. Older people with stiffer crystalline lenses, show a bigger change in ciliary muscle in order to accommodate more accurately, while young people with easily deformable lenses and bigger leads of accommodation exhibit less ciliary muscle change although their accommodative response is more accurate. Our findings support the Fincham's theory of presbyopia.



## **3.2 INTRODUCTION**

According to the last report on world population ageing published by the United Nations<sup>1</sup>, by 2050 the number of older people will exceed the number of adolescents and youth. As a consequence, the number of presbyopes and needs for presbyopia correction will increase considerably.

There are different theories of presbyopia development some of which are mutually exclusive. While authors like Gullstrand expanded the popular Helmholtz's theory of accommodation and attributed the loss of accommodative capacity to the crystalline lens<sup>2</sup>, others like Duane<sup>3</sup> and Schachar<sup>4</sup> claimed the opposite referring to the ciliary muscle as the ultimate structure of the eye causing presbyopia. In between these two theories, there is the one proposed by Fincham<sup>5</sup> who suggested that the reduction in accommodation is primarily lenticular but also stated that the amount of ciliary muscle response required to reach a given accommodative stimulus increases with age.

Almost all the current solutions for presbyopia are static approaches and most effort is focused on developing dynamic corrections in order to restore the accommodative ability, allowing subjects to retrieve a young dynamic visual function. Accommodating intraocular lenses (IOLs) are currently the most popular approach.<sup>6, 7</sup> Most accommodating IOL designs rely on the ciliary muscle contraction to change the refractive power of the lens to facilitate vision over a range of distances. However, none of the designs take into account the changes in ciliary muscle function with age and accommodation.<sup>8</sup>

Very few studies have looked at the changes in ciliary muscle as a function of age and accommodation because the highly pigmented area of the iris located in front of the ciliary region has traditionally hampered the assessment of the ciliary muscle in-vivo. Nonetheless, in the last decade, the development of imaging technologies such as magnetic resonance imaging (MRI) and optical coherence tomography (OCT), have added a new insight.<sup>9-19</sup>

Strenk et al.<sup>12</sup> were the first to use MRI to study the ciliary muscle. This imaging technology produces undistorted images and allows the direct visualization of the intraocular structures during accommodation. Diverse studies have been published in which the ciliary muscle anteroposterior thickness, ciliary ring diameter and circumferential space are evaluated as a function of age and at different accommodative demands.<sup>9, 11, 12</sup> However MRI images are not taken in natural conditions of vision and are critical to eye positioning. Also, the resolution, signal to noise ratio and the acquisition time along with the accommodative stimuli presentation are constraints of this technique.<sup>12</sup> It is therefore more convenient and accessible to assess the ciliary muscle in a non-contact, non-invasive and rapid acquisition fashion by means of Anterior-Segment Optical Coherence Tomography (AS-OCT).

The first study using Visante AS-OCT was published in 2009 where accommodative fluctuations were related to the thickness of the ciliary muscle measured at one single point in children (8 to 15 years).<sup>16</sup> From then on, thickness has been measured in several different points of the ciliary muscle and its role on presbyopia has been of interest. Sheppard and Davies investigated the changes in ciliary muscle

thickness (CMT) with accommodation depending on the refractive condition<sup>18</sup> and age.<sup>19</sup> In the latter study, Sheppard and Davies<sup>19</sup> analysed the CMT with age and accommodation and documented a thickening with accommodation of a single point of the ciliary muscle (located at 25% of the overall length of the muscle), Richdale and colleagues<sup>15</sup> measured the CMT at different points of the muscle and analysed the interaction between age and accommodation as well as the effect of age up to 50 years. They<sup>15</sup> did not find a statistically significant effect of age in the ciliary muscle or interaction between age and accommodation. This result is however, only valid for predominantly pre-presbyopic participants as their sample included emmetropes up to the age of 50 years.<sup>15</sup> Also, this is not likely to be the kind of population accommodating IOLs are targeted to, as most of the people needing and willing to wear this kind of correction will be well over the age of 50 to 55 years when the accommodative ability is completely lost.<sup>20</sup>

Later, other groups used more sophisticated set up<sup>14, 21</sup> or imaging devices to study ciliary muscle changes.<sup>17, 22</sup> Lewis et al.<sup>21</sup> and Lossing et al.<sup>14</sup> coupled the AS-OCT to a PowerRefractor to simultaneously, but not necessarily in a synchronized way, measure the accommodative response and CMT. This evaluation was, however, only done in a cohort of children<sup>21</sup> and young adults (up to 28 years)<sup>14</sup>. Consequently only the influence of accommodation in CMT was assessed but not the effect of age in CMT changes. More recently, Ruggeri and colleagues<sup>22</sup> and Shao et al.<sup>17</sup> developed a custom AS-OCT with which the lens and ciliary muscle can be imaged at the same time but they did so in a very scarce (2 participants<sup>22</sup>) and young cohort (age range, 20-39 years<sup>17</sup>), using a manual approach to segment the

ciliary muscle images and without determining the accommodative responses of the subjects.

Due to the emergence of new ways to assess the ciliary muscle in-vivo, diverse methods to measure its thickness have been proposed. While some authors do the ciliary muscle segmentation manually<sup>22, 23</sup>, others<sup>24, 25</sup> have developed softwares capable of almost automatically delimitating the ciliary muscle. These differences in image processing along with the diverse equipment, procedures and analysis used between peer-reviewed publications have contributed to the often variable results in ciliary muscle characteristics.

Therefore, it seems important to understand ciliary muscle changes in more detail to improve the current dynamic approaches for presbyopia correction which rely on the ciliary muscle functionality. The aim of this study is to evaluate the changes in the ciliary muscle characteristics in an age divided cohort at different accommodative levels.

## **3.3 METHODS**

### **3.3.1 Subjects**

A cross-sectional study was conducted including 61 participants aged between 18 and 75 years. Ciliary muscle measurements were taken for 0 D, 2.5 D and 4.0 D accommodative demands. Of the 61 subjects tested, only 49 had usable data from which only 18 participants had repeated data for different accommodative levels; this is valid measurements at each of the three different accommodative vergences measured. The quality of the ciliary muscle images in the apex, the difficulty of segmenting that part and the differences in image centration between images, reduced the amount of eligible data. The 18 subjects sub-sample was divided into three different age groups (Age group 1: 18 to 29 years, n=4; Age group 2: 30 to 40 years, n=8 and Age group 3: 40 years and over, n=6). Complete demographic data from the 3 samples is included in Table 3.1

Table 3.1: Demographic data.

Maximum Sample size (n)	Description	Accommodative demand presented (D)	Age group	Sample size (n)	Mean age $\pm$ SD (years)	Gender Male (n)	Gender Female (n)	Mean Spherical equivalent $\pm$ SD (D)		
61	Total number of subjects tested	0, 2.5 and 4	All	61	33 $\pm$ 15	25	36	-1.36 $\pm$ 1.93		
			1	33	23 $\pm$ 3	10	23	-1.56 $\pm$ 1.77		
			2	13	33 $\pm$ 2	8	5	-1.39 $\pm$ 1.70		
			3	15	56 $\pm$ 12	7	8	-0.84 $\pm$ 2.48		
Maximum Sample size (n)	Description	Accommodative demand presented (D)	Age group	Sample size after CM analysis (n)	Mean age $\pm$ SD (years)	Gender Male (n)	Gender Female (n)	Mean Spherical equivalent $\pm$ SD (D)		
49	Total number of subjects with usable data after CM analysis	0	All	19	41 $\pm$ 16	12	7	-1.41 $\pm$ 2.10		
			1	4	25 $\pm$ 4	1	3	-2.14 $\pm$ 2.41		
			2	8	33 $\pm$ 2	7	1	-1.36 $\pm$ 1.59		
			3	7	59 $\pm$ 13	4	3	-1.00 $\pm$ 2.71		
		2.5	All	43	33 $\pm$ 16	20	23	-1.52 $\pm$ 1.90		
			1	23	23 $\pm$ 3	8	15	-1.61 $\pm$ 1.75		
			2	10	34 $\pm$ 3	7	3	-1.16 $\pm$ 1.59		
		4	3	10	58 $\pm$ 12	5	5	-1.67 $\pm$ 2.68		
			All	49	33 $\pm$ 16	22	27	-1.52 $\pm$ 1.81		
			1	28	23 $\pm$ 3	9	19	-1.44 $\pm$ 1.54		
		18	Total number of subjects with usable repeated data for the different accommodative levels	0, 2.5 and 4	2	11	33 $\pm$ 2	8	3	-1.65 $\pm$ 1.72
					3	10	60 $\pm$ 11	5	5	-1.61 $\pm$ 2.72
All	18				39 $\pm$ 13	12	6	-0.63 $\pm$ 1.73		
1	4				25 $\pm$ 4	1	3	-1.68 $\pm$ 2.45		
2	8	33 $\pm$ 2	7	1	-0.58 $\pm$ 1.43					
3	6	57 $\pm$ 13	4	2	0.34 $\pm$ 1.24					

Only healthy participants over 18 years of age, astigmatism less than 1.25 D and no history of ocular pathology or surgery were enrolled in this study. Participants with history of any systemic pathology or using any topical or systemic medication which could affect accommodation were excluded from the study. Ciliary muscle images and refraction measurements were taken from all the subjects. The left eye was used for all measurements. This is due to the external design of the device (i.e. the arm that connects the chin and head rest is situated on the left) as it is only possible to turn the gaze to the right to see an external target. Hence participants were positioned as right as possible on the chin rest and the left eye was the one situated in front of the device and used to take the ciliary muscle measurements. The mean spherical equivalent refraction (M) of the 18 subjects sub-sample was -0.63 D (range +1.58 D and -4.26 D). The study followed the tenets of the Declaration of Helsinki and written informed consent was obtained from all participants after the nature and possible consequences of the study had been explained. The project protocol was approved by the Research Ethics Committee of the University of Manchester.

### **3.3.2 Accommodative response**

The accommodative response of each individual was measured using the irx3 Wavefront Aberrometer (Imagine-Eyes, Orsay, France) which is a Hartmann-Shack based equipment that allows the measurement of ocular aberrations. Measurements were taken using the accommodation procedure available in the

software. A series of several fixed stimulus measurements are taken every time the internal target moves at the predefined steps. Nine refraction measurements were taken, from 0 D to 4 D of accommodation in 0.50 D steps. Paraxial M was calculated from the defocus ( $Z(2,0)$ ) and spherical aberration ( $Z(4,0)$ ) terms using the paraxial curvature matching formula proposed by Thibos et al.<sup>26</sup>, for each of the refraction measurement taken. The slope of the linear fit to the data corresponding to the accommodative response encountered from when a 1.5 D accommodative stimulus was presented up to the 4 D stimulus, was obtained using MATLAB (MathWorks, Natic, MA). The first three refraction measurements (at 0, 0.50 and 1 D stimulus) from the accommodative measurements were discarded as they include the subject's tonic accommodation. Four accommodative response function measurements were performed for each subject and the slope results were averaged.

### **3.3.3 Ciliary muscle images**

The Visante AS-OCT (Carl Zeiss Meditec, Dublin, CA). was used to capture images of the ciliary muscle. For this purpose, the set up showed in Figure 3.1 was put into place.



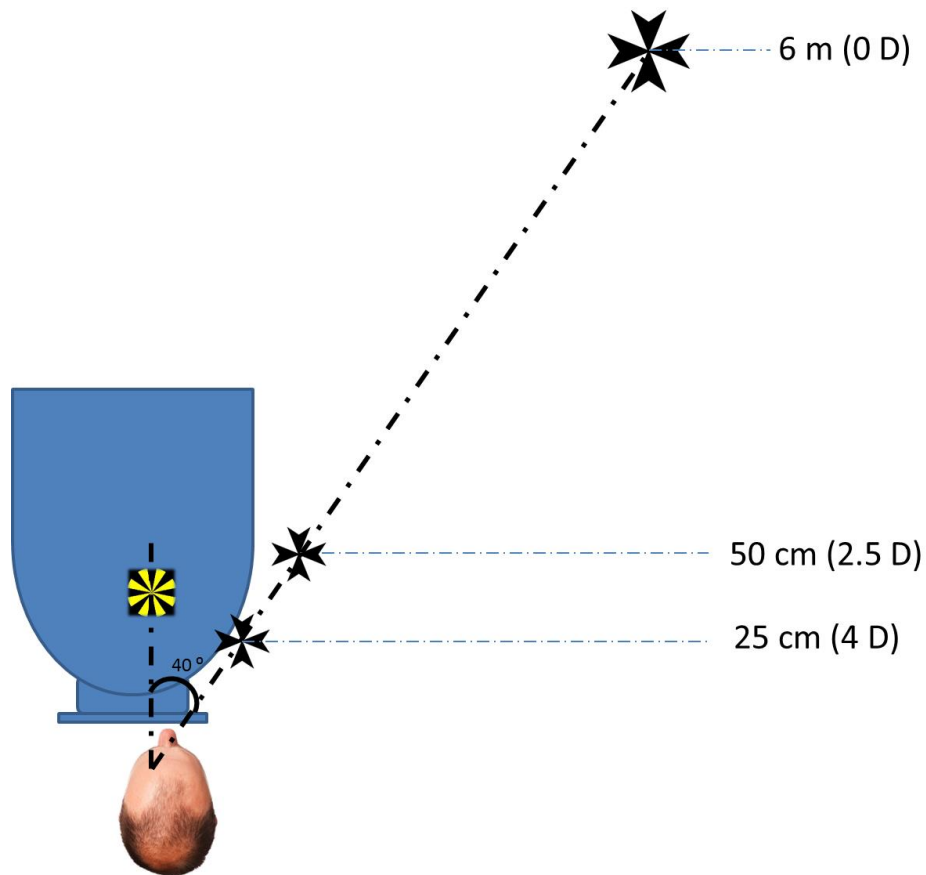


**Figure 3.1:** Schematic diagram of the laboratory set up for imaging the ciliary muscle with Visante AS-OCT.

The scan mode selected to capture the images was “Enhanced High Resolution Corneal”. In this mode, each column of the final image corresponds to 4 scans that were registered and averaged by the Visante’s software. Once positioned appropriately, the participants were asked to fixate at the centre of the internal target in the OCT. Meanwhile the examiner aligned the image optimally as a reflection normal to the cornea was visible in the screen. Subsequently, the participants were asked to only turn their gaze to their right hand side and fixate at the centre of the external Maltese cross target while keeping their head in the same position. The left eye and therefore the temporal ciliary muscle was examined. To

ensure all the subjects could perceive the targets sharply, their prescription was corrected with daily disposable soft contact lenses (CLs). The CLs prescription was chosen based on the spherical equivalent obtained from aberrometry measurements rather than performing a sight test. In order to evaluate the changes in CMT with accommodation, a target was presented at different distances. The distant target was presented on the far wall (6 m) and the accommodative targets mounted on an adjustable rod which was externally situated creating an angle of approximately 40 degrees between the target and examined eye. The Maltese cross was moved along the rod to generate a 2.5 D (40 cm) and 4 D (25 cm) stimulus. Three OCT images were taken at each of the three possible positions of the target which were shown in a random order and results averaged for each participant.

A MATLAB code was developed following that from Kao et al.<sup>24</sup> in order to obtain the dimensions of the ciliary muscle from Visante AS-OCT raw image binary files. The images were imported into MATLAB in grey scale and a size of 512 by 1024 pixels (4 x 10 mm). Afterwards they were resized to 512 by 1280 pixels (4 x 10.2 mm) to maintain the original aspect ratio. After that, two vertical lines delimiting the original image (image length 1024 pixels) were drawn.

Subsequently, unlike the algorithm presented by Kao et al.<sup>24</sup> where one single point corresponding to the scleral spur was selected, two points were located manually by one examiner (ISF). The examiner was masked to the subject and accommodative state of the image as the identification numbers automatically assigned by the device were used to analyse the images. ISF selected the scleral spur and the end of

the ciliary muscle within the vertical boundaries previously shown. This approach, despite of being slower, increases the robustness of the ciliary muscle segmentation. Then, the image was cropped horizontally in order to select the area of interest at 128 pixels to the left and 896 pixels to the right of the scleral spur and down sampled to one-fourth to reduce the analysis time. New pixels around the edges of the resized image were introduced in order to better delimitate the boundaries of the image.

To extract the ocular structure from the background in the image, the average of the grey scale image was obtained and set as a threshold beyond which, the contour of the ocular surface was taken. The images provided by Visante AS-OCT did not have enough quality for the apex of the ciliary muscle to be detected in an accurate and robust way for all subjects. The signal-to-noise ratio was very poor and it is not easily differentiated. Besides, the poorer contrast in ciliary muscle accommodating images has already been acknowledged by another author.<sup>14</sup> Therefore, similarly to the algorithm proposed by Kao et al.<sup>24</sup>, a diamond shape was obliquely superimposed and based on it, a region of interest delimited by the diamond shape and the two selected points was manually obtained.

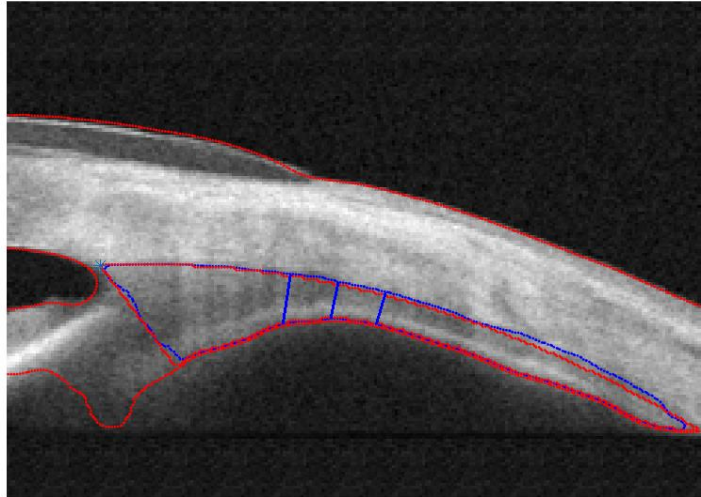


**Figure 3.2:** Example of a ciliary muscle segmentation by using the MATLAB code developed. Red line delimits the ocular structure and blue line the ciliary muscle region along with the pigmented epithelium. Transversal blue lines normal to the ciliary muscle curvature represent the thickness measurements taken with the custom software.

An edge-based active contour model based on the publication of Li et al.<sup>27</sup> was then applied to extract the ciliary muscle from the ocular structures. Since binary files from Visante AS-OCT do not need geometric adjustments for distortion, only a refractive adjustment was performed. The refractive index applied was  $n = 1.56$  as it was the experimentally obtained by Kao et al.<sup>24</sup> for infrared light travelling through human sclera and ciliary muscle tissue fixed in 10% formalin. Figure 3.2 shows the result of a ciliary muscle segmentation image. CMT was measured tracing lines normal to the local curvature of the segmented ciliary muscle at 2 (CMT2), 2.5 (CMT25) and 3 (CMT3) mm from the scleral spur. No thickness measurements were taken in the anterior part of the ciliary muscle as an artificial shape had been included to facilitate the delimitation of that area. However, the variation of CMT2, CMT25 and CMT3 with accommodation and age, if any should

be proportional in a linear way<sup>15</sup> to the variation of the CMT in the most anterior part. For this purpose a linear regression analysis was applied to Kao's et al.<sup>24</sup> cross-sectional study data with a refractive index of  $n = 1$  and  $n = 1.38$ . Figure 3.3 shows CMT at 1 mm from the scleral spur predicted from CMT data at 2 and 3 mm, in both cases. Despite the slightly smaller values obtained from the linear regression, they are within the standard deviation limits and therefore this could be a valid method to obtain the CMT in the anterior part. Thus, in our study the thickness at 1 mm from the scleral spur was obtained by fitting a linear regression to the averaged data.

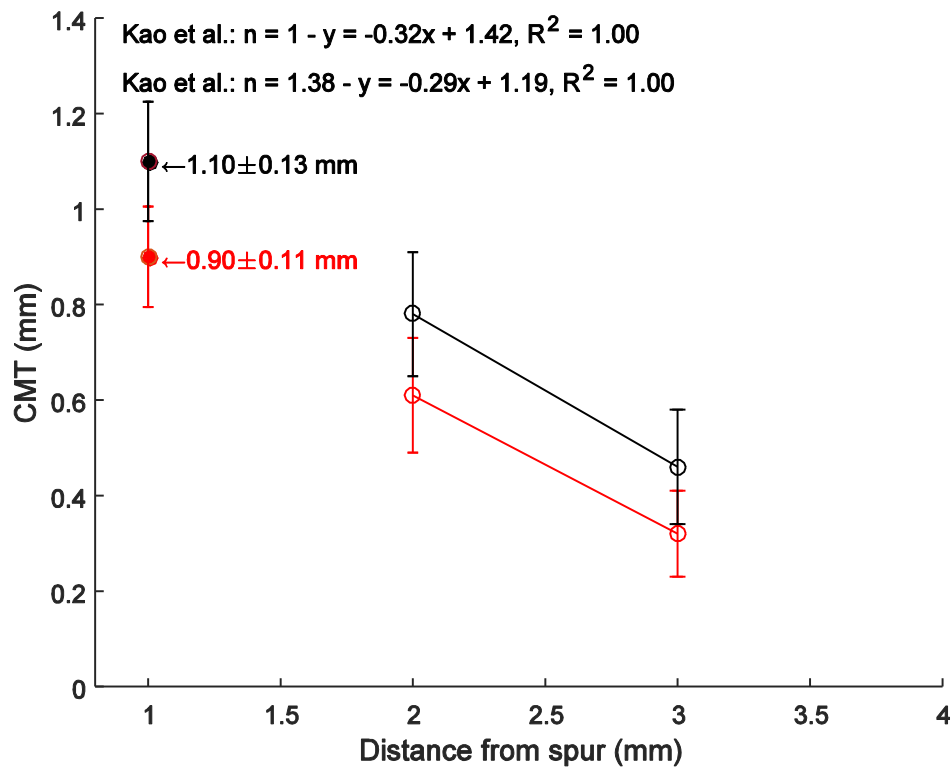


**Figure 3.3:** Linear regression fitted to Kao et al.<sup>24</sup> data from mean CMT2 and mean CMT3.

Black and red lines and dots represent data from Kao's et al.<sup>24</sup> algorithm data with a refractive index of  $n = 1$  and  $n = 1.38$ , respectively. Mean CMT values at 1 mm from the scleral spur empirically obtained by Kao et al.<sup>24</sup> were  $1.15 \pm 0.09$  and  $0.92 \pm 0.09$  for  $n = 1$  and  $n = 1.38$ , respectively.

The data analysed in this study was carefully visually inspected to meet good standards criteria (delimitation lines not exceeding the boundaries of the muscle, image centred so the totality of the muscle can be seen and thickness lines covering the whole width of the muscle) and provide high quality results.

### **3.3.4 Statistical analysis**

Statistical analysis was carried out using MATLAB. Linear regression analysis was performed to the CMT data in order to determine its relationship with age, distance from the scleral spur and slope of the accommodative response. CMT measurements were classified according to age group and stimulus vergence at which the image was taken. Normality was tested using Kolmogorov-Smirnov, which revealed that the data did not have a normal distribution. Therefore, non-parametric tests such as Friedman were carried out in order to find differences in the CMT when measurements were repeated at different accommodative demands. All the tests were calculated for a confidence interval at 0.05 significance level.

## **3.4 RESULTS**

The relationship between CMT2, CMT25 and CMT3 with age at the three different accommodative demands (0, 2.5 and 4 D) is presented in Figures 3.4 and 3.5. The uniformity in CMT with age is more apparent when all subjects (n=49) from whom

CMT data was available are included in the analysis (Figure 3.4). Despite the low linear regression slope, a slight increase in CMT with age is apparent from the data of the 18 subject sub-sample. However, as shown from the p-values displayed for each of the linear regression equations, the correlation between CMT and age was not statistically significant ( $p > 0.05$ ) for any of the points of the ciliary muscle measured at any of accommodative demands presented.

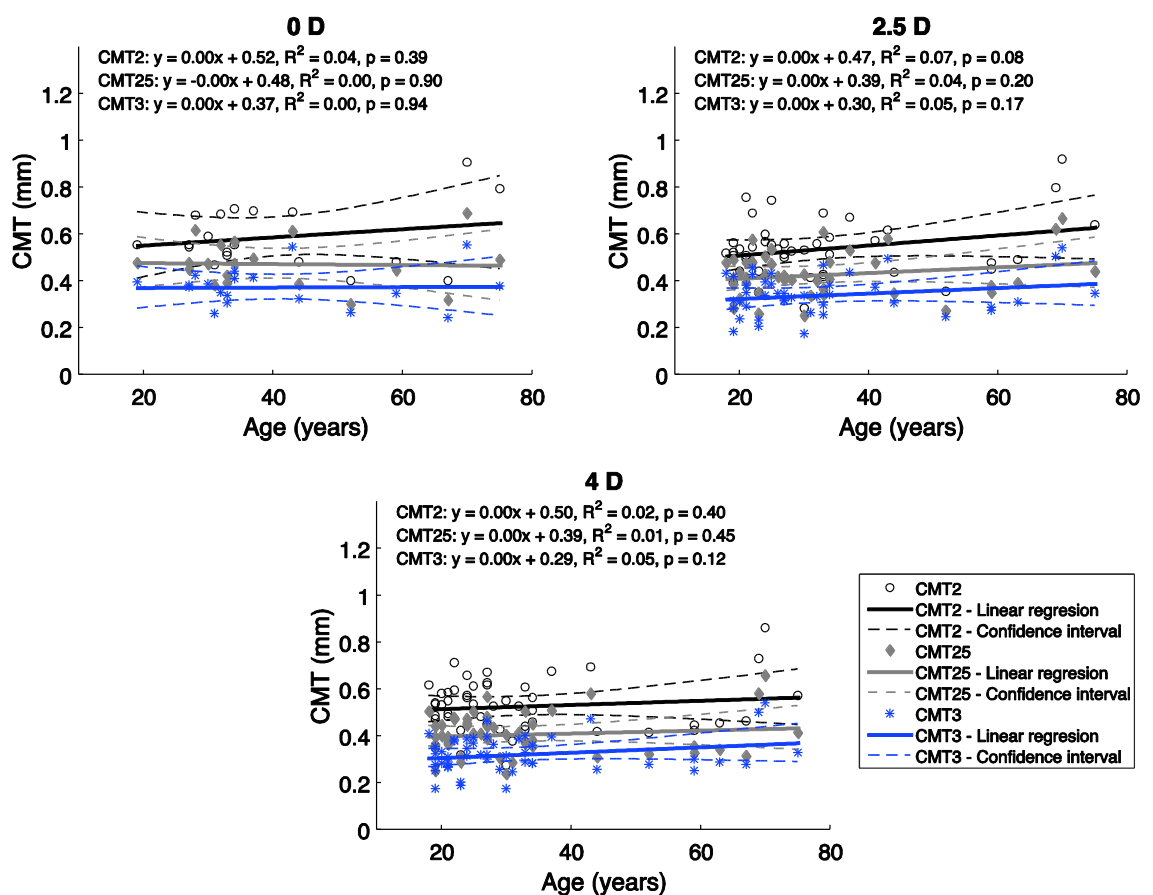


**Figure 3.4:** CMT relationship with age at the three different accommodative demands for a sample of 49 subjects. Dots, solid and dashed lines represent the CMT values, linear regression and confidence intervals for a 0.05 of significance level. Black colour corresponds to CMT2, grey to CMT25 and blue to CMT3. The linear equations for the three respective CMT linear regressions are also displayed on top of each graph.

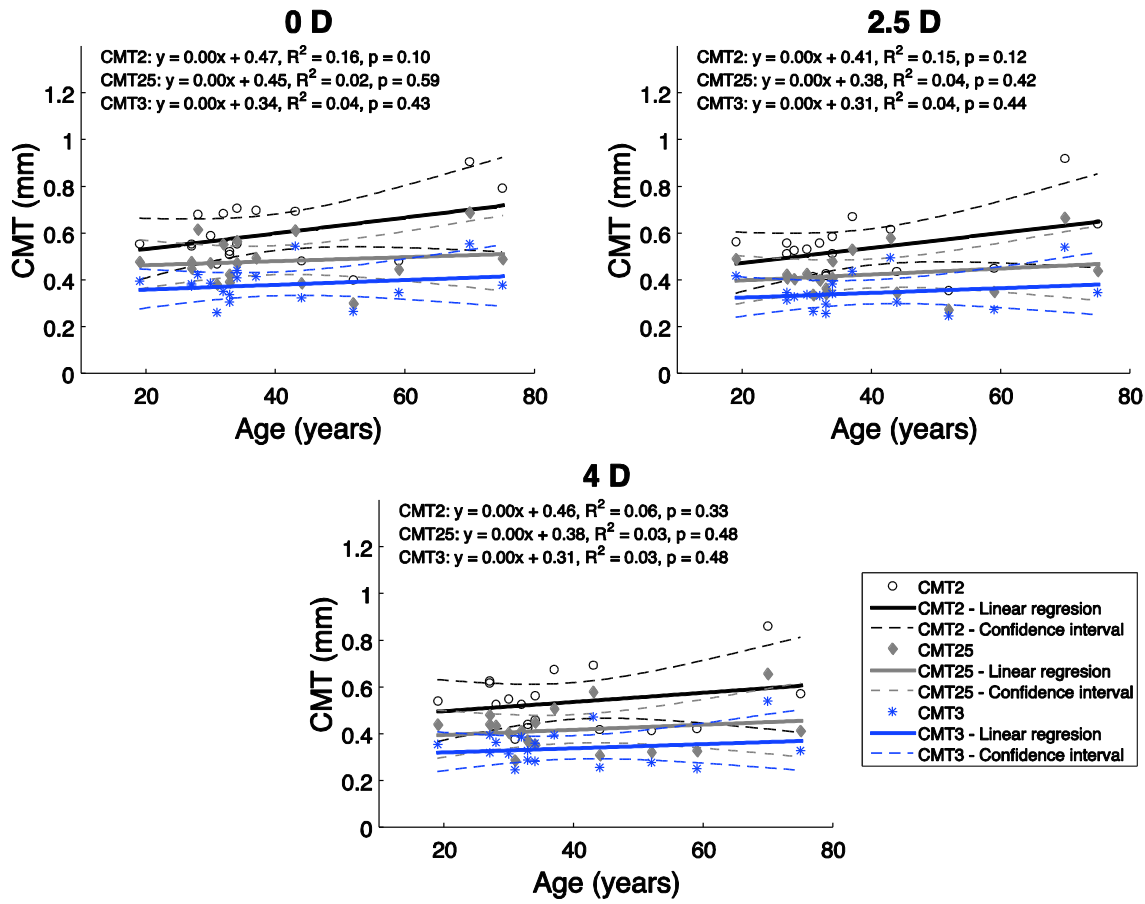


**Figure 3.5:** CMT relationship with age at the three different accommodative demands for a sample of 18 subjects. Dots, solid and dashed lines represent the CMT values, linear regression and confidence intervals for a 0.05 of significance level. Black colour corresponds to CMT2, grey to CMT25 and blue to CMT3. The linear equations for the three respective CMT linear regressions are also displayed on top of each graph.

Figure 3.6 shows the values of CMT2, CMT25 and CMT3 plotted against accommodation for all the 18 subjects who had valid measurements at every accommodative demand. Friedman test for repeated measures revealed that there was a statistically significant reduction in CMT depending on the accommodative demand  $a$ , for all CMT2, CMT25 and CMT3. In order to allow for multiple comparisons between accommodative states for the same CMT point, Wicoxon test was run. It revealed that statistical significance exists for all CMT2, CMT25 and



CMT3 when compared at unaccommodated state and both at 2.5 and 4 D but not when the ciliary muscle thickness at the three different points from the scleral spur was compared between the two accommodated states (2.5 and 4 D). These results are presented in Table 3.2.

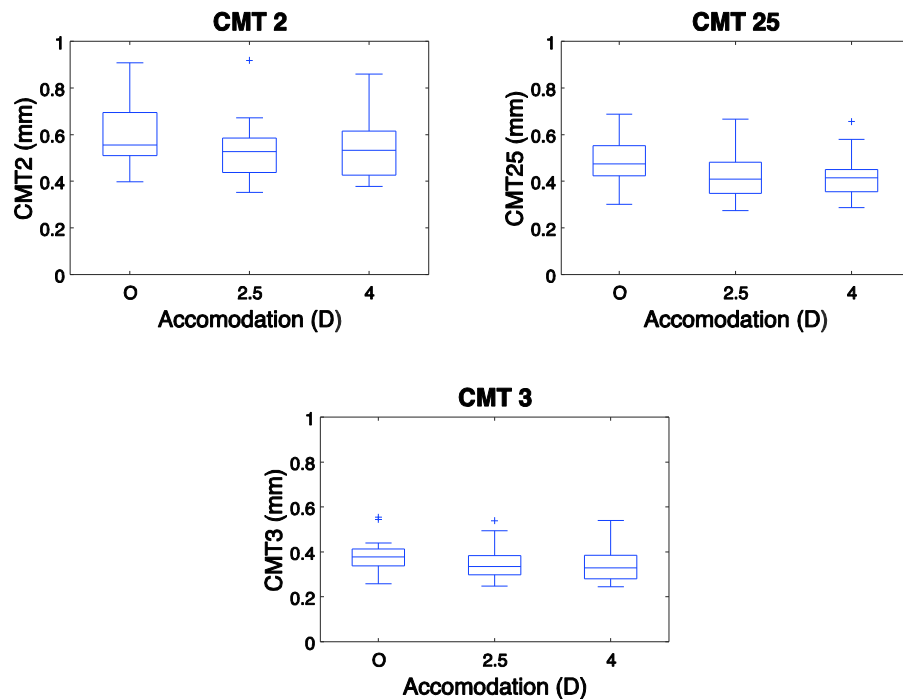
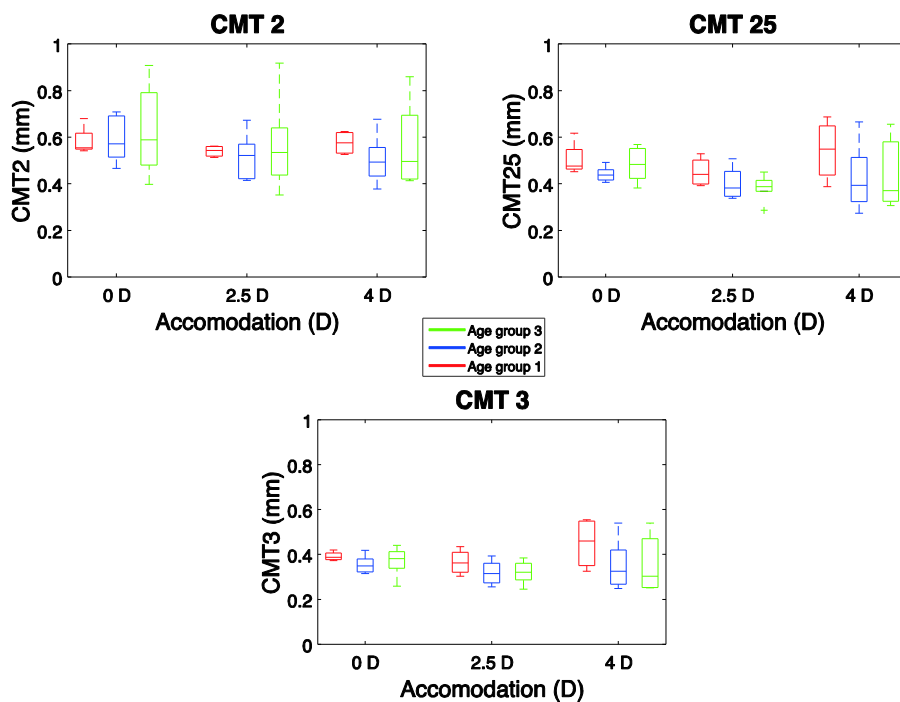


Figure 3.6: CMT at three different accommodative stimulus. Boxplots with medians (lines), 25 % to 75 % quartiles (boxes), ranges (whiskers) and outliers (+).

**Table 3.2:** Mean and standard deviation for CMT2, CMT25 and CMT3 at the different accommodative demands. P-value for Friedman and Wilcoxon tests for the different comparisons. Asterisks (\*) indicate statistically significant differences ( $p < 0.05$ ) in CMT with accommodation.

	CMT2			CMT25			CMT3		
	0 D	2.5 D	4 D	0 D	2.5 D	4 D	0 D	2.5 D	4 D
<b>Mean CMT (mm)</b>	0.60	0.54	0.54	0.48	0.43	0.42	0.38	0.35	0.34
	±	±	±	±	±	±	±	±	±
	0.13	0.13	0.12	0.10	0.10	0.09	0.08	0.08	0.08
<b>Friedman test</b>	<b>p-value</b>	0.02*		0.02*		0.01*			
<b>Multiple comparison test</b>	<b>0 Vs 2.5</b>	0.002*		0.001*		0.003*			
	<b>0 Vs 4</b>	0.012*		0.001*		0.005*			
	<b>2.5 Vs 4</b>	0.913		0.500		0.616			

When results were divided according to the subject's age group (Figure 3.7), Friedman test showed that CMT2 and CMT25 were significantly different ( $p < 0.05$ ) with accommodation in age group 2. Besides, CMT3 was significantly different ( $p < 0.05$ ) in age group 3 while no significant change in CMT with accommodation was observed for age group 1 in any of the points of the ciliary muscle measured. The older age group presented the biggest deviation of data at all the conditions measured. This can be due to the more heterogeneous nature of age group three as it included a wider age range of participants. This bigger deviation of data can also be seen in Table 3.3.



**Figure 3.7:** CMT for age groups 1 (red boxes), 2 (blue boxes) and 3 (green boxes) at three different accommodative stimulus. Boxplots with medians (lines), 25 % to 75 % quartiles (boxes), ranges (whiskers) and outliers (+).

As described in the methods section, CMT at 1 mm from the scleral spur (CMT1) was theoretically calculated. Mean CMT2, CMT25 and CMT3 and standard deviation

are plotted. A linear regression was fitted to them in order to obtain the ciliary muscle dimensions in the anterior part. These results are shown in Table 3.3 and Figure 3.8. Morphologically, the section of the ciliary muscle is thicker on the anterior part and it gets thinner the further away from the scleral spur. However, this thinning of the ciliary muscle depending on the distance from the scleral spur, is only statistically significant at 0 D for age group 2 and for age groups 1 and 2 when subjects were accommodating to a 2.5 D target. This is shown in the three graphs from Figure 3.8 where a slight reduction of the mean CMT can be seen with accommodation.

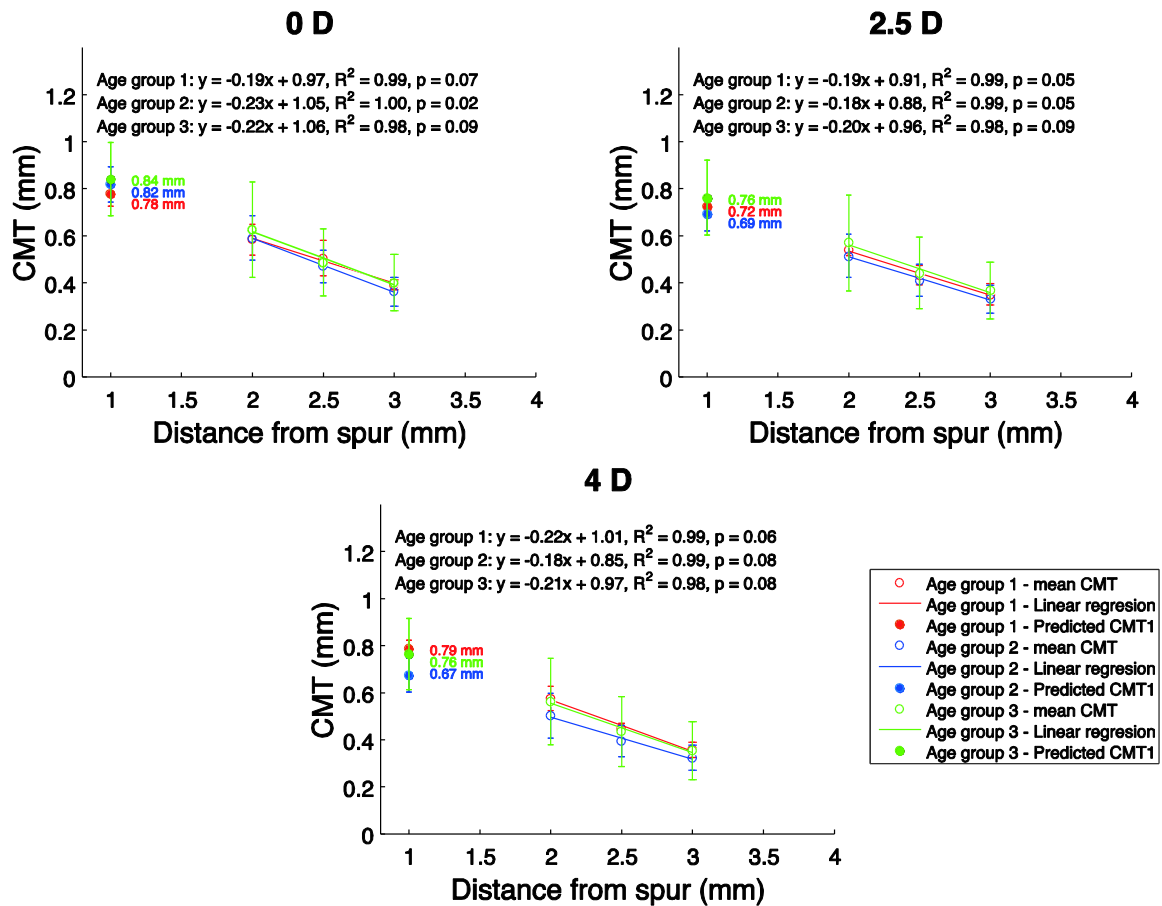


**Figure 3.8:** Mean CMT (open dots) and standard deviation for the 3 different points of the ciliary muscle at which thickness was measured and extrapolation of the mean CMT (solid dots) and standard deviation at 1 mm from the scleral spur. Data for the three age groups (red: age group 1, blue: age group 2 and green: age group 3) is shown. Solid lines represent the linear fit to the mean CMT data in each group. Linear equations and p-value for each of the regressions is displayed on top of each graph for the three age groups.

**Table 3.3:** Mean and standard deviation for CMT1, CMT2, CMT25 and CMT3 at the different accommodative demands and age groups. P-value for the linear relationship between the empirically obtained CMT and the distance it was measured at each accommodative demand presented, is also shown. Asterisks (\*) indicate statistically significant differences ( $p < 0.05$ ) in CMT.

Age group	0 D				2.5 D				4 D			
	CMT1	CMT2	CMT25	CMT3	CMT1	CMT2	CMT25	CMT3	CMT1	CMT2	CMT25	CMT3
<b>Mean</b>	0.78	0.58	0.51	0.39	0.72	0.54	0.43	0.35	0.79	0.58	0.45	0.36
<b>CMT</b>	±	±	±	±	±	±	±	±	±	±	±	±
<b>(mm)</b>	0.05	0.07	0.08	0.02	0.04	0.02	0.04	0.05	0.03	0.05	0.02	0.03
<b>p-value</b>			0.07				0.05*				0.06	
<b>Mean</b>	0.82	0.59	0.47	0.36	0.69	0.51	0.41	0.33	0.67	0.50	0.39	0.32
<b>CMT</b>	±	±	±	±	±	±	±	±	±	±	±	±
<b>(mm)</b>	0.07	0.09	0.07	0.06	0.07	0.09	0.07	0.06	0.07	0.10	0.07	0.05
<b>p-value</b>			0.02*				0.05*				0.08	
<b>Mean</b>	0.84	0.63	0.49	0.40	0.76	0.57	0.44	0.37	0.76	0.56	0.44	0.35
<b>CMT</b>	±	±	±	±	±	±	±	±	±	±	±	±
<b>(mm)</b>	0.16	0.20	0.14	0.12	0.16	0.20	0.15	0.12	0.15	0.18	0.15	0.12
<b>p-value</b>			0.09				0.09				0.08	

In order to investigate the relationship between CMT and accommodative response accuracy, the slope of the accommodative response function was plotted against the absolute value of CMT slope for each participant. In Figure 3.9, two subjects (from age group 3) out of the 18 included in the repeated measures sub-sample, were discarded from this data analysis as acquisition errors in their accommodative response slope measurements with the irx3 were encountered. Despite the fact that any of the linear regressions were statistically significant ( $p > 0.05$ ), age group 1 presented a negative slope for all the CMT measurements. Therefore, the more accurate the accommodation in age group 1, the lower the changes in ciliary muscle tend to be. In age group 2 and 3, the opposite effect is found where accommodative accuracy is accompanied by a larger change in CMT.

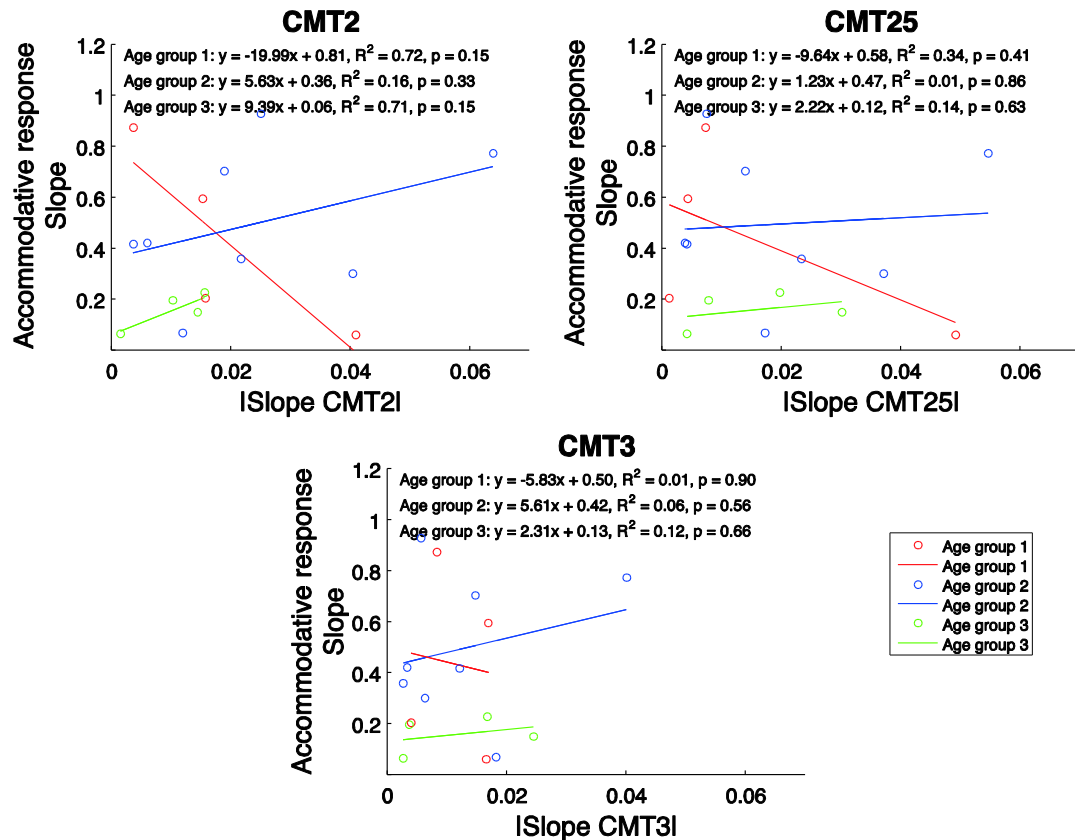


**Figure 3.9:** Accommodative response slope and absolute value of the CMT slope for the 3 different points of the ciliary muscle at which thickness was measured and age groups (red dots: age group 1, blue dots: age group 2 and green dots: age group 3). Solid lines represent the linear fit to the data in each group. Linear equations and p-value for each of the regressions is displayed on top of each graph for the three age groups.

### 3.5 DISCUSSION

Gaining a better understanding of the accommodative ability and the ageing effects is vital to improve the current methods of presbyopia correction and the level of vision care that can be provided.

This is (to our knowledge) the first study in which the accommodative response accuracy has been related to the ciliary muscle characteristics in an age diverse cohort including presbyopic subjects at least up to 70 years of age. While many

studies have related the accommodative response to the changes in the ciliary muscle, none of them has looked into the relationship between how accurate a person is accommodating and in consequence how much his or her ciliary muscle is changing. With this purpose, we assessed the slope of the accommodative response versus the slope of the ciliary muscle with accommodation. Our results suggested that subjects in age group 1 who are younger and therefore still have deformable crystalline lenses, do not need to produce that much change in the ciliary muscle to reach the right accommodative response. Also it is widely accepted that at the beginning of the accommodative response there is a lead of accommodation.<sup>28</sup> In spite of this part of the accommodative response being removed from our data, young people with bigger accommodation capacity may exhibit an over-accommodation that leads to a lesser change in the ciliary muscle in order to accurately accommodate. On the contrary subjects in age groups 2 and 3 needed a bigger change in ciliary muscle in order to reach the accommodative demand, which could be due to their stiffer lenses which are more difficult to mould. Shao et al.<sup>17</sup> found that the same amount of contraction of the ciliary muscle results in less lens reshaping in older compared to younger subjects.

A limitation in our study was the amount of lost data. The lack of optimal quality of the ciliary muscle images in the apex and the subsequent difficulty of segmenting that part of the apex reduced the amount of eligible data and made it more difficult to process. During image acquisition, centring and aligning of the eye was done following the standard procedure for measurements in which the patient was fixating inside the device. We, as previous authors did, asked the participant to



move the gaze and depending on the eyes' configuration in the face, the location of the ciliary muscle changes and small adjustments to the centration are necessary. This leads to a less homogenous set of images and thus the variety of conditions for which the image analysis software needs to be accurate is higher. We developed a software based on the popular algorithm used by Kao et al.<sup>24</sup> Our programme is capable of segmenting images of the ciliary muscle in different accommodative states in an almost automatic fashion. When it comes to the segmentation programmes, the validity of the OCT inbuilt software calipers to measure the thickness and the number of manually selected landmarks required has been questioned along with the index of refraction used for refractive correction of the images and the ciliary muscle zone to be measured.<sup>29</sup> The inbuilt software calipers do not fit the curved shape of the ciliary muscle and sclera but our software has overcome this problem by fitting the best degree 1 polynomials to the contour. However, we have not evaluated the repeatability. Laughton et al.<sup>25</sup> showed that with their not fully automated software, 60 % of the differences in thickness encountered were due to the manual selection of the ciliary muscle edges. It is likely that the repeatability is higher the less manually selected positions within the muscle are needed. We used two landmarks to increase the precision of the segmentation and an index of refraction of  $n = 1.56$ . Kao's et al.<sup>24</sup> and Laughton's et al.<sup>25</sup> softwares use an index of refraction of 1.38 for the ciliary muscle. If we had used this same index, our results might be more comparable between studies. However, we only used this parameter as a matter of conversion from the thickness in pixels to obtain the final CMT in millimeters. It would be ideal to be able to alter the AS-OCT interface so the examined eye can be properly aligned once the

subjects have turned their gaze. Also, more consensus about ciliary muscle dimensions would be gained if a totally examiner independent and robust enough software was designed in order to outline the ciliary muscle in any kind of AS-OCT image acquired. Therefore, robust image processing along with careful data acquisition are of importance in order to have good quality data that enables one to infer sound conclusions.

On the other hand and despite the fact that Sheppard and Davies<sup>18</sup> documented an increase in overall ciliary muscle length in longer eyes, the muscles were not significantly thicker at any of the proportional or fixed measures of the ciliary muscle. Hence, this is not likely to have affected our results. Because of the difference in refraction in our sample, the maximum difference in axial length between subjects would be 2.97 mm. Selecting the ciliary muscle points at a fixed distance from the scleral spur, would only represent a span in ciliary muscle overall length of approximately 0.6 mm, which is smaller than the measurement error<sup>18</sup> obtained when measuring the length of the temporal ciliary muscle ( $4.810 \pm 0.690$  mm).

- *Refractive range in our data set: [+1.58 D to -4.26 D]*
- *For an approximate power of the total emmetrope eye of 50 D and a mean index of refraction of the ocular media of 1.337:*

$$AL_1 = 1.337 / (50 - 1.58) = 27.61 \text{ mm}$$

$$AL_2 = 1.337 / (50 + 4.26) = 24.64 \text{ mm}$$

$$AL_1 - AL_2 = 2.97 \text{ mm difference in axial length}$$

- Linear equation from Sheppard and Davies<sup>18</sup> figure 4:

$$Y = 205.1 \times AL - 205.15$$

$$Y_1 = 205.1 \times 27.61 - 205.15 \rightarrow y_1 = 5457.661$$

$$Y_2 = 205.1 \times 24.64 - 205.15 \rightarrow y_2 = 4848.514$$

$$y_1 - y_2 = 609.14 \mu\text{m} = 0.6 \text{ mm of change in ciliary muscle overall length}$$

Our measurements taken at 2 mm and further posterior to the scleral spur of the temporal ciliary muscle, agree with Shao et al<sup>17</sup> who also found that the thickness of the ciliary muscle, in particular the maximum thickness, is age independent. On the contrary, Sheppard and Davies<sup>19</sup> found less homogeneous results in their data set. The temporal CMT only remained constant with age when measured at 2mm from the spur in myopes and at 25 % of the overall length in myopes and emmetropes. They show the linear correlation coefficient for ciliary muscle thickness and age which was below 0.5 in every case indicating a weak correlation.<sup>19</sup> Our data also showed statistically insignificant correlation between CMT and age (Figure 3.4). It is unlikely that this would be significant increasing the sample size as we showed data not only for the 18 subjects who had valid repeated measures of their ciliary muscle at the three different accommodative demands presented but also for the 49 patients that had usable data at any of the accommodative demands. In both case scenarios, the relationship between age and CMT was not statistically significant. Sheppard and Davis<sup>19</sup> also assessed the nasal ciliary muscle and found it to be invariant with age at all the ciliary muscle points measured as Richdale et al.<sup>15</sup>

did. When compared to the overall thickness any potential effect of ageing on the ciliary muscle seems of little clinical significance.

In general, the values we encountered for the disaccommodated ciliary muscle dimensions for the particular age group tested in each publication, are in agreement with those found by previous authors using AS-OCT imaging technology (Table 3.4).

**Table 3.4:** Comparison of CMT results at 3 different distances from the scleral spur (1, 2 and 3 mm) in disaccomadated state from previous publications with the results from the present study for the particular age group tested. The region of the ciliary muscle assessed in each publication is included: N (Nasal), T (Temporal).

<b>CMT</b>	<b>Reference</b>	<b>Region</b>	<b>Mean CMT <math>\pm</math> SD (mm)</b>	<b>Mean CMT <math>\pm</math> SD (mm) from the present study</b>
<b>CMT 1mm</b>	I. Lossing et al. <sup>14</sup>	T	Visit 1: $0.775 \pm 0.066$ / Visit 2: $0.775 \pm 0.066$	$0.82 \pm 0.07$ (Age group 2)
	II. Richdale et al. <sup>15</sup>	N	$0.80 \pm 0.10$	$0.82 \pm 0.07$ / $0.84 \pm 0.16$ (Age groups 2 & 3)
<b>CMT 2 mm</b>	I. Lossing et al. <sup>14</sup>	T	Visit 1: $0.558 \pm 0.081$ / Visit 2: $0.566 \pm 0.075$	$0.59 \pm 0.09$ (Age group 2)
	II. Richdale et al. <sup>15</sup>	N	$0.498 \pm 0.11$	$0.59 \pm 0.09$ / $0.63 \pm 0.20$ (Age groups 2 & 3)
	III. Sheppard & Davies <sup>18</sup>	T	$0.405 \pm 0.058$	$0.58 \pm 0.07$ (Age group 1)
<b>CMT 3 mm</b>	I. Lossing et al. <sup>14</sup>	T	Visit 1: $0.354 \pm 0.068$ / Visit 2: $0.354 \pm 0.065$	$0.36 \pm 0.06$ (Age group 2)
	II. Richdale et al. <sup>15</sup>	N	$0.27 \pm 0.08$	$0.36 \pm 0.06$ / $0.40 \pm 0.12$ (Age groups 2 & 3)

Some authors<sup>18</sup> showed slightly lower values but these differences can be attributed to the difference in refractive index used or ciliary muscle dimensions calculation which was not obtained by a semi-automatic software but with the calipers from the Visante AS-OCT inbuilt software. However, when compared with other authors that used a similar algorithm to detect the ciliary muscle boundaries, our results are in agreement<sup>14</sup> or within the standard deviation values<sup>15</sup> of the CMT measurements in the temporal part.

The literature on ciliary muscle changes with accommodation shows thickening of the anterior part of the ciliary muscle up to about 2 mm from the scleral spur. This thickening stretches the posterior part and a thinning is seen from 2 mm posterior to the spur.<sup>14, 15, 18</sup> This is in agreement with our results for the ciliary muscle measured at 2, 2.5 and 3 mm from the spur for 3 different accommodative demands. Although this is the general trend, when the sample is divided according to age we found no significant changes in the younger ciliary muscles with accommodation which matches the results of Sheppard and Davies<sup>18</sup> whose cohort included subjects from 19 to 34 years old. Their<sup>18</sup> results showed no significant change in the ciliary muscle measured at 50% or at 75% of the overall ciliary muscle length posterior to the scleral spur (approximately 2.4 mm and 3.6 mm respectively according to their mean overall length). However, when it comes to an older cohort like the ones in the studies of Richdale et al.<sup>15</sup> and Lossing et al.<sup>14</sup>, the significant changes in CMT2 and CMT3 we encountered in age groups 2 and 3 as well as the thickness values at 4D of accommodative stimulus are in agreement.

As previously mentioned, the Visante AS-OCT does not provide high definition around the inner apex of the ciliary muscle and images are non-uniform between participants, which makes difficult to accurately measure the muscle in that point for every subject. Therefore, the anterior CMT was calculated by extrapolating the data in the most posterior part. As shown in Table 3.4, our results match those from Richdale et al.<sup>15</sup> when measured at 1 mm from the scleral spur in the dissaccommodated ciliary muscle. The trend with accommodation (increase in thickness with accommodation) does not match, probably because other authors superimpose artificial shapes in the ciliary muscle apex so the segmentation is easier but due to the resolution it is still difficult to accurately select the edges and the high variability in results could lead to misestimations.

In summary, we investigated the ciliary muscle changes in thickness with accommodation and its relationship with the accommodative response accuracy. Our results support the Fincham's theory of presbyopia showing no age related changes in the ciliary muscle with age but with accommodation. Younger subjects exhibited a smaller ciliary muscle change with accommodation in relation with their accommodative response accuracy when compared with the two older groups of subjects. This means that the ciliary muscle might be more active in older than younger people but results will be different between different accommodative demands. Lots of individual variability has been found in our data. Thus, ideally ciliary muscle function with accommodation should be measured before implanting accommodating IOLs.

### 3.6 REFERENCES

1. United Nations. Department of Economic and Social Affairs, Population Division (2015). World Population Ageing 2015. (ST/ESA/SERA/390).
2. von Helmholtz H, Southall JP. Mechanism of accommodation. 1924.
3. Duane A. The accommodation and donders'curve and the need of revising our ideas regarding them: an experimental study. *JAMA* 1909;52:1992-1996.
4. Schachar RA. The mechanism of accommodation and presbyopia. *Int Ophthalmol Clin* 2006;46:39-61.
5. Fincham EF. The proportion of ciliary muscular force required for accommodation. *J Physiol* 1955;128:99-112.
6. Charman WN. Developments in the correction of presbyopia II: surgical approaches. *Ophthalmic Physiol Opt* 2014.
7. Charman WN. Developments in the correction of presbyopia I: spectacle and contact lenses. *Ophthalmic Physiol Opt* 2014;34:8-29.
8. Sheppard AL, Bashir A, Wolffsohn JS, Davies LN. Accommodating intraocular lenses: a review of design concepts, usage and assessment methods. *Clin Exp Optom* 2010;93:441-452.
9. Kasthurirangan S, Markwell EL, Atchison DA, Pope JM. MRI study of the changes in crystalline lens shape with accommodation and aging in humans. *J Vis* 2011;11.
10. Koretz JE, Strenk SA, Strenk LM, Semmlow JL. Scheimpflug and high-resolution magnetic resonance imaging of the anterior segment: a comparative study. *J Opt Soc Am A Opt Image Sci Vis* 2004;21:346-354.



11. Strenk. Magnetic resonance imaging of the anteroposterior position and thickness of the aging, accommodating, phakic, and pseudophakic ciliary muscle. *J Cataract Refract Surg* 2010;36:235-241.
12. Strenk SA, Semmlow JL, Strenk LM, Munoz P, Gronlund-Jacob J, DeMarco JK. Age-related changes in human ciliary muscle and lens: a magnetic resonance imaging study. *Invest Ophthalmol Vis Sci* 1999;40:1162-1169.
13. Strenk SA, Strenk LM, Guo S. Magnetic resonance imaging of aging, accommodating, phakic, and pseudophakic ciliary muscle diameters. *J Cataract Refract Surg* 2006;32:1792-1798.
14. Lossing LA, Sinnott LT, Kao CY, Richdale K, Bailey MD. Measuring changes in ciliary muscle thickness with accommodation in young adults. *Optom Vis Sci* 2012;89:719-726.
15. Richdale K, Sinnott LT, Bullimore MA, et al. Quantification of age-related and per diopter accommodative changes of the lens and ciliary muscle in the emmetropic human eye. *Invest Ophthalmol Vis Sci* 2013;54:1095-1105.
16. Schultz KE, Sinnott LT, Mutti DO, Bailey MD. Accommodative fluctuations, lens tension, and ciliary body thickness in children. *Optom Vis Sci* 2009;86:677-684.
17. Shao Y, Tao A, Jiang H, et al. Age-related changes in the anterior segment biometry during accommodation. *Invest Ophthalmol Vis Sci* 2015;56:3522-3530.
18. Sheppard AL, Davies LN. In vivo analysis of ciliary muscle morphologic changes with accommodation and axial ametropia. *Invest Ophthalmol Vis Sci* 2010;51:6882-6889.
19. Sheppard AL, Davies LN. The effect of ageing on in vivo human ciliary muscle morphology and contractility. *Invest Ophthalmol Vis Sci* 2011;52:1809-1816.

20. Duane A. Studies in Monocular and Binocular Accommodation, with Their Clinical Application. *Trans Am Ophthalmol Soc* 1922;20:132-157.
21. Lewis HA, Kao CY, Sinnott LT, Bailey MD. Changes in ciliary muscle thickness during accommodation in children. *Optom Vis Sci* 2012;89:727-737.
22. Ruggeri M, de Freitas C, Williams S, et al. Quantification of the ciliary muscle and crystalline lens interaction during accommodation with synchronous OCT imaging. *Biomed Opt Express* 2016;7:1351-1364.
23. Shao Y, Tao A, Jiang H, et al. Simultaneous real-time imaging of the ocular anterior segment including the ciliary muscle during accommodation. *Biomed Opt Express* 2013;4:466-480.
24. Kao CY, Richdale K, Sinnott LT, Grillott LE, Bailey MD. Semiautomatic extraction algorithm for images of the ciliary muscle. *Optom Vis Sci* 2011;88:275-289.
25. Laughton DS, Coldrick BJ, Sheppard AL, Davies LN. A program to analyse optical coherence tomography images of the ciliary muscle. *Cont Lens Anterior Eye* 2015;38:402-408.
26. Thibos LN, Hong X, Bradley A, Applegate RA. Accuracy and precision of objective refraction from wavefront aberrations. *J Vis* 2004;4:329-351.
27. Li C, Xu C, Gui C, Fox MD. Distance regularized level set evolution and its application to image segmentation. *IEEE Trans Image Process* 2010;19:3243-3254.
28. Morgan Jr MW. Accommodation and its relationship to convergence. *Optom Vis Sci* 1944;21:183-195.
29. Bailey MD. How should we measure the ciliary muscle? *Invest Ophthalmol Vis Sci* 2011;52:1817-1818.

## **4 CHANGES IN ACCOMMODATIVE FLUCTUATIONS WITH AGE AND MULTIFOCAL CONTACT LENSES**

### **CONTRIBUTIONS**

The study was designed by me and my supervisor, Hema Radhakrishnan and we obtained ethics approval for the study. The participants' recruitment and data collection was done by me and I analysed the data using a MATLAB code that I wrote. I also wrote the manuscript which was revised and finalised with the support of my supervisor.

### **PUBLISHING OF THE PAPER**

Authors for this study are Irene Siso-Fuertes and Hema Radhakrishnan. This paper will be submitted with the title: "Changes in accommodative fluctuations with age and multifocal contact lenses". Target journal: *Optometry and Vision Science (OVS)*. To be submitted.

### **PRESENTATION AT CONFERENCE**

Part of the results from this study were presented in the form of a poster at:

Siso-Fuertes, I. & Radhakrishnan. 2016. Effects of different multifocal contact lenses on accommodation and ocular aberrations. *Proceedings of Association for Research in Vision and Ophthalmology (ARVO) Annual Meeting, 2016, E-abstract.*

## **4.1 ABSTRACT**

**PURPOSE:** To study the changes in accommodative and disaccommodative microfluctuations with age, including presbyopic individuals, and with multifocal contact lenses (MFCLs) fitted in young subjects.

**METHODS:** 61 subjects in an age range of 18 to 70 years were recruited and accommodative responses measured with a Hartmann-Shack Wavefront Aberrometer. Static accommodation measurements were taken by presenting fixed stimuli from 0 D to 4 D of accommodation in 0.50 D steps and the slope of the response calculated. Dynamic accommodative and disaccommodative responses were continuously measured at approximately 12 Hz while subjects changed their focus from distance to two stimuli (2.5 D and 4 D) and back to a non-accommodating state.. Accommodative and disaccommodative amplitude, time constants and the magnitude of paraxial equivalent refraction (M), higher order aberrations (HOAs) and spherical aberration (SA) fluctuations (RMS deviation) were calculated from the sustained accommodation states of the dynamic measurement. Results were compared by age group, stimulus magnitude or part of the accommodative response.

A sub-sample of 32 young subjects (18 to 29 years) was fitted with two different MFCLs (PureVision 2 For Presbyopia (centre-near design) and Proclear Multifocal (centre-distance design)). Static and dynamic accommodation was measured with the MFCLs.

**RESULTS:** Age had a significant effect on amplitude of accommodation and disaccommodation. A significant difference ( $p = 0.03$ ) in the magnitude of accommodative fluctuations (paraxial M RMS deviation) between age groups was found for the 2.5 D stimulus, with subjects in the third decade of life having the largest fluctuations. No significant difference between age groups was found during accommodation either in HOA and SA RMS deviation or in time constants. The correlation between the slope of the accommodative response and either the magnitude of the fluctuations during accommodation or the accommodative time

constants was not statistically significant for any of the age groups or accommodative stimuli.

When young participants were fitted with the two MFCLs and compared with the naked eye situation, no significant ( $p > 0.05$ ) differences between conditions were found in paraxial M RMS deviation or accommodative time constants. Significant differences ( $p = 0.02$ ) in disaccommodative time constants were found with the 2.5 D stimulus.

**CONCLUSION:** Age-related changes are found in both static and dynamic accommodation. Accommodative fluctuations increase in the third decade of life. The relationship between the magnitude of fluctuations and possible blur tolerance suggests that fluctuations in accommodation may play a role in controlling the accommodation system. Accommodation performance is not altered in young individuals fitted with MFCLs.

## **4.2 INTRODUCTION**

Due to the dynamic nature of accommodation, fluctuations in the dioptric power of the eye happen in short time intervals and are known as microfluctuations. Microfluctuations are often analysed in the time domain by obtaining the overall root mean square (RMS) value or in the frequency domain (by doing their Fourier transform). According to this last analysis, the spectrum of microfluctuations is divided into two components: low (LFC; at  $< 0.5$  Hz) and high (HFC; at  $>0.5 - 2$  Hz).<sup>1,2</sup>

Microfluctuations in accommodation were first studied by Collins.<sup>3</sup> Since these early reports several studies pointed to a theory that microfluctuations might act as a fine-tuning system that controls accommodation and helps optimising the accommodative performance. Such role has traditionally been attributed to the LFC which most authors agree to be under neurological control and related to stimulus characteristics and respiration frequency.<sup>1, 2, 4-7</sup> A recent article showed similar findings and considers that microfluctuations could be used to determine accommodation direction.<sup>8</sup> On the other hand HFC have been proved to be part of the “noise” of the accommodative system itself as they are mainly generated by the pulse.<sup>2, 6, 9</sup> The pulse and cardiopulmonary system have been claimed to be the cause of the microfluctuations in aberrations that shows a high correlation when the mechanical rhythms affecting the crystalline lens and the choroid are in phase<sup>9,10</sup>

It is of importance to further investigate the fluctuations in the optics of the human eye during steady-state viewing as they have an impact on the visual performance.

They also affect the measurement of refraction (i.e. the temporal variations in accommodation might affect the reliability of measurements of refraction) as well as the development of more accurate techniques to measure aberrations, more realistic eye models or any simulations using adaptive optics. Microfluctuations have been studied extensively in young subjects but since the world population is ageing and the proportion of people over 60 will increase considerably by 2050<sup>11</sup>, it is important to understand how microfluctuations change in the older age groups. Microfluctuations in accommodation and higher order aberrations (HOAs) have thus far only been assessed in participants under the age of 50 years.<sup>12</sup> Most of the changes in the microfluctuations are likely to appear after the onset of presbyopia (over 50 years of age) as a change in other optical parameters such as aberrations have been reported in this age group which will result in an increased depth of focus (DoF).<sup>13</sup> Microfluctuations are believed to be related to the DoF of the eye.<sup>14</sup> Altering DoF is being investigated as a potential method of correcting presbyopia. One of the latest trends in intraocular lenses (IOLs) design is to create an extended DoF implant. The increased DoF with age is due to changes such as a peripheral abrupt decline in refractive index of the lens and/or an increase in the size of the central refractive index region within the crystalline lens.<sup>15, 16</sup> These factors will also influence the accommodation dynamics making it important to understand the fluctuations in accommodation in the presbyopic population.

Most patients seeking contact lens correction for presbyopia are fitted with simultaneous vision multifocal contact lenses (MFCLs). According to an international survey 29 % of the presbyopic CL users are fitted with MFCLs.<sup>17</sup> For

this reason the question whether the low percentage (29 %) of success of these lenses is due to the necessity of remaining accommodative ability for a correct performance, arises. Over the last few years, in addition to presbyopia correction, simultaneous vision MFCLs have also been used for other purposes such as myopia control.<sup>18</sup> The simultaneous vision MFCLs are likely to interact with the accommodative fluctuations and alter the dynamic visual quality. Hence, it is important to understand how the MFCLs influence the accommodative fluctuations of the eye. Madrid-Costa et al.<sup>19</sup> evaluated the dynamics of accommodation during MFCL wear, in terms of the accommodative response and its peak velocity and time constant. This was done in a small sample of 10 subjects, without assessing the disaccommodative dynamics. The current study investigates the MFCLs performance at different viewing distances in young people who are able to accommodate.

There are a scarce number of publications that look into the implication of age on accommodative fluctuations but in most of the studies a general reduction in both frequency components of the accommodative fluctuations with age has been reported.<sup>1, 12, 20-22</sup> Heron and Schor<sup>22</sup>, found no significant differences between old and young subjects when their average accommodative response was between 1 and 1.50 D and Toshida et al.<sup>1</sup> only assessed the influence of age in the HFC of the fluctuations. Others like Candy and Bharadwaj<sup>21</sup> and Anderson et al.<sup>20</sup> quantified the fluctuations by the RMS deviation finding a reduction in adults with respect to new-borns (up to 30 weeks) and an increase in fluctuations in the 3<sup>rd</sup> decade of life. The differences between these studies reported in the literature can often be



attributed to the differences in techniques, conditions and metrics used for analysing the changes in microfluctuations with age. Substantial intersubject differences<sup>6</sup> also make comparisons difficult between studies. All these studies describe the changes in microfluctuations with age in a largely pre-presbyopic population. To our knowledge, this is the first experimental study aimed at understanding the changes in microfluctuations with age by extending the age range to 70 years. This will give us further insights into the stability of accommodation measured both during accommodation and disaccommodation states in the presbyopic population in comparison to the pre-presbyopic individuals. The second part of this study aims to assess the accommodative and disaccommodative performance in both static and dynamic conditions with MFCLs. This is intended to provide extended knowledge on quality of vision through two different designs of MFCLs and in consequence, the accommodation and its fluctuations when wearing them.

## **4.3 METHODS**

### **4.3.1 Experiment 1: Age-related changes in accommodation**

#### **4.3.1.1 Subjects**

A power analysis was performed using previous data from Radhakrishnan et al.<sup>13</sup> for a power of 80% and a significance level of 0.05. According to the results from this analysis, the recruitment target was 27 subjects distributed within three

different age groups. Finally, 61 subjects in an age range of 18 to 70 years were recruited and divided into the three different age groups. Age group 1 included 32 participants from 18 to 29 years with a mean age of  $22.7 \pm 3.2$  years and a mean equivalent refraction (M) of  $-1.61 \pm 1.77$  D. Age group 2 consisted of 13 subjects between 30 to 39 years with a mean age of  $33.3 \pm 2.4$  years and a mean M of  $-1.39 \pm 1.70$  D. Age group 3 comprised 11 people of 40 years and over with a mean age of  $53.7 \pm 10$  years and a mean M of  $-0.80 \pm 1.99$  D. Habitual correction with astigmatism higher than 1.25 D, any history of ocular or systemic pathology, surgery, or using any topical or systemic medication that could affect accommodation was considered as exclusion criteria. This study followed the tenets of the Declaration of Helsinki and was approved by the Research Ethics Committee of the University of Manchester. Informed consent was obtained from all participants after the nature and possible consequences of the study were explained.

#### **4.3.1.2 Protocol**

Distance and near visual acuity (VA) were measured for all participants wearing their habitual correction for distance. Secondly, objective measurements of refraction were taken using the irx3 Wavefront Aberrometer (Imagine-Eyes, Orsay, France). The irx3 is a Hartmann-Shack based aberrometer that also provides a spherical equivalent which is the spherical error that best matches the measured wavefront error. Based on the spherical equivalent results, the refractive error of each subject was corrected by using the Badal system incorporated in the device.

Subsequently, static and dynamic accommodative responses were measured. For both, static and dynamic accommodative response measurements, pupil size, stimulus, time and Zernike coefficients up to the 6<sup>th</sup> order were available for every measurement point taken. Paraxial M was calculated from the pupil size, defocus (Z(2,0)) and spherical aberration (Z(4,0)) terms from each data point using the paraxial curvature matching formula proposed by Thibos et al.<sup>23</sup> This has been shown to be the most accurate way of predicting subjective refraction.<sup>23</sup>

Measurements were only taken from the left eye of all participants who were instructed to fixate the internal target in the aberrometer, the Snellen E, while their right eye was covered with a patch. Once the participants were positioned in the chin and headrest, the pupil was centered and aligned following the recommendations of the manufacturer. The instructions given to every subject were: "Please, keep the letter E as clear as possible all the time and blink whenever you want but please keep your head still".

#### **4.3.1.3 Static accommodative response measurements**

Static accommodation measurements were taken using the accommodation setting in the irx3 where the internal target moves at 0.50 D steps and the starting point was set to be each participant's spherical equivalent refraction. In this study nine fixed stimulus measurements were taken, this is, from 0 D to 4 D of accommodation in 0.50 D steps. Four repetitions were made for each participant and centration and alignment were corrected during the measurements when required.

The first three refraction measurements (at 0, 0.50 and 1 D stimulus) from the static

accommodative measurements were discarded as they include the subject's tonic accommodation. Subsequently, MATLAB (MathWorks, Natic, MA) was used to obtain the slope of the linear fit to the data corresponding to the paraxial M encountered from when a 1.5 D accommodative stimulus was presented up to the 4 D stimulus.

#### **4.3.1.4 Dynamic accommodative response measurements**

The dynamic measurements were obtained using a custom program developed for the irx3 by the manufacturer. The accommodative stimulus was altered by using the internal Badal system in the irx3 to present a distance target for approximately 10 seconds which was then changed to an accommodative target (either 2.5 or 4 D presented in a randomised order) for the next 10 seconds approximately. Following this, the target was once again changed to a distance target for around 10 seconds to assess the disaccommodation state of the eye. In total measurements were obtained over 30 seconds of duration and frequency of approximately 12 Hz. The measurements of the accommodative stimulus curve followed a "Battlement-like" (Figure 4.1, it looks like the footprint of a castle) pattern. In this curve, the first flat part would show the dynamic refraction changes under a relaxed accommodative state following which the next stimulus stage represents the dynamics of accommodative state and the final recovery phase shows the dynamics of disaccommodation. The starting point for dynamic measurements was set as the spherical equivalent of each participant. Due to the software characteristics, the duration and nature of the pattern were not exactly the same for every measurement as this depended on various characteristics such as blinks. The points

in which blinks were detected were automatically deleted and three dynamic accommodative response measurements were performed per participant and accommodative demand.

A custom MATLAB code was developed in order to automatically read and process the dynamic accommodative response measurements (see Appendix). Figure 4.1 shows an example which is representative of the data for dynamic accommodation measurements.

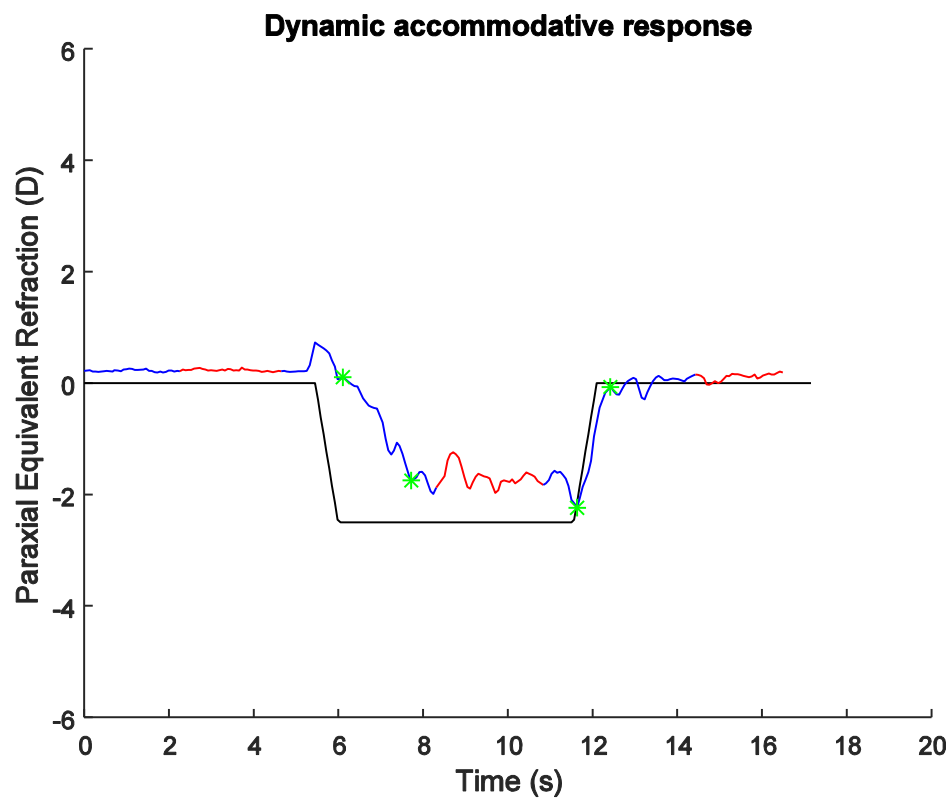


**Figure 4.1:** Example of dynamic accommodative response measurement when a 2.5 D stimulus was presented to a young subject (age group 1). Red lines in the graph are the portions of sustained accommodative response. Green asterisks delimitate the transition zones between accommodative states.

The accommodative fluctuations analysed in this study were calculated from three different intervals of sustained accommodative response (red lines in Figure 4.1) within the three parts of the measurement (relaxed accommodation, accommodation and recovery). In every case, these intervals were delimited starting at the 31<sup>st</sup> point after the stimulus was presented or switched, to 10 measurement points before the stimulus was switched again. A transition section (blue lines between asterisks in Figure 4.1) was also delimited for accommodation and disaccommodation. Following a similar approach to the one used by Kasthurirangan et al.<sup>24</sup>, the accommodative transition section starts in the fourth consecutive point of change after the stimulus was switched, in which the paraxial M was decreasing. The end of the accommodative transition section was set in the first point of four consecutive increasing paraxial M points. The same criteria but for decreasing paraxial M points was used to define the disaccommodative transition section i.e, disaccommodation started at the fourth consecutive increasing paraxial M point after the stimulus was switched and ended in the first point of four consecutive decreasing paraxial M points.

The dynamic accommodative response measurements were found to be highly variable within the three repetitions for the majority of the 61 participants included in the study. The differences could be attributed to the inconsistencies in measurements which depended on the blink responses of the participants. The changes in tear film between blinks led to significant changes in the aberration profile of the eye<sup>25</sup> and therefore it was decided to allow participants to blink normally during the dynamic measurements. To ensure that the data was

consistent, visual inspection of every measurement was performed in order to discard any spurious data. Individual data was included in the analysis only if: an accommodative effort could be seen, peaks in the response were not higher than half the amplitude of the accommodative response, the transition zone was correctly delimited and no points from it were included in the sustained accommodative response portions. These criteria led to a large amount of excluded data.

For the data that was included, the following parameters were calculated:

*Accommodative and Disaccommodative amplitude*

Accommodative amplitude was obtained from the difference between the mean paraxial M during the sustained accommodation and relaxed accommodation states. Similarly, disaccommodative amplitude was calculated from the difference in diopters between the sustained accommodation and recovery states.

*RMS deviation*

To quantify the magnitude of the amplitude of fluctuations in accommodation and aberrations during the sustained responses, the approach proposed by Anderson et al.<sup>20</sup> was followed to calculate the RMS deviation:

$$RMSdeviation = \sqrt{\frac{1}{n} \sum_{i=1}^n (x_i - \bar{x})^2}$$

**Equation 4.1:** RMS deviation, where  $n$  is the number of values,  $x_i$  is each individual value and  $\bar{x}$  is the mean value.

We used this time-domain analysis in order to quantify the microfluctuations in paraxial M, HOAs (up to the 4th order) and spherical aberration (Z(4,0)).

### Time Constants

Time constant values represent the time taken to achieve 63% of the response. Amplitude data was used to calculate the response levels when 10% and 90% of the accommodative response amplitude was reached within the transition sections previously delimited. These were the cut off points for which the corresponding times ( $t_{10}$  and  $t_{90}$ ) with the response levels were taken.  $t_{10}$  and  $t_{90}$  were then used to obtain the time constant ( $\tau$ ) for accommodation as well as for disaccommodation applying the following equation<sup>26</sup>:

$$\tau = \frac{t_{90} - t_{10}}{\ln 9}$$

**Equation 4.2:** Time constant calculation.  $t_{10}$  and  $t_{90}$  are the times in seconds at which the accommodative response was 10% and 90% of the accommodative amplitude, respectively. The difference is divided by the natural logarithm of 9 in order to obtain the time constant ( $\tau$ ) in seconds.

### **4.3.2 Experiment 2: Accommodation through MFCLs**

The same 32 subjects from Age group 1 (18 to 29 years) that participated in Experiment 1, were recruited to participate in this Experiment 2. The mean age and mean spherical equivalent refraction of the sample were  $22.7 \pm 3.2$  years and  $-1.61 \pm 1.77$  D, respectively.

Objective measurements of refraction were taken from the left eye of all participants using the aberrometer. The refractive error of each subject was



corrected by means of two different MFCLs whose distance power would match each participant's spherical equivalent provided by the aberrometer.

#### **4.3.2.1 Contact lenses**

In this study the MFCLs chosen to be fitted in randomised order were: PureVision 2 for Presbyopia (Bausch & Lomb, Rochester, NY, USA) and Proclear Multifocal (Cooper Vision, Fairport, NY, USA). The PureVision2 for Presbyopia has an aspheric multifocal, centre-near design within the 14.00 mm of diameter and is available in "Low" and "High" addition. In this study the "High" addition version was used which delivers an effective addition power of 1.54 D<sup>27</sup> with a smooth transition towards the distance power.

The Proclear Multifocal fitted in this study had a simultaneous vision multifocal, centre-distance design with 2.00 D of addition. The powers are distributed across the 14.4 mm diameter with the most minus distance power allocated in the central 4.6 mm of the contact lens.<sup>28</sup> This MFCL has previously been used for myopia control studies.<sup>29-31</sup> The fit of each lens was made in successive random order and assessed after allowing at least 5 minutes for the lens to settle. Distance and near VA as well as static and dynamic accommodative response were measured for all participants with both types of MFCLs.

#### **4.3.2.2 Static and dynamic accommodative response measurements**

Static and dynamic accommodative responses were measured following almost the same protocol and identical individual data eligibility criteria and analysis as in Experiment 1. The only difference in taking the measurements was that the starting

point either for the static or dynamic approach, was set to 0 D as each participant's refractive error was corrected by the MFCL.

### **4.3.3 Statistics**

The Statistics and Machine Learning Toolbox™ included in MATLAB was used to implement Kolmogorov-Smirnov test to determine whether the data was normally distributed. Subsequently, non-parametric test were applied for parameters that were not normally distributed. In order to check the individual effects of age, stimulus (2.5 D or 4 D) or part of the accommodative response (relaxed accommodation, accommodation and recovery) in the different dependent variables assessed in this study (accommodative and disaccommodative amplitude, time constants and RMS deviation of the paraxial M, HOAs and spherical aberration(SA)), Kuskal – Wallis Test available in the toolbox was used. All statistical test were performed for a significance level of 0.05.

## **4.4 RESULTS**

### **4.4.1 Experiment 1**

After visual inspection of the dynamic accommodative response measurements analysed with our algorithm, a total of 76 measurements were considered as usable data which resulted in 53 measurements once averaged per subject and these were taken into account for data analysis.

Exact number, distribution and demographics of the subjects included in this experiment are shown in Table 4.1. Age group 1 comprised 22 subjects with a mean age of  $22.2 \pm 3.3$  and a mean spherical equivalent of  $-1.2 \pm 1.8$  D. Age group 2 consisted of 10 participants with a mean age of  $32.8 \pm 2.1$  and a mean spherical equivalent of  $-1.2 \pm 1.6$  D. Finally, age group 3 included 8 participants with a mean age of  $56.9 \pm 10.8$  years and a mean spherical equivalent of  $-1.7 \pm 1.9$  D. The reduction in sample size due to the high variability of results and inconsistencies in measurements resulted in a confidence level of the sample of no more than 40 %.

All the included subjects reached a distance visual acuity of 0.0 logMAR or better with their habitual correction. Similarly, wearing their habitual distance correction, all subjects from age groups 1 and 2 and 50 % of the subjects in age group 3 reached a near VA of N5 or better. The remaining 50 % of subjects in age group 3 was divided into the 25 % of participants reaching a distance corrected near visual acuity (DCNVA) of 8N and the other 25 % a DCNVA of 10N.

**Table 4.1:** Number, distribution and demographics of subjects and continuous accommodative response measurements included in the study.

	Age group 1		Age group 2		Age group 3	
<b>No total of subjects</b>	22		10		8	
<b>Mean age ± SD (years)</b>	22.2 ± 3.3		32.8 ± 2.1		56.9 ± 10.8	
<b>Age range (years)</b>	18 to 29		30 to 37		41 to 70	
<b>Spherical equivalent, M (D)</b>	-1.2 ± 1.8		-1.2 ± 1.6		-1.7 ± 1.9	
<b>% of myopes (M&lt;-0.50 D) within the age group</b>	40.9		70.0		62.5	
<b>Distribution of subjects according to the data included in the study</b>						
<b>Accommodative stimulus presented (D)</b>	<b>2.5</b>	<b>4</b>	<b>2.5</b>	<b>4</b>	<b>2.5</b>	<b>4</b>
No of subjects for each accommodative demand	18	12	5	8	5	5
No of subjects included in both accommodative demands	8		3		2	
No of total measurements that were later averaged per subject	25	17	9	13	7	5

The dynamic accommodation metrics used in this study were calculated for an average interval of  $2.18 \pm 0.17$  seconds of sustained accommodative response. The dynamic data for approximately  $2.32 \pm 0.07$  seconds on average at the start of each dynamic state (i.e. after the stimulus was switched) was discarded from analysis to ensure only the sustained response was included. Figure 4.2 shows the accommodative amplitude for the 3 different age groups when the 2.5 D and 4 D stimuli were presented. Kruskal Wallis test showed that age had a significant effect on amplitude of accommodation ( $p < 0.002$ ) and disaccommodation ( $p < 0.02$ ). The magnitude of stimulus only had a significant effect in amplitude of accommodation ( $p = 0.001$ ) and disaccommodation ( $p = 0.006$ ) in age group 1.

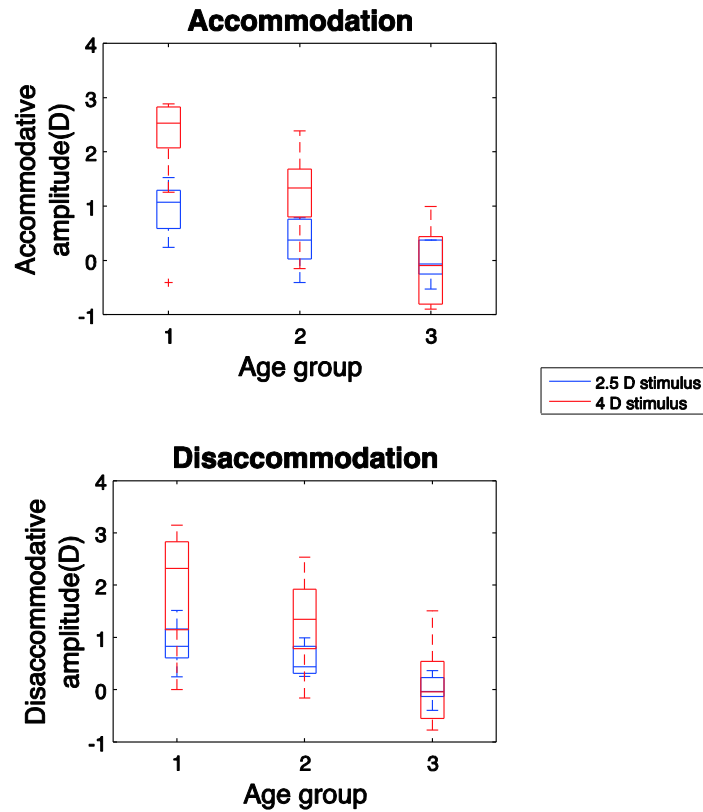


**Figure 4.2:** Accommodative and disaccommodative amplitude for the 3 age groups and two different accommodative stimuli (blue boxplots: 2.5 D and red boxplots: 4 D). Boxplots with medians (lines), 25 % to 75 % quartiles (boxes), ranges (whiskers) and outliers (+).

Figure 4.3 shows RMS deviation calculated for the paraxial M for the three different age groups. The first stimulus level (0 D) in Figure 4.3 refers to the initial resting state, the second stimulus level (2.5 or 4 D) refers to the fully accommodated state and the final stimulus (0 D on the right hand side of the graph) represents the disaccommodated state. A rise in the magnitude of fluctuations can be seen with accommodation for both levels of accommodative demand. Kruskal-Wallis test showed a significant difference in the RMS deviation for accommodation ( $p = 0.03$ ) between age groups for a 2.5 D stimulus. This difference was not evident for the 4 D stimulus ( $p = 0.63$ ) There were no significant differences in the relaxed and

dissaccommodated state between the three age groups for both 2.5 and 4 D stimulus levels.

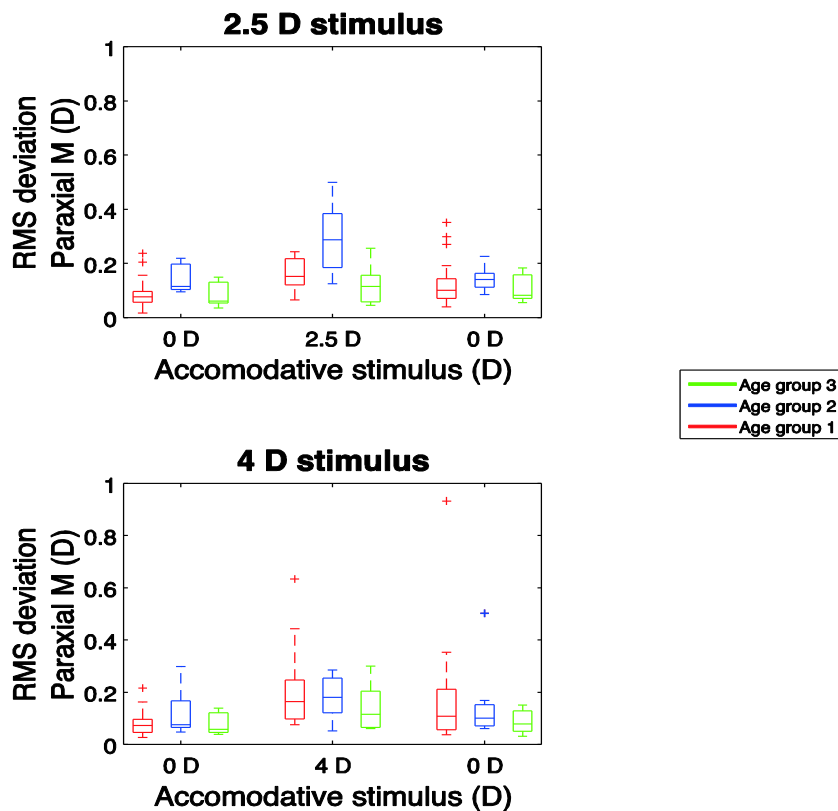


**Figure 4.3:** RMS deviation of the paraxial M for the 3 age groups (red boxplots: age group 1, blue boxplots: age group 2 and green boxplots: age group 3) and two different accommodative stimulus. Boxplots with medians (lines), 25 % to 75 % quartiles (boxes), ranges (whiskers) and outliers (+).

A statistically significant difference was found in the magnitude of fluctuations between relaxed, accommodated and disaccommodated states in age group 1 for both stimulus demands ( $p = 0.005$  for 2.5D;  $p = 0.02$  for 4D). A clinically but not statistically significant difference can also be seen in age group 2 between the relaxed, accommodated and disaccommodated states when a 2.5 D stimulus ( $p = 0.084$ ) was presented but not for the 4D stimulus ( $p = 0.28$ ). No significant differences were found in the relaxed, accommodated and disaccommodated states for age group 3 at both stimulus levels ( $p > 0.05$ ). No significant difference in

RMS deviation was found in the accommodated and disaccommodated state between the two stimulus demands (2.5 D and 4 D) for all three age groups ( $p>0.05$ ). However, it can be noticed that in age group 2 higher magnitude of fluctuations is evident for the 2.5 D stimulus when compared to the 4 D stimulus. This age group would have been able to accommodate to the 2.5D stimulus but not so well for the 4D stimulus and therefore demonstrates lower fluctuations at this higher stimulus level. In contrast, the median RMS deviation while accommodating to a 4D stimulus in age groups 1 and 2 is very similar although age group 1 shows higher dispersion of the data.

The HOAs up to 4<sup>th</sup> order and fourth order SA for all three dynamic accommodation states (Figure 4.4) showed no statistically significant difference between age groups or accommodative stimulus level. The effect of age was only statistically significant in the recovery state when the 2.5 D stimulus was presented.

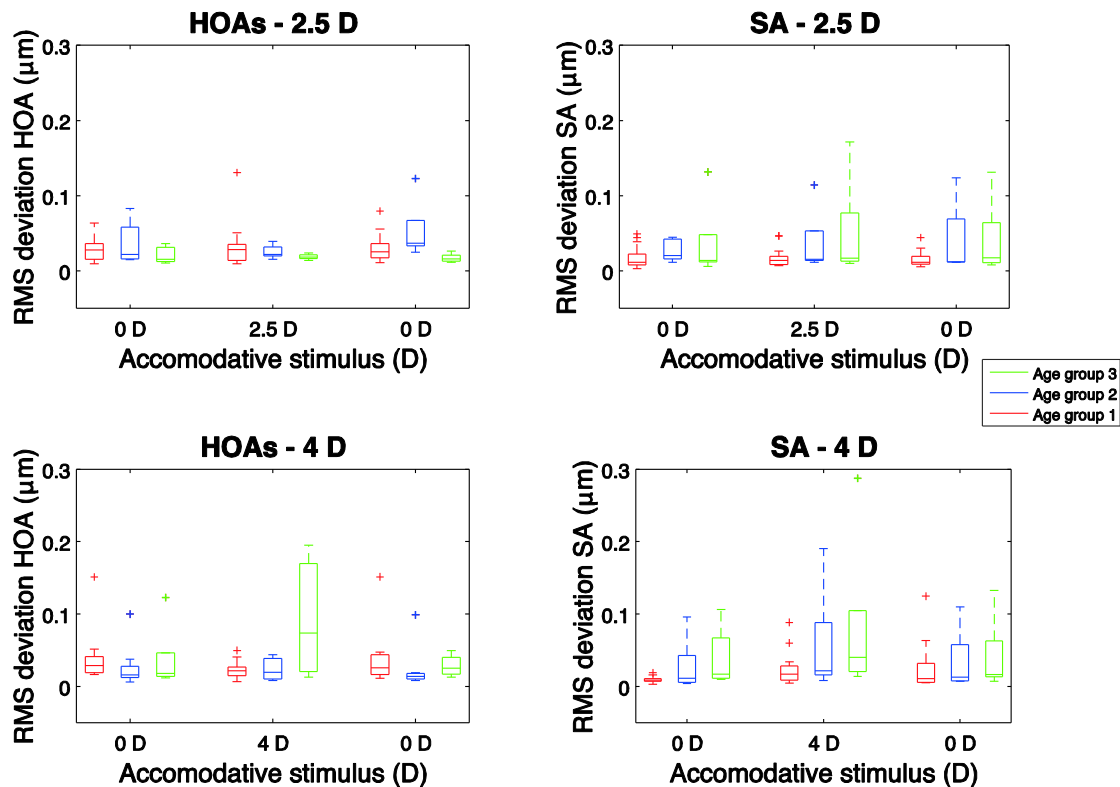


**Figure 4.4:** RMS deviation of the HOA and SA for the 3 age groups (red boxplots: age group 1, blue boxplots: age group 2 and green boxplots: age group 3) and two different accommodative stimuli. Boxplots with medians (lines), 25 % to 75 % quartiles (boxes), ranges (whiskers) and outliers (+). One spurious data point in the HOAs – 2.5 D graph was deleted ( $0.52 \mu\text{m}$ ) for 0 D stimulus (initial resting state) to expand the scale.

Time constants for accommodation and disaccommodation for the three groups are shown in Figure 4.5. Although subjects from age group 1 were fully able to accommodate to the 2.5D and 4D targets which was not the case in other age groups, differences in time constants between the age groups were not significant ( $p > 0.05$ ). No statistically significant differences were found between time constants for the two accommodative demands for any of the age groups.

Kruskall-Wallis test showed that in age group 1 the time constants are significantly different between accommodation and disaccommodation for the two



accommodative demands ( $p = 0.014$  for 2.5D and  $p = 0.013$  for 4D). On the contrary, no significant differences between accommodation and disaccommodation time constants were found for the other two age groups for both accommodative demands ( $p > 0.05$ ).

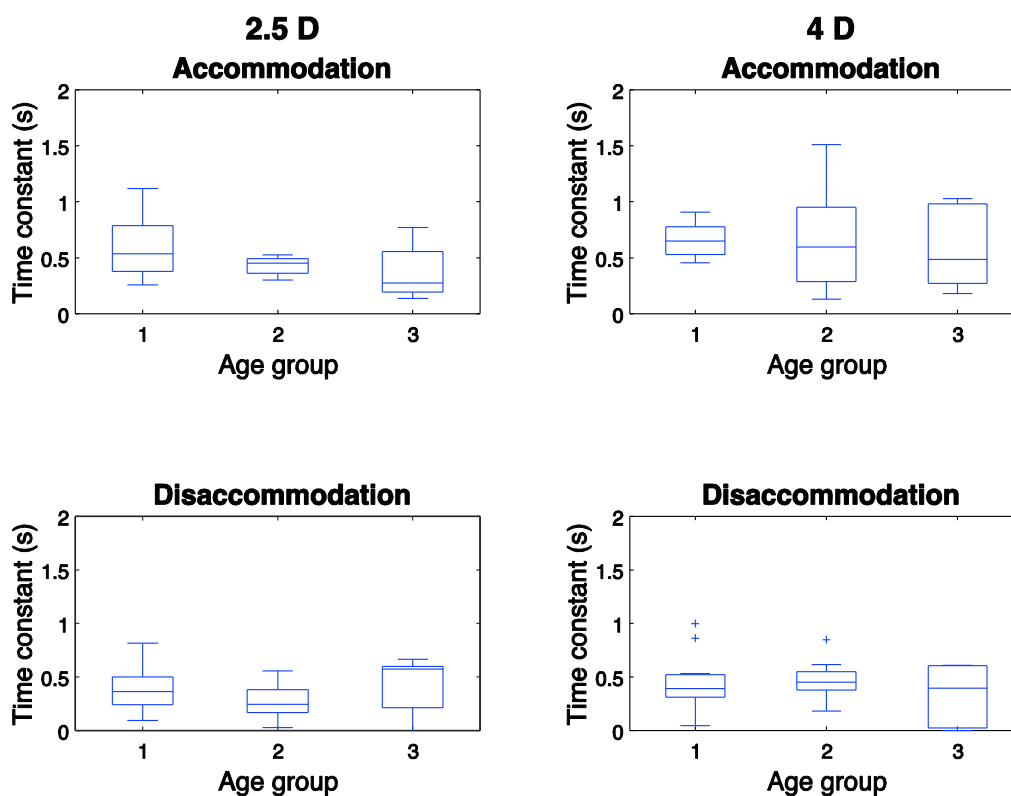


**Figure 4.5:** Accommodative and disaccommodative time constants for the 3 age groups and two different accommodative stimuli (top and bottom left boxplots: 2.5 D and top and bottom right boxplots: 4 D). Boxplots with medians (lines), 25 % to 75 % quartiles (boxes), ranges (whiskers) and outliers (+).

The relationship between microfluctuations and accommodative response is shown in Figure 4.6 where the slope of the accommodative response is plotted against the RMS deviation for the paraxial M. The correlation between the slope of the accommodative response and the magnitude of the fluctuations during accommodation was not statistically significant for any of the age groups or

accommodative stimuli. When the 2.5 D stimulus was presented, age groups 1 and 2 presented a positive slope for the linear regression. However, the slope of the linear regression for age group 3 was negative and the slope of the accommodative response for these subjects was almost zero. These findings on age group 3 were consistent when a 4 D stimulus was presented.

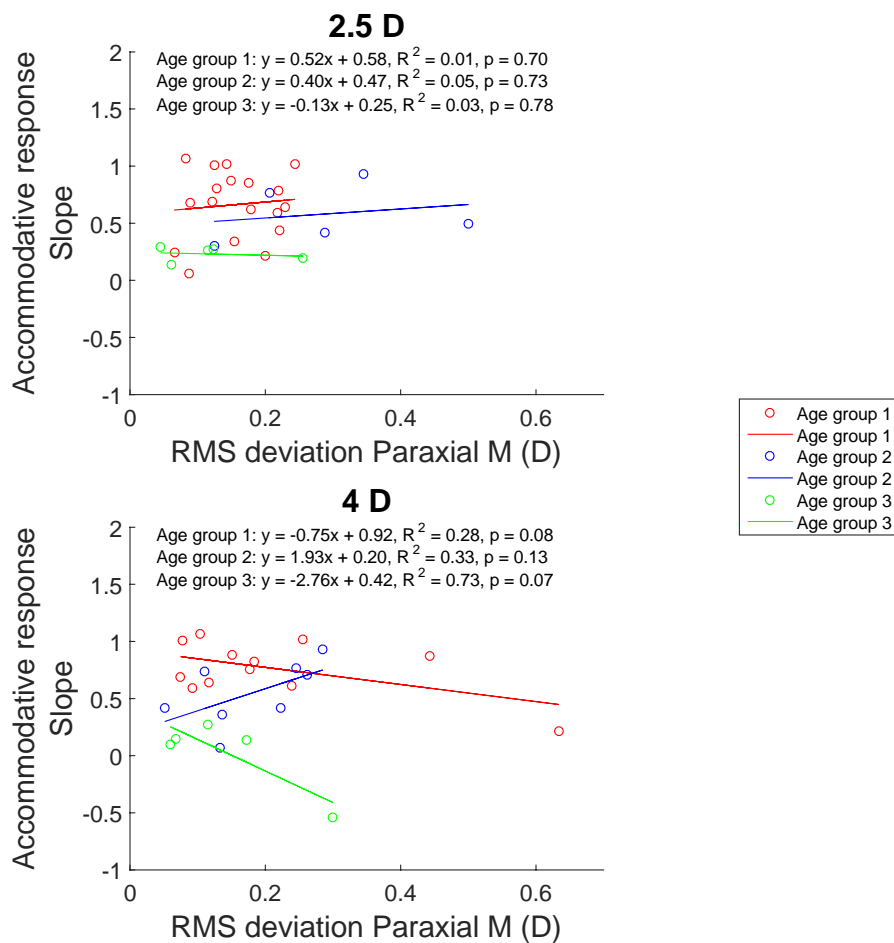


**Figure 4.6:** Accommodative response slope and RMS deviation of the paraxial M for the 3 age groups (red dots: age group 1, blue dots: age group 2 and green dots: age group 3) and two different accommodative stimulus. Solid lines represent the linear fit to the data in each group. Linear equations and p value for each of the regressions is displayed on top of each graph for the three age groups.

A negative slope of the linear regression was found for age groups 1 and 3 when the 4 D stimulus was presented while the slope of the linear regression for age group 2

was positive. The accommodative response for subjects in age group 3 is almost zero with a spurious negative accommodative response value; whilst subjects in age group 1 showed a high variability in accommodative response leading to a spurious value far from the point cloud which made the negative slope of the regression appear erroneously steep. This positive slope of the linear regression when the 2.5 D stimulus was presented and negative slope of the linear regression for the 4 D accommodative demand shown in the results of age group 1, can also be seen in Figure 4.7. Participants from age group 1 are divided according to their refraction into myopes and emmetropes (-0.50 D to +0.50 D). Emmetropes have smaller fluctuations and more accurate accommodation at both accommodative demands. Myopes show these characteristics only when a 4 D stimulus was presented. However, when the 2.5 D stimulus was presented, a positive correlation was found between accommodative response slope and RMS deviation of the paraxial refraction for myopes.

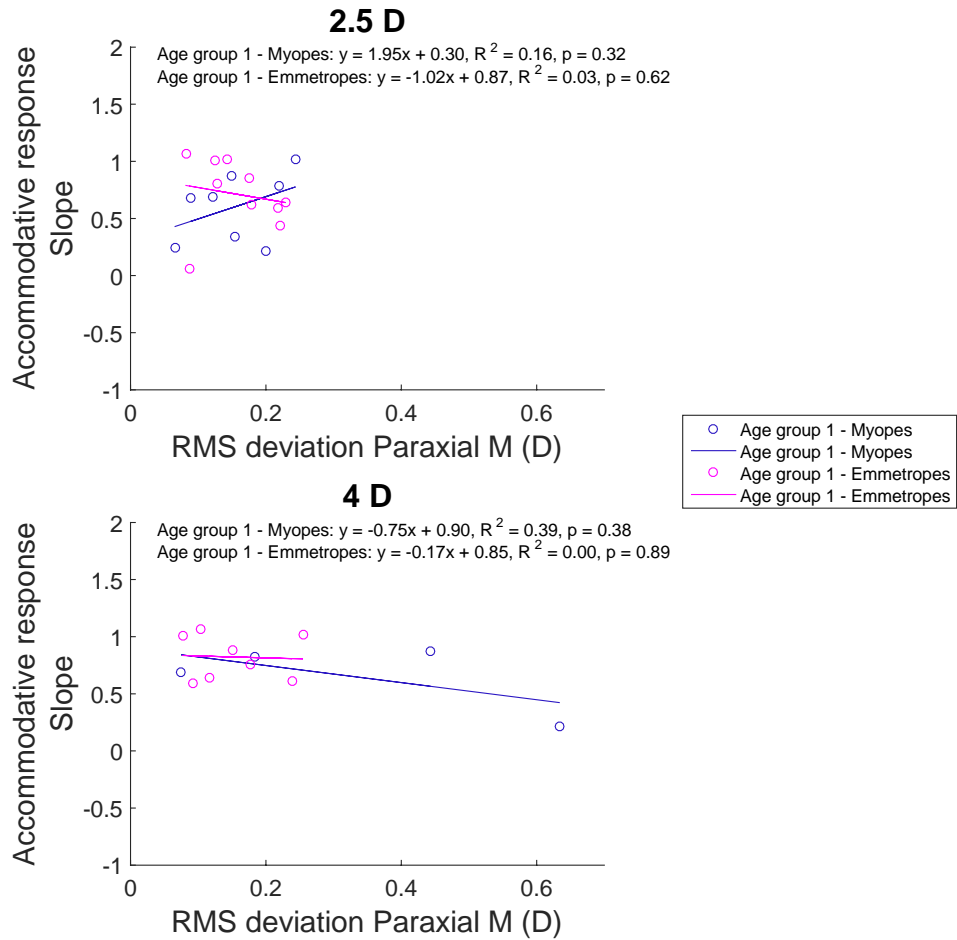


**Figure 4.7:** Accommodative response slope and RMS deviation of the paraxial M for age group 1. Subjects are divided according to their refractive error (blue dots: myopes (<-0.50 D), magenta dots: emmetropes (-0.50 to +0.50 D)) and two different accommodative stimulus. Solid lines represent the linear fit to the data in each subgroup. Linear equations and p value for each of the regressions is displayed on top of each graph for the two subgroups.

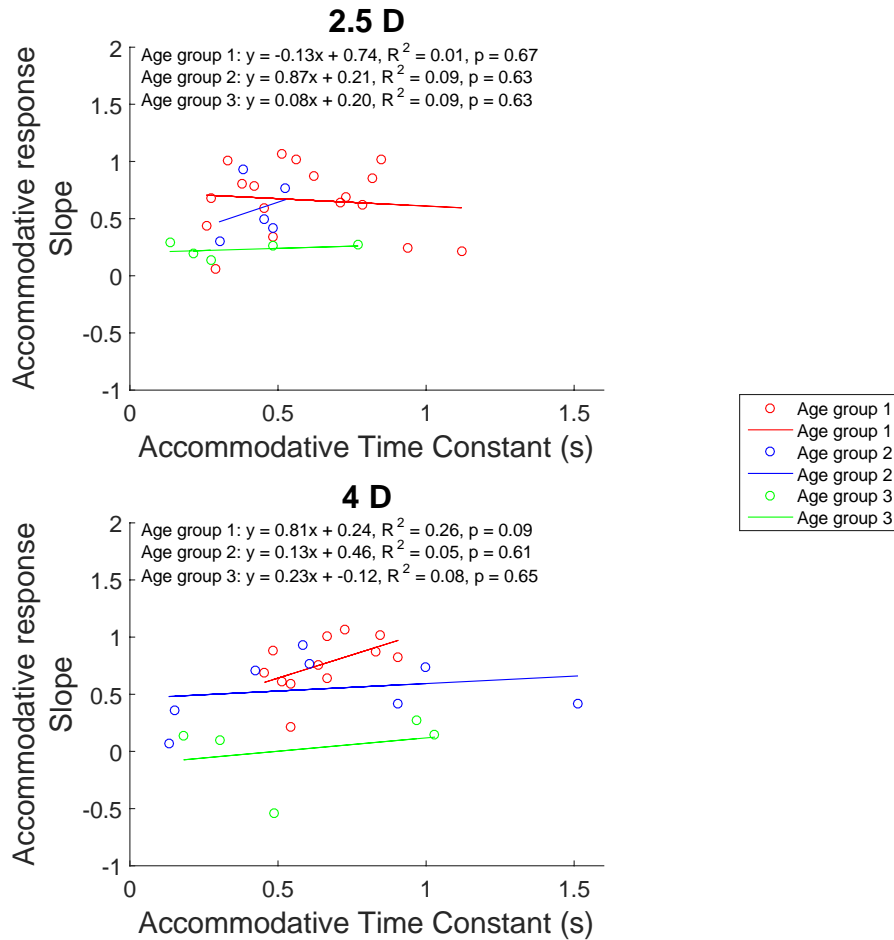


**Figure 4.8:** Accommodative response slope and time constant for the 3 age groups (red dots: age group 1, blue dots: age group 2 and green dots: age group 3) and two different accommodative stimulus. Solid lines represent the linear fit to the data in each group. Linear equations and  $p$  value for each of the regressions is displayed on top of each graph for the three age groups.

Figure 4.8 shows the relationship between the accommodative response slope and the time constant for the different age groups. No statistically significant correlation between the slope of the accommodative response and the accommodative time constants was found for any of the age groups or accommodative stimuli. All three age groups presented a positive slope of the linear regression at the 4 D stimulus level. A bigger value of the accommodative response slope indicates a more accurate accommodative response (i.e. if a subject would

accommodate the same dioptric amount that was presented to them, the accommodative response slope would be 1) A positive slope of the linear regression was found for age groups 2 and 3 at a 2.5 D of stimulus level (Figure 4.8). This means that the more accurate these subjects accommodate, the longer they take to reach that accommodative level, as the accommodative time constant is also higher. However, the slope of the linear regression for age group 1 was negative when the 2.5 D stimulus was presented.

This negative tendency of the regression curve is evident at 2.5 D of accommodative target in the group of myopes shown in Figure 4.9, who were the main contributors. In Figure 4.9 participants from age group 1 are divided according to their refraction into myopes and emmetropes (-0.50 D to +0.50 D). A positive slope of the linear regression was found for emmetropes at both accommodative demands and myopes when a 4 D stimulus was presented. No statistically significant correlation between the slope of the accommodative response and the accommodative time constants was found for any of the age groups or accommodative stimuli.

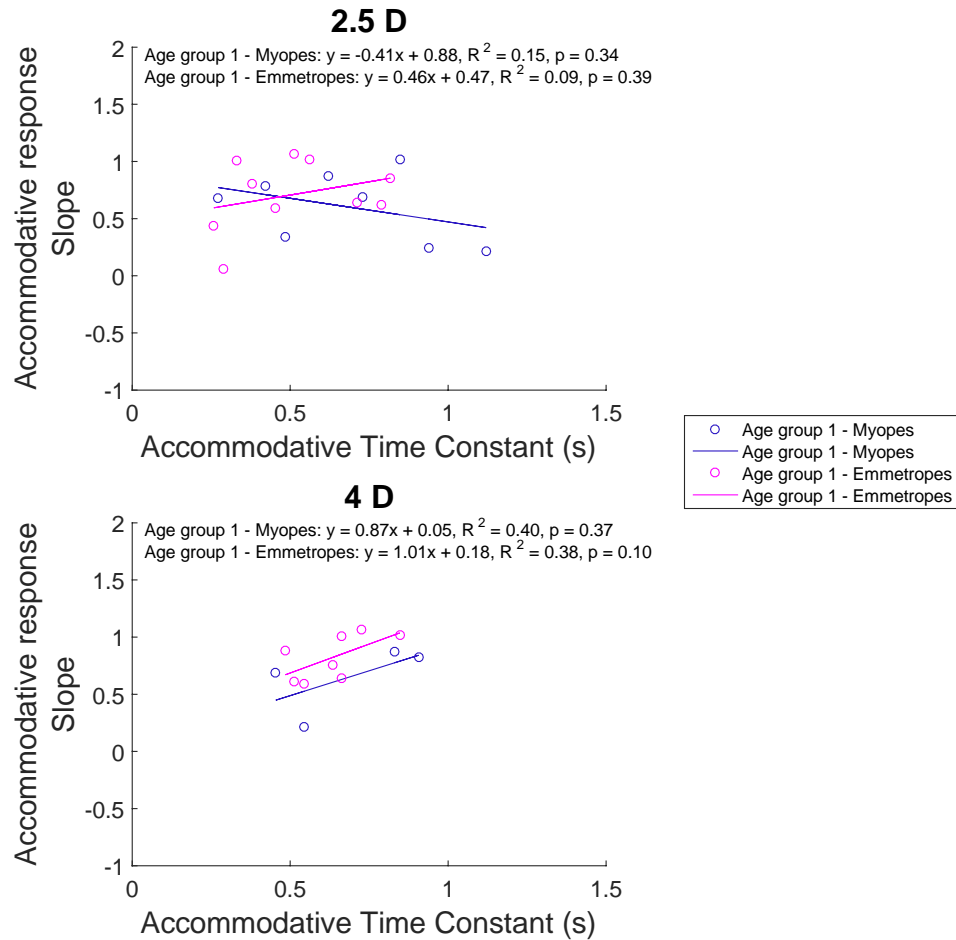


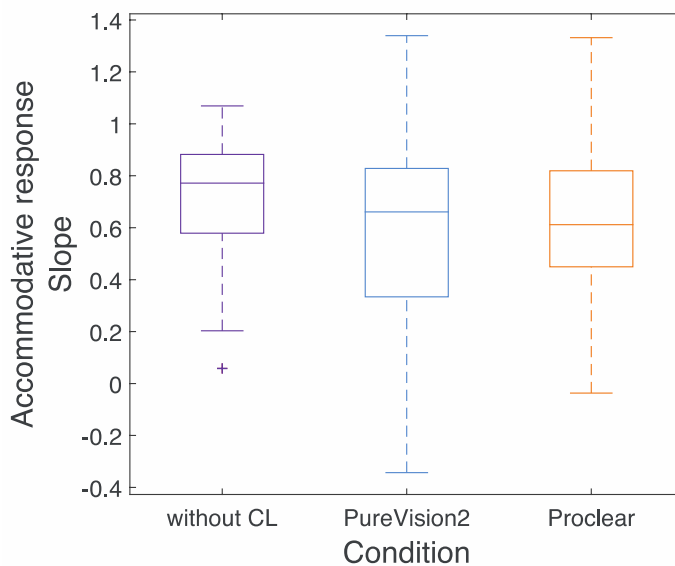
**Figure 4.9:** Accommodative response slope and time constant for age group 1. Subjects are divided according to their refractive error (blue dots: myopes (<-0.50 D), magenta dots: emmetropes (-0.50 to +0.50 D)) and two different accommodative stimulus. Solid lines represent the linear fit to the data in each subgroup. Linear equations and p value for each of the regressions is displayed on top of each graph for the two subgroups.

#### 4.4.2 Experiment 2

After visual inspection of the dynamic accommodative response data with both types of MFCLs analysed with our algorithm, results were added to the naked eye results obtained from Experiment 1 for the younger age group. In total, 111 measurements were considered as usable which resulted in 83 once averaged per subject and these were taken into account for calculation of the time constants and

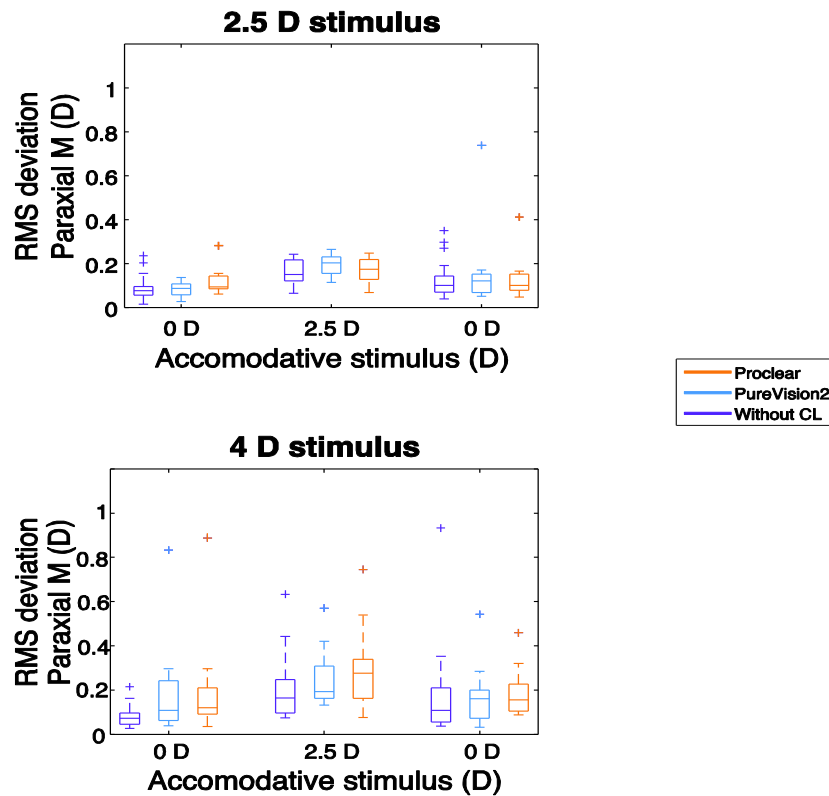
RMS deviation. All the included subjects reached a distance visual acuity of 0.0 logMAR or better either with their habitual correction or any of the two MFCLs fitted.

Accuracy of the accommodative response is represented by its slope which is plotted in Figure 4.10 for the three different conditions tested. Although Kruskal-Wallis non-parametric test did not reveal statistically significant differences ( $p = 0.72$ ) between conditions, a higher variability in results can be seen for both CL designs.



**Figure 4.10:** Slope of the accommodative response for the 3 conditions (purple boxplots: without contact lenses, blue boxplots: PureVision 2 and orange boxplots: ProcLEAR). Boxplots with medians (lines), 25 % to 75 % quartiles (boxes), ranges (whiskers) and outliers (+).





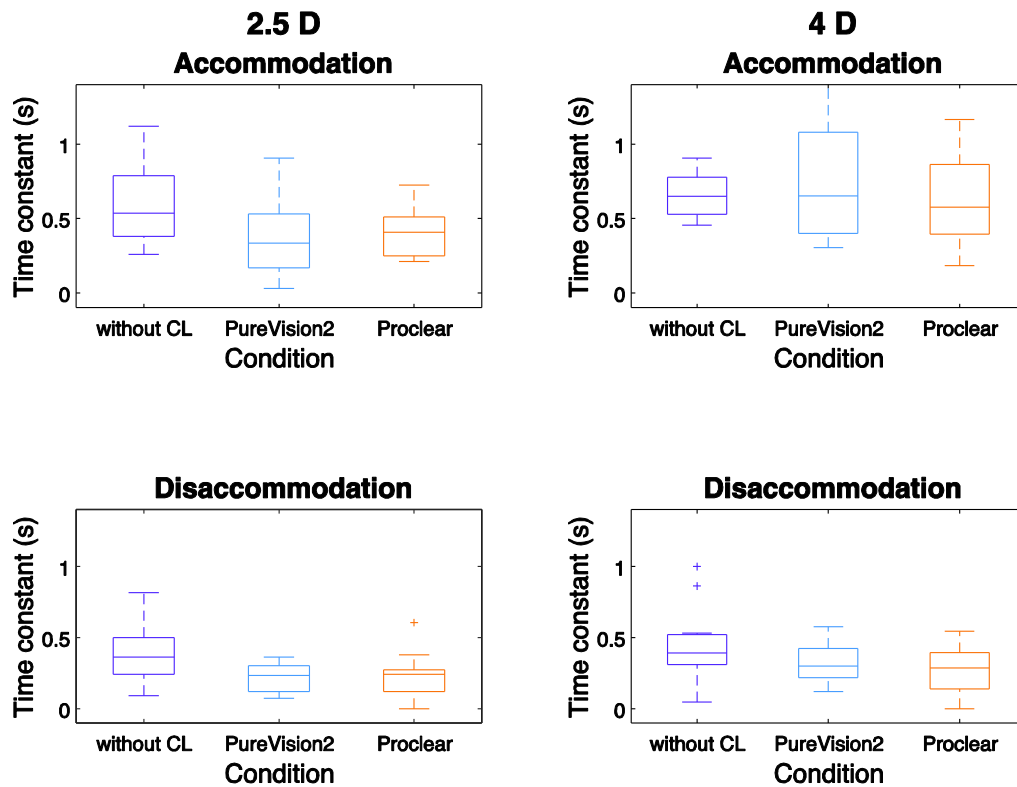
**Figure 4.11:** RMS deviation of the paraxial M for the 3 conditions (purple boxplots: without CLs, blue boxplots: PureVision2 and orange boxplots: Proclear) and two different accommodative stimuli. Boxplots with medians (lines), 25 % to 75 % quartiles (boxes), ranges (whiskers) and outliers (+).

Figure 4.11 shows RMS deviation calculated for the paraxial M for the three different conditions tested. A rise in the magnitude of fluctuations can be seen with accommodation for both levels of accommodative demand. However, Kruskal-Wallis test showed no significant difference in the RMS deviation at any of the accommodative levels (relaxed, accommodated, disaccommodated) between conditions for both the 2.5 and 4 D stimuli.

The same statistical test showed significant differences ( $p = 0.03$ ) in accommodative time constant between the two different accommodative stimuli when participants

#### *Chapter 4: Accommodative fluctuations with age and multifocal contact lenses*

were fitted with the PureVision 2. However, no statistically significant differences in accommodative time constants were found in participants who were not wearing contact lenses ( $p > 0.05$ ) or were fitted with the Proclear multifocal contact lens ( $p=0.07$ ) when they were accommodating to the two different accommodative targets. Similarly, no significant differences ( $p > 0.05$ ) were found in disaccommodative time constants for all three conditions for the two accommodative stimuli (2.5 and 4 D). When the effect on accommodative and disaccommodative time constants of the three different conditions (without CL, PureVision2 and Proclear) at the two different accommodative stimuli was assessed, Kruskal-Wallis test only showed significant differences ( $p = 0.02$ ) in disaccommodative time constant when the 2.5 D stimulus was presented. Accommodative and disaccommodative time constants are plotted in Figure 4.12 from which closer time constant values between conditions and less dispersion of the data can be seen when the accommodative stimulus is higher.



**Figure 4.12:** Accommodative and disaccommodative time constants for the 3 conditions tested and two different accommodative stimuli (top and bottom left boxplots: 2.5 D and top and bottom right boxplots: 4 D). Boxplots with medians (lines), 25 % to 75 % quartiles (boxes), ranges (whiskers) and outliers (+).

With the purpose of assessing the relationship between the accuracy of the accommodative response and the time taken to accommodate, the slope of the accommodative response was plotted against the accommodative time constant (Figure 4.13). Only when participants were not wearing CLs and a higher accommodative stimulus was presented (4 D) the relationship was closer to statistical significance ( $p = 0.09$ ).

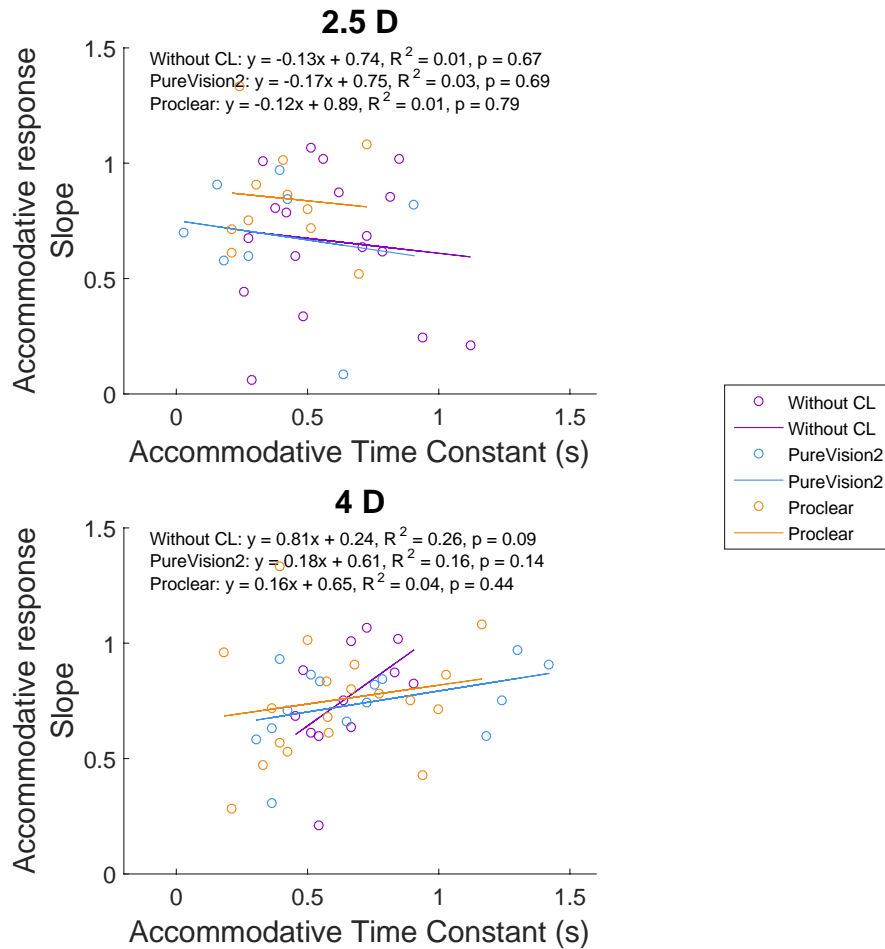


**Figure 4.13:** Accommodative response slope and time constant for the conditions tested (purple boxplots: without contact lenses, blue boxplots: PureVision 2 and orange boxplots: ProcLEAR) and two different accommodative stimulus. Solid lines represent the linear fit to the data in each group. Linear equations and p value for each of the regressions is displayed on top of each graph for the three conditions.

## 4.5 DISCUSSION

This is the first study in which accommodative fluctuations have been assessed in people over 50 years of age and for relaxed accommodation, accommodation and recovery states.

The results show an increase in the accommodative fluctuations in the 3<sup>rd</sup> decade of life which concur with the findings of Anderson et al.<sup>20</sup> The oldest age group included in Anderson et al.<sup>20</sup> was in the 32-38 year range.

On the other hand, publication from Krueger<sup>32</sup>, cited by Charman and Heron<sup>2</sup>, reported that the amplitude of the fluctuations increases with increasing age. Heron and Schor<sup>22</sup> also showed that the differences in amplitude of the spectrum between young and old subjects was not significant when they reached the maximum accommodative response (1 to 1.50 D) for the stimulus presented. It could be that the differences in Heron and Schor's<sup>22</sup> sample between young and older (still capable of accommodating) bridged the gap if higher accommodative stimuli were presented. The present study, uses higher accommodative stimuli to participants in all three age groups and assesses the impact of real world accommodative demands on the response elicited by different age groups. The fluctuations in accommodation reach maximal activity in the centre of the individuals' accommodative range.<sup>1, 33, 34</sup> As shown in the publications of Toshida et al.<sup>1</sup> and Mieke and Denieul<sup>33</sup>, for subjects in their 30's, this peak would be around 3 D of accommodative stimulus. This is in agreement with our results as subjects in age group 2 are the ones that show the bigger fluctuations when they were presented a 2.5 D stimulus that would be in the middle of their amplitude of accommodation under the measurement conditions used.

A Badal system incorporated in the aberrometer was used to present the target at the different vergences. It is well documented that the under-accommodation or lag of accommodation is higher with enclosed Badals and in monocular viewing.<sup>35-37</sup>

This way, proximal and vergence accommodation are not acting while reflex and

voluntary accommodation are being stimulated so the accommodative amplitude would be reduced. This could be the reason behind the subtle differences in mean and standard deviation of the RMS deviation in accommodative conditions between our study and Anderson's et al.<sup>20</sup> as they used an open-field photorefractor. The use of the Badal system could also have accounted for the lack of accommodative response of most of the subjects in age group 3. There were only three participants over 60 years of age (i.e. with no existent accommodation capacity) but the rest of the subjects were all younger presbyopes from 40 years on, who still retain some accommodation capacity.

The bigger lags due to our measurement conditions could explain the higher magnitude of fluctuations for the subjects in age group 2, not only when accommodating at 2.5 D but also the slightly higher values encountered at 4 D of accommodation. It has been suggested that fluctuations in accommodation could be a mechanism to compensate the intrinsic lag to the accommodative function when it is moderate.<sup>34</sup> However, this compensation of lag by an increase in accommodative microfluctuations is not very likely to be happening to our sample as the reduced RMS deviation in the older age group, who because of their accommodative inability has bigger lags, does not match this compensation theory. Some of the differences in accommodative fluctuations in age group 2 can be attributed to the large proportion of myopes in this group (70 %; Table 4.1) as myopes have been shown to have higher accommodative fluctuations than emmetropes.<sup>38-41</sup>

The low magnitude of difference between disaccommodation and recovery states could also be linked to the refractive error of the participants. The results indicate

that most of the subjects were either unable or found it hard to completely disaccommodate. This difficulty to disaccommodate is in agreement with the results reported by Allen et. al<sup>26</sup> who also found longer time constants for disaccommodation.

Knowing the extent of microfluctuations has an impact not only in the vision research field but also in the daily practice. It would be particularly useful to develop more realistic eye models that could better predict the objective DoF as it has been demonstrated that the RMS value of the fluctuations is correlated to the objective DoF<sup>42</sup> and therefore improve the current solutions for presbyopia which rely on this factor. It could also be useful for practitioners as a tool to assess the stability of the accommodative response when wearing different types of correction including IOLs implanted after cataract surgery. This would help to understand the origin of the fluctuations and whether they disappear when the natural crystalline lens has been removed as to the authors' knowledge no studies addressing this question have been published

In an attempt to answer this question, we also looked into the influence of fluctuations in driving the accommodative response. With this purpose we evaluated the relationship between the slope of the accommodative response and the RMS deviation of the paraxial M when two different stimuli were presented. Subjects in age group 3 showed a very low slope of the accommodative response indicating that they barely accommodate to the targets. In age groups 1 and 2, those subjects whose accommodation is more accurate present higher magnitude of fluctuations. Thus, fluctuations could be understood as a signal fine-tuning

system that provides a temporal cue for detecting the correct direction and magnitude of the accommodative stimulus. This is in agreement with those studies that attribute the fluctuations in accommodation playing a role in controlling the accommodation system.<sup>2, 8, 43</sup> If one compares subjects in different age groups, those in age group 1 are the ones that accommodate more accurately but whose maximum magnitude of fluctuations is smaller probably because this is an easily reachable accommodative stimulus for them. Subjects in age group 2 are still able to accommodate but their accommodative system is being more stressed and the target is closer to the middle of their accommodative range and as stated before this could be why they exhibit higher magnitude of fluctuations.<sup>33</sup> Young (age group 1) myopes showed that when higher accommodative demand was presented (4 D) improved accommodative accuracy led to lower accommodative fluctuations. This can be because 4 D is too much blur to tolerate; however when the accommodative stimulus is not that high (2.5), it is feasible that in cases where blur tolerance is high (for example in myopes), higher fluctuations in accommodation help in driving accommodation in the right direction.<sup>41</sup>

The increase in SA with increasing age is well documented<sup>13</sup>, a bigger dispersion of the data within our age groups could be expected. Like Zhu et al.<sup>5</sup>, the present study found an increase in the fluctuations of SA with accommodation but in a much smaller magnitude than for the paraxial M, which also includes the contribution of defocus. In addition, age groups 2 and 3 include subjects that struggle more to accommodate both at 2.5 D and 4 D stimulus. In these groups, the increase in SA fluctuations could be linked to a balance of defocus during accommodation.<sup>44</sup>



The present study found no statistically significant differences with age in accommodative time constants. Time constants for the younger subjects for accommodation are similar to those found by Radhakrishnan et al.<sup>26</sup> but almost double in magnitude that those from Mordi et al.<sup>12</sup> across different age groups which, as found in the former study may be due to the high proportion of myopes in our cohort. As the accommodative stimuli presented were in a different portion of the accommodative amplitude for each age group, we found higher values in dissaccommodation time constants in age groups 2 and 3 after viewing a 4 D stimulus which would have challenged their accommodative capability.<sup>45</sup> In general the more accurate subjects accommodate the more time they invest on reaching that accommodative target. However, the opposite behaviour was found in the case of myopes in age group 1. These were the subjects whose magnitude of fluctuations and therefore the amount of blur generated was higher as they accommodate more accurately. Because they are more tolerant to blur, it may be that at this stage they are able to more quickly detect the accommodative cues. Those with more accurate accommodation in this myopic group reached that accommodative state in less time. Because of their age group these are also the subjects whose crystalline lens is softer and more easily deformable.

In Experiment 2, the relationship between the slope of accommodative response and accommodative time constants when participants were fitted with the MFCLs, mimicked that of the naked eye situation. The accuracy of accommodative response and the extent of accommodative fluctuations in MFCL wearing participants, suggest that accommodation is used by young people fitted with MFCLs. Therefore, accommodative function is preserved in young subjects fitted

with MFCLs used in this study, which is in agreement with the vast majority of studies.<sup>19, 46, 47</sup>

When participants were wearing the MFCLs, higher variability in slope of the accommodative response data was found, which can be attributable to the two different foci generated by these MFCLs and the contribution of different parts of the CLs, as data were obtained for natural pupils. The discrimination between both foci might be different in older subjects whose neural processing may still play a role providing benefit to these individuals from the use of MFCLs. The generation of the near and distance foci when participants were fitted with the MFCLs, may also be the explanation of the slightly lower values in accommodative time constants when the accommodative stimulus (2.5 D) was closer to the addition provided by the lenses (PureVision 2: +2.5 D of add, Proclear: +2.00 D of add). Median accommodative time constant was found to be lower with the 2.5 D stimulus than with the 4 D stimulus for all the situations (without CLs and with the two MFCLs), which is in agreement with the results of Madrid-Costa et al.<sup>19</sup> although the values encountered in our study are lower. It could be that participants took longer to reach the 63 % of the accommodative response when the stimulus presented was 4 D as it was higher than the CLs' addition. However, these differences in accommodative time constants between conditions were not statistically significant as in the study from Madrid-Costa et al.<sup>19</sup> Measurements of visual performance such as visual acuity, contrast sensitivity, stereoacuity and glare would provide more information about the performance of these MFCLs, however this was beyond the scope of this thesis.

In spite of the agreement in results with previous published studies,<sup>2,20,33,47</sup> the main limitation of our two experiments was the difficulty of acquiring and analysing dynamic accommodation data. This led to a large amount of excluded data, reducing significantly the sample size. This reduction in number of participants made our results less generalizable and hence, less accurate to describe the entire population.

From the cohort of participants in this study, it can be concluded that ageing affects accommodative fluctuations but not time constants. Time constants are usually higher when accommodation is more accurate but do not change with age. There is an increase in the accommodative fluctuations in the 3<sup>rd</sup> decade of life when the accommodative system is more stressed as the accommodative stimulus presented is in the middle of the amplitude of accommodation range. A higher magnitude of fluctuations leads to a more accurate accommodation in the younger age groups. However, when blur tolerance is possibly higher as in the case of younger myopes accommodating to a high accommodative demand (4 D) and presbyopes, more accurate accommodation is achieved with less fluctuations. This suggests that accommodative microfluctuations have the function in controlling the accommodation system to some extent. MFCLs do not interfere in the accommodative and disaccommodative performance in both static and dynamic conditions in young individuals.

## 4.6 REFERENCES

1. Toshida K, Okuyama F, Tokoro T. Influences of the accommodative stimulus and aging on the accommodative microfluctuations. *Optom Vis Sci* 1998;75:221-226.
2. Charman WN, Heron G. Fluctuations in accommodation: a review. *Ophthalmic Physiol Opt* 1988;8:153-164.
3. Collins G. The electronic refractionometer. *Clin Exp Optom* 1939;22:122-132.
4. Collins M, Davis B, Wood J. Microfluctuations of steady-state accommodation and the cardiopulmonary system. *Vision Res* 1995;35:2491-2502.
5. Zhu M, Collins MJ, Iskander DR. The contribution of accommodation and the ocular surface to the microfluctuations of wavefront aberrations of the eye. *Ophthalmic Physiol Opt* 2006;26:439-446.
6. Charman WN, Heron G. Microfluctuations in accommodation: an update on their characteristics and possible role. *Ophthalmic Physiol Opt* 2015;35:476-499.
7. Gray LS, Winn B, Gilmartin B. Effect of target luminance on microfluctuations of accommodation. *Ophthalmic Physiol Opt* 1993;13:258-265.
8. Metlapally S, Tong JL, Tahir HJ, Schor CM. Potential role for microfluctuations as a temporal directional cue to accommodation. *J Vis* 2016;16:19.
9. Zhu M, Collins MJ, Robert Iskander D. Microfluctuations of wavefront aberrations of the eye. *Ophthalmic Physiol Opt* 2004;24:562-571.

10. Muma M, Iskander DR, Collins MJ. The role of cardiopulmonary signals in the dynamics of the eye's wavefront aberrations. *IEEE Trans Biomed Eng* 2010;57:373-383.
11. United Nations. Department of Economic and Social Affairs, Population Division (2015). World Population Ageing 2015. (ST/ESA/SERA/390).
12. Mordi JA, Ciuffreda KJ. Dynamic aspects of accommodation: age and presbyopia. *Vision Res* 2004;44:591-601.
13. Radhakrishnan H, Charman WN. Age-related changes in ocular aberrations with accommodation. *J Vis* 2007;7:11.11-21.
14. Day M, Seidel D, Gray LS, Strang NC. The effect of modulating ocular depth of focus upon accommodation microfluctuations in myopic and emmetropic subjects. *Vision Res* 2009;49:211-218.
15. Kasthurirangan S, Markwell EL, Atchison DA, Pope JM. In vivo study of changes in refractive index distribution in the human crystalline lens with age and accommodation. *Invest Ophthalmol Vis Sci* 2008;49:2531-2540.
16. Moffat BA, Atchison DA, Pope JM. Age-related changes in refractive index distribution and power of the human lens as measured by magnetic resonance micro-imaging in vitro. *Vision Res* 2002;42:1683-1693.
17. Morgan PB, Efron N, Woods CA. An international survey of contact lens prescribing for presbyopia. *Clin Exp Optom* 2011;94:87-92.
18. Walline JJ, Greiner KL, McVey ME, Jones-Jordan LA. Multifocal contact lens myopia control. *Optom Vis Sci* 2013;90:1207-1214.

19. Madrid-Costa D, Ruiz-Alcocer J, Radhakrishnan H, Ferrer-Blasco T, Montes-Mico R. Changes in accommodative responses with multifocal contact lenses: a pilot study. *Optom Vis Sci* 2011;88:1309-1316.
20. Anderson HA, Glasser A, Manny RE, Stuebing KK. Age-related changes in accommodative dynamics from preschool to adulthood. *Invest Ophthalmol Vis Sci* 2010;51:614-622.
21. Candy TR, Bharadwaj SR. The stability of steady state accommodation in human infants. *J Vis* 2007;7:4.1-16.
22. Heron G, Schor C. The fluctuations of accommodation and ageing. *Ophthalmic and Physiol Opt* 1995;15:445-449.
23. Thibos LN, Hong X, Bradley A, Applegate RA. Accuracy and precision of objective refraction from wavefront aberrations. *J Vis* 2004;4:329-351.
24. Kasthurirangan S, Vilupuru AS, Glasser A. Amplitude dependent accommodative dynamics in humans. *Vision Res* 2003;43:2945-2956.
25. Montes-Mico R, Alio JL, Munoz G, Perez-Santonja JJ, Charman WN. Postblink changes in total and corneal ocular aberrations. *Ophthalmology* 2004;111:758-767.
26. Radhakrishnan H, Allen PM, Charman WN. Dynamics of accommodative facility in myopes. *Invest Ophthalmol Vis Sci* 2007;48:4375-4382.
27. Madrid-Costa D, Ruiz-Alcocer J, Garcia-Lazaro S, Ferrer-Blasco T, Montes-Mico R. Optical power distribution of refractive and aspheric multifocal contact lenses: Effect of pupil size. *Cont Lens Anterior Eye* 2015;38:317-321.
28. Wagner S, Conrad F, Bakaraju RC, Fedtke C, Ehrmann K, Holden BA. Power profiles of single vision and multifocal soft contact lenses. *Cont Lens Anterior Eye* 2015;38:2-14.

29. Kang P, Fan Y, Oh K, Trac K, Zhang F, Swarbrick HA. The effect of multifocal soft contact lenses on peripheral refraction. *Optom Vis Sci* 2013;90:658-666.
30. Kang P, McAlinden C, Wildsoet CF. Effects of multifocal soft contact lenses used to slow myopia progression on quality of vision in young adults. *Acta ophthalmol* 2017;95:e43-e53.
31. Rosen R, Jaeken B, Lindskoog Petterson A, Artal P, Unsbo P, Lundstrom L. Evaluating the peripheral optical effect of multifocal contact lenses. *Ophthalmic Physiol Opt* 2012;32:527-534.
32. Krueger H. Schwankungen der Akkommodation des menschlichen Auges bei mon-und binokularer Beobachtung. *Graefe's Arch Clin Exp Ophthal* 1978;205:129-133.
33. Mieke C, Denieul P. Mean response and oscillations of accommodation for various stimulus vergences in relation to accommodation feedback control. *Ophthalmic Physiol Opt* 1988;8:165-171.
34. Plainis S, Ginis HS, Pallikaris A. The effect of ocular aberrations on steady-state errors of accommodative response. *J Vis* 2005;5:466-477.
35. Jaschinski W. Fixation disparity and accommodation for stimuli closer and more distant than oculomotor tonic positions. *Vision Res* 2001;41:923-933.
36. Aldaba M, Otero C, Pujol J, Atchison DA. Does the Badal optometer stimulate accommodation accurately? *Ophthalmic Physiol Opt* 2017;37:88-95.
37. Radhakrishnan H, Charman WN. Age-related changes in static accommodation and accommodative miosis. *Ophthalmic Physiol Opt* 2007;27:342-352.

38. Day M, Strang NC, Seidel D, Gray LS, Mallen EA. Refractive group differences in accommodation microfluctuations with changing accommodation stimulus. *Ophthalmic Physiol Opt* 2006;26:88-96.
39. Harb E, Thorn F, Troilo D. Characteristics of accommodative behavior during sustained reading in emmetropes and myopes. *Vision Res* 2006;46:2581-2592.
40. Lin H, Drobe B, Jin W, Lin M, Chen Y, Chen H. Effects of Near Addition Lenses and Prisms on Accommodative Microfluctuations in Chinese Children. *Optom Vis Sci* 2016;93:488-496.
41. Seidel D, Gray LS, Heron G. Retinotopic accommodation responses in myopia. *Invest Ophthalmol Vis Sci* 2003;44:1035-1041.
42. Yao P, Lin H, Huang J, Chu R, Jiang BC. Objective depth-of-focus is different from subjective depth-of-focus and correlated with accommodative microfluctuations. *Vision Res* 2010;50:1266-1273.
43. Winn B, Gilmartin B. Current perspective on microfluctuations of accommodation. *Ophthalmic Physiol Opt* 1992;12:252-256.
44. Lopez-Gil N, Fernandez-Sanchez V, Legras R, Montes-Mico R, Lara F, Nguyen-Khoa JL. Accommodation-related changes in monochromatic aberrations of the human eye as a function of age. *Invest Ophthalmol Vis Sci* 2008;49:1736-1743.
45. Shirachi D, Liu J, Lee M, Jang J, Wong J, Stark L. Accommodation dynamics I. Range nonlinearity. *Am J Optom Physiol Opt* 1978;55:631-641.
46. Montes-Mico R, Madrid-Costa D, Radhakrishnan H, Charman WN, Ferrer-Blasco T. Accommodative functions with multifocal contact lenses: a pilot study. *Optom Vis Sci* 2011;88:998-1004.



47. Ruiz-Alcocer J, Madrid-Costa D, Radhakrishnan H, Ferrer-Blasco T, Montes-Mico R. Changes in accommodation and ocular aberration with simultaneous vision multifocal contact lenses. *Eye Contact Lens* 2012;38:288-294.

## **5 ACCOMMODATION AND OCULAR ABERRATIONS WITH TWO GENERATIONS OF MULTIFOCAL CONTACT LENSES**

### **CONTRIBUTIONS**

The study was designed by me and my supervisors during my placement at the University of Valencia (Spain), Robert Montes-Mico. The data collection was done by me along with the data analysis. I wrote the first draft of the manuscript which was revised and finalised with support from the co-authors.

### **PUBLISHING OF THE PAPER**

Authors for this study are Irene Sisó-Fuertes, Caridad Pérez-Vives, Teresa Ferrer-Blasco, Hema Radhakrishnan and Robert Montes-Micó. This paper will be submitted with the title: "Accommodation and ocular aberrations with two generations of multifocal contact lenses". Target journal: Journal of Optometry. To be submitted.

### **PRESENTATION AT CONFERENCE**

This work was presented in the form of a poster:

Siso-Fuertes, I., Perez-Vives, C., Ferrer-Blasco, T., Radhakrishnan, H., Montes-Mico, R. 2015. Accommodation and ocular aberrations with two simultaneous vision multifocal contact lenses. Proceedings of European Academy of Optometry and Optics (EAOO) Annual Meeting, 2015.

## 5.1 ABSTRACT

**PURPOSE:** To investigate the improvements achieved, if any, by the PureVision2 High add bi-aspheric multifocal contact lens (MFCL) with respect to its predecessor PureVision High add lens in terms of visual acuity, accommodative response and ocular aberrations.

**METHODS:** Fifteen eyes from non-presbyopic subjects were fitted with the PureVision Multifocal and PureVision 2 for Presbyopia, both in high addition. Each individual wore each of the MFCLs in successive random order. Corrected distance visual acuity (CDVA), distance corrected near visual acuity (DCNVA), accommodative response obtained from defocus terms and higher-order aberrations; were assessed in all cases for every type of MFCL.

**RESULTS:** PureVision 2 High add provided significantly ( $p < 0.05$ ) better DCNVA while differences were not found in CDVA when comparing lenses. Statistically significant ( $p < 0.05$ ) differences in terms of accommodative response were found between the three accommodative states analysed (0 D, 2.5 D and 4 D) but not ( $p > 0.05$ ) between MFCLs at each accommodative demand. Higher-order aberrations assessment showed a statistically significant increase towards negative values in vertical coma ( $Z_3^{-1}$ ) and spherical aberration ( $Z_4^0$ ) in both MFCLs wearers with accommodation. PureVision High Add showed greater aberration coefficients than the other CL analysed when the 2.5 D stimulus was presented.

**CONCLUSION:** Results obtained in this study from aberration data indicate that simultaneous vision MFCLs studied do not reduce accommodative function when fitted in non-presbyopic subjects. It appears that some improvements in visual performance have been attained with the PureVision 2 High Add design.

## **5.2 INTRODUCTION**

In 1864, Donders and Moore<sup>1</sup> noticed that the range of distances for which the eye is able to focus clearly (amplitude of accommodation), progressively declines with age and it becomes manifested when the near point no longer coincides with the normal near working distance. Subsequently other authors<sup>2-5</sup> have found that the decrease is almost linear and it reaches zero at about 50 years of age leading to presbyopia. As life expectancy becomes greater, the number of presbyopes increases too. Hence, diverse solutions to correct presbyopia have been developed in recent years. Regarding contact lens (CL) correction, monovision and bi- or multi-zone CLs based on either simultaneous or alternating vision have been the most accepted alternatives to correct presbyopia.<sup>6</sup>

In simultaneous vision multifocal contact lenses (MFCLs), both distance and near correction zones are allocated within the pupillary area. Thus, light that comes from far and near objects goes through both zones. This means that in every case the lens wearer has a clear image in the retina of the observed object but also a blurry image from the out-of-focus image. Therefore these kinds of MFCLs are strongly dependent on the pupil size and also their quality of the retinal image depends on the lens power profile, and the lens centration with respect to the visual axis.<sup>7</sup> Consequently, the satisfaction of MFCL wearers varies widely. An example of this kind of simultaneous focus MFCL is the PureVision Multifocal. Despite the fact that the contact lens industry has increased its activity, the last international survey (among 38 countries) reveals that the rate of prescribing MFCLs is still very low.<sup>8</sup>

The transition zone between the distance and near power zones enlarges the depth of focus (DoF) aiming to increase the range of distances in which an image appears acceptably sharp. Non-presbyopic subjects wearing MFCLs have not shown the expected reduction in accommodation that should happen when positive additions are prescribed for near tasks.<sup>9</sup> This has been assessed in terms of defocus, pupil function and higher-order aberrations. Some investigations<sup>10-12</sup> have assessed the accommodative response in non-presbyopic subjects explained as the combined effect of the eye and the respective corrective lens. When comparing the results obtained by single vision CLs wearers and PureVision MFCL fitted subjects, no statistically significant differences in accommodation<sup>10-12</sup>, peak velocity<sup>10</sup>, time constant<sup>10</sup> and latency<sup>10</sup> have been found. Moreover, Montes-Micó et al.<sup>11</sup> measured the accommodative facility using flippers and found no differences between lenses. When the same experiment was performed in reference to pupil function, the results of amplitude of constriction, constriction per diopter of accommodation and transience showed no accommodative effort.<sup>10</sup> These same outcomes were found by Ruiz-Alcocer et al.<sup>12</sup> when assessing ocular aberrations (spherical aberration and root-mean-square [RMS]) in both kinds of CL wearers. However, when comparing MFCLs with single vision CLs, monocular near VA has been reported to be similar whilst distance VA is always better with the single vision CLs in non-presbyopic people.<sup>11, 12</sup> Furthermore, contrast sensitivity function<sup>11, 13, 14</sup> and stereoacuity<sup>13, 15, 16</sup> assessment exposes that in spite of being slightly low, MFCLs provide good visual performance and balance of real-world visual function. One of the latest additions to the growing market of MFCLs whose main goal is providing spectacle-free vision correction for the presbyopic population, is the

PureVision2 for Presbyopia (Bausch & Lomb, Rochester, NY). Hartmann-Shack wavefront based analysis provided by the manufacturer showed a new aspheric multifocal design near centre 3-Zone Progressive.

The aim of this study is to assess whether both generations of MFCLs (PureVision Multifocal and PureVision2 for Presbyopia) provide clear enough images from near objects. The study also aims to compare the changes in accommodation and ocular aberrations between the two generations of MFCLs.

## **5.3 METHODS**

### **5.3.1 Subjects**

This study included 15 eyes from non-presbyopic subjects whose mean age was  $28 \pm 4$  years (range from 25 to 38). All of them were healthy volunteers from the University of Valencia staff. Despite all the subjects being members of the staff, all of them were volunteer participants and were not coerced to participate. Standard safeguards were applied to protect the confidentiality of their personal information. None of the participants had used any topical or systemic medication which could affect accommodation. Their mean spherical refractive error was  $-0.34 \text{ D} \pm 0.97$ . Eyes whose astigmatism was 0.75 D or higher, were not included in the study. Table 5.1 shows the demographic information about the participants. In addition none of the participants have had corneal refractive surgery or any other kind of surgery that could distort the measurements. All participants were informed

about the details of this study, and following the Helsinki Declaration a written informed consent was obtained from each participant.

**Table 5.1:** Demographic information for all 8 subjects.

No of participants (n)	No of eyes (n)	Mean age $\pm$ SD (years)	Age range (years)	Gender		Mean Spherical equivalent $\pm$ SD (D)
				Male (n)	Female (n)	
9	15	28 $\pm$ 4	25 to 38	4	5	-0.34 $\pm$ 0.97

### 5.3.2 Contact lenses

MFCLs chosen for this study were PureVision Multifocal and PureVision2 for Presbyopia both in High addition as the transition zone is more abrupt, thus making their effect and possible changes more pronounced. The distance power was selected for refractive error correction if any. The PureVision Multifocal has a front surface aspheric and back surface spherical, centre-near design with an optical zone of 8.00 mm and a total lens diameter of 14.00 mm.

The PureVision2 for Presbyopia has new aspheric multifocal design near centre 3-Zone Progressive within the 14.00 mm of diameter that delivers more add power towards the centre of the lens and a wider intermediate zone in order to get a gradual transition towards the distance vision zone where power is constant. Both contact lenses had a base curve radius of 8.6 mm and the fit of each lens was made in successive random order and assessed after allowing at least 5 minutes for the lens to settle without changing any of the contact lens parameters. This was done prior to making any aberrations measurement..

### **5.3.3 Experimental procedure**

Once participants were distance corrected, visual acuity was measured for distance (6m) and near (40 cm) using a snellen chart in photopic conditions ( $85 \text{ cd/m}^2$ ) and results converted to logMAR units. We used the wavefront sensor incorporated in the crx1 Adaptive Optics Visual Simulator (Imagine Eyes) which is a Hartmann-Shack based equipment that allows the acquisition of the different Zernike polynomials. The aberrometer has a square array of 1024 lenslets and measurements are made at a wavelength of 850 nm. The observer viewed a Maltese cross generated on a micro-display through the adaptive optics system and an artificial pupil. The micro-display subtended a visual angle of  $114 \times 86$  with a resolution of  $800 \times 600$  pixels and having a luminance of about  $85 \text{ cd/m}^2$

Measurements were taken at three different vergences. One for distance (0 D), another at 40 cm (2.50 D) and the last one at 4 D in order to assess the accommodative effort in three situations. All the subjects were encouraged to keep the stimulus as clear as possible at each accommodative demand. They were also asked to blink freely in order to distribute homogeneously their tear film and to avoid any possible artefacts. Measurements were obtained monocularly with the fellow eye covered with a patch and using the measurements of all microlenses available in the circle of maximum diameter allowed by the aberrometer optics (6.5 mm) and the subject's eye pupil. Individual pupil size was measured but in order to collect the data we used the same pupil diameter for every subject so the effect of the lens could be assumed to be constant for every subject. Thus, as suggested by Bara et al.<sup>17</sup> aberrations data were rescaled down for the desired 4 mm pupil size.



Three measurements were taken at each accommodative demand so possible errors while data acquisition, were minimized. Moreover, we took into account that there is some latency between the onset of a stimulus and the initiation of an accommodative response. Thus, in order to get data when the accommodative response had already started, aberrations were recorded after 1 second of looking at the fixation target.<sup>18</sup> Power vectors of equivalent sphere (M) were obtained from defocus terms in accordance to the following expression:<sup>19</sup>

$$M = -\frac{4\sqrt{3} C_2^0}{r^2}$$

**Equation 5.1:** *Surface fitting procedure that minimizes the RMS of the wave aberration using the second-order Zernike coefficients.*<sup>19</sup>

Where, 'r' is the pupil radius for the appropriate Zernike term. The mean value for the three measurements was calculated. In order to obtain the accommodative response to any near stimulus the difference between the mean-equivalent sphere refraction measured with the near stimulus and those at the far point, was taken. The sign was reversed to make the response positive. All the described measurements were performed for every subject wearing the two different MFCLs. Obtained data was statistically analysed using SPSS 20 for Windows (SPSS Inc., Chicago, IL). Repeated Measures ANOVA was performed to test whether changes in accommodation and ocular aberrations are produced for the different accommodated states.

## 5.4 RESULTS

In this study, visual performance, accommodative response and high-order aberrations were evaluated.

Subjectively and in terms of corrected distance visual acuity (CDVA), no statistically significant differences were found between both generations of MFCLs ( $t(14)=0.791$ ,  $p=0.442$ ). Distance corrected near visual acuity (DCNVA) showed a statistically significant difference between MFCLs ( $t(14)=3.327$ ,  $p=0.005$ ). Figure 5.1 shows that PureVision 2 High add provides better acuity for near tasks than its predecessor with a mean DCNVA of 0.06 logMAR against the mean DCNVA of 0.14 logMAR achieved by PureVision High add wearers.

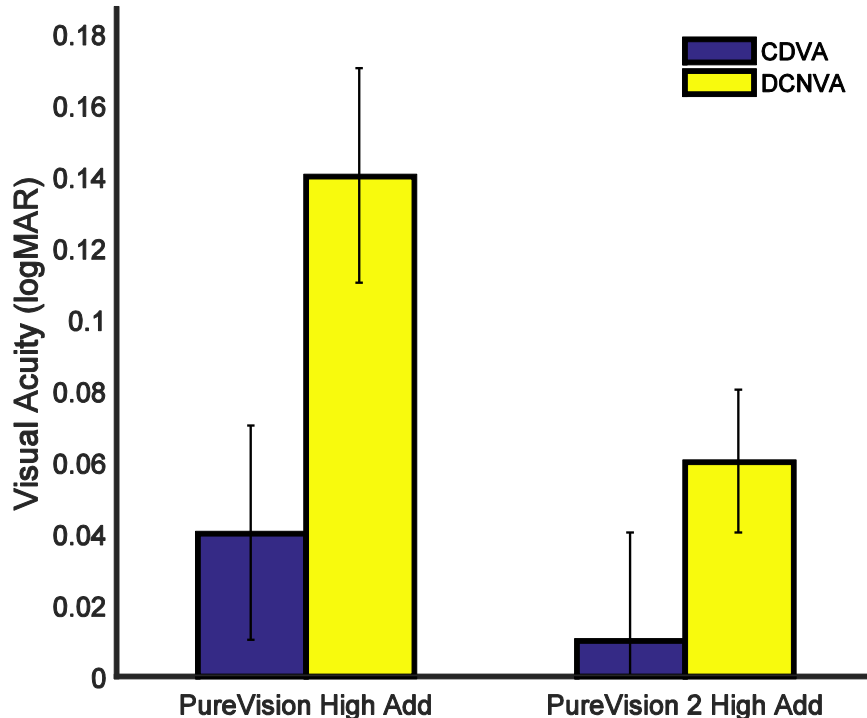


**Figure 5.1:** Mean CDVA and mean DCNVA in photopic conditions for subjects wearing the two types of simultaneous vision MFCLs. Error bars represent standard error.

Figure 5.2 shows the accommodative response that represents the combined effect of any correcting lens and the eye. Statistically significant differences between the three accommodative states (0 D, 2.5 D and 4 D) have been found for PureVision High Add (F, ANOVA(2,28)=181.161,  $p < 0.01$ ) and PureVision 2 High Add (F, ANOVA(2,28)=196.879,  $p < 0.01$ ). Figure 5.2 shows the accommodative response function with the two generations of MFCL which show very similar regression.

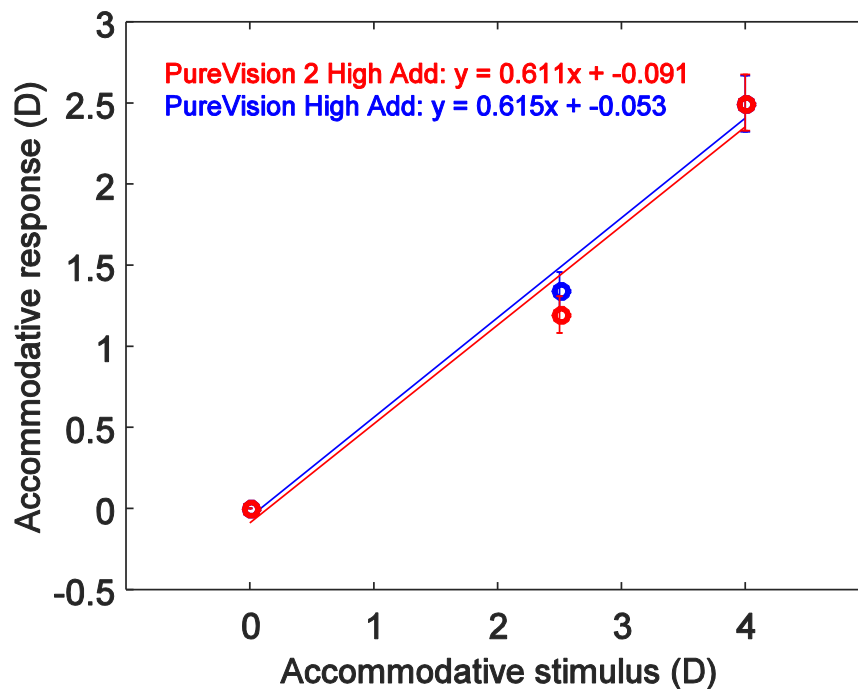
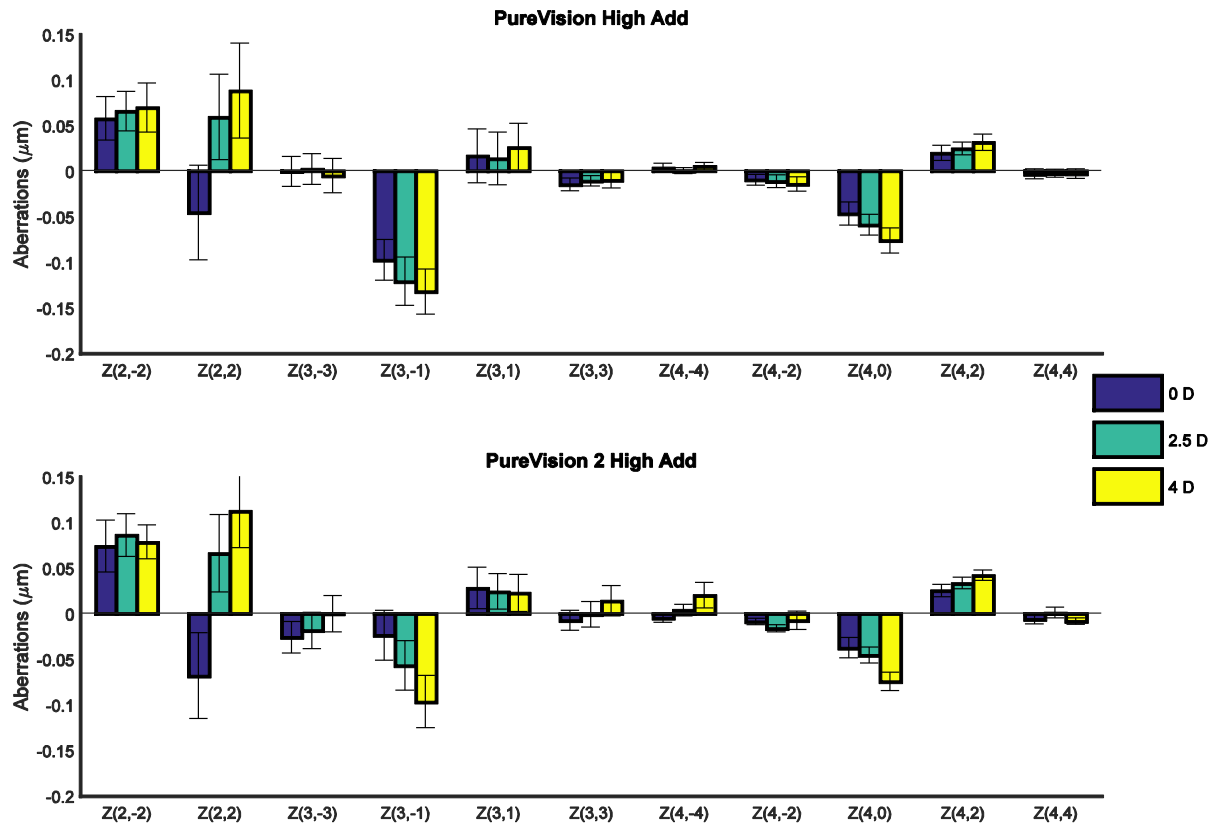


**Figure 5.2:** Mean stimulus-response function for each MFCL. The lines represent the best linear trend for each condition. Blue line refers to the PureVision High Add and red line represents the PureVision 2 High Add. Linear equations for each of the regressions is displayed on top of the graph for both conditions. Error bars represent standard error of the means.

Ocular aberrations with accommodation were assessed up to the 4<sup>th</sup> order since it has been demonstrated that the ocular wavefront aberration for small or medium

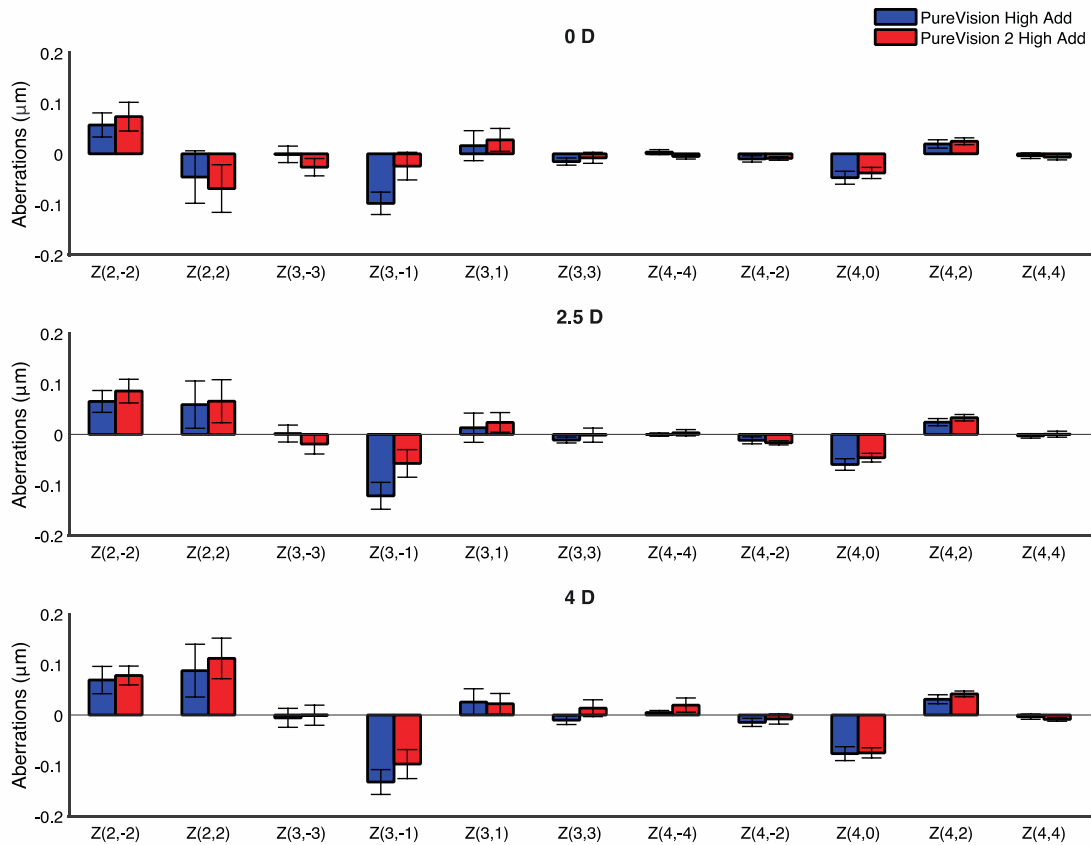
pupils is well depicted by using only Zernike polynomial terms up to the fourth-order.<sup>20</sup> Results of Repeated Measures ANOVA expose that statistically significant changes in several ocular aberrations are produced for the different accommodated states for each of the two MFCLs.

Figure 5.3 shows mean Zernike aberration coefficients when the three accommodative stimuli (0 D, 2.5 D and 4 D) were presented to PureVision and PureVision 2 High Add wearers. We found a statistically significant ( $p < 0.05$ ) increase towards negative values in vertical coma ( $Z_3^{-1}$ ) and spherical aberration ( $Z_4^0$ ). On the other hand, a statistically significant ( $p < 0.05$ ) positive shift in vertical astigmatism ( $Z_2^2$ ) was found in both MFCLs for all accommodated states.



**Figure 5.3:** Mean Zernike aberration coefficients when the three accommodative stimuli (0 D, 2.5 D and 4 D) were presented for the PureVision High Add and PureVision 2 High Add, respectively. Error bars represent standard error of the means.

Figure 5.4 shows mean Zernike aberration coefficients comparing the two types of simultaneous vision MFCLs for the three accommodative stimuli (0 D, 2.5 D and 4 D), respectively. For the 0 D stimulus, differences between both MFCLs were statistically significant ( $p < 0.05$ ) in vertical coma ( $Z_3^{-1}$ ). When the 2.5 D stimulus was presented we found greater and statistically significant ( $p < 0.05$ ) coefficients for PureVision High Add than for PureVision 2 High Add when vertical coma ( $Z_3^{-1}$ ) and spherical aberration ( $Z_4^0$ ) were assessed.



**Figure 5.4:** Mean Zernike aberration coefficients when the two types of simultaneous vision MFCLs were worn for the three accommodative stimuli (0 D, 2.5 D and 4 D), respectively. Error bars represent standard error of the means.

Finally, no statistically significant differences ( $p < 0.05$ ) in any Zernike coefficient were found between both MFCLs for the 4 D stimulus

## **5.5 DISCUSSION**

Some studies have assessed accommodative response and ocular aberrations in simultaneous vision MFCLs<sup>10-12, 21</sup> but this is the first study to investigate it in subjects wearing PureVision 2 High Add.

When evaluating results of monocular CDVA in PureVision High Add wearers, our results (CDVA=0.04 logMAR) coincide with those found by Ruiz-Alcocer et al.<sup>12</sup> and Llorente-Guillemot et al.<sup>21</sup> They encountered a CDVA of 0.06 logMAR and 0.03 logMAR, respectively. Despite the good results achieved and agreement between studies, even with those that measure it binocularly and after having worn them for one month;<sup>13, 15</sup> it should be taken into account that it has been suggested that the performance of MFCLs is always better and more likely to be similar to real life conditions in binocular than in monocular viewing<sup>22</sup> and can be improved over time due to possible neuroadaptation.<sup>23</sup> DCNVA results for PureVision High Add (DCNVA=0.14 logMAR) were worse than those found in other studies.<sup>11, 12, 15, 21</sup> This can be due, in part, to the different test charts used between studies. We used a Snellen chart that in some publications<sup>24, 25</sup> has been reported to result in an overestimation or underestimation of visual acuity because of the irregular size progression of the letters on the chart and the lack of a standardised scoring system. Significant differences were found in non-rotationally symmetric aberrations such as vertical coma between the two MFCLs. These differences in aberrations could have led to the differences in DCNVA between the two lens conditions, as the accommodative function was basically the same for the two MFCLs.

It is of interest to investigate how non-presbyopic subjects fitted with simultaneous vision MFCLs respond to objects over a range of distances. We did so monocularly in order to eliminate accommodation due to convergence that is present under binocular conditions<sup>26</sup> and therefore obtain the true accommodative response from the combined effect of the correcting lens and the eye. We explored the accommodative function for 2.5 D and 4 D of accommodative stimulus. We chose these vergences, in part, because they are the most studied vergences that will allow us to compare our results with those from previous publications and these distances also correspond to the distances at which daily tasks are performed. Large lags found in this study were expected due to the use of a Badal system and are in agreement with those found by Madrid-Costa et al.<sup>10</sup>, Ruiz-Alcocer et al.<sup>12</sup> and Montés-Micó et al.<sup>11</sup> when evaluating accommodative response with PureVision High Add wearers. Montés-Micó et al.,<sup>11</sup> also found the accommodative response change per dioptre of accommodation was of 0.460 D which is approximately 0.25 D lower than our results provided by the slope of the linear regression for PureVision High Add. We found very similar results for PureVision 2 High Add. Similar to previous comparison of MFCLs with single vision CLs,<sup>10-12</sup> our results indicate that both kinds of simultaneous vision MFCLs used in this study do not reduce accommodation in any way.

When no accommodative stimulus was presented, we found the negative spherical aberration ( $Z_4^0$ ) which is expected in a centre-near MFCL. This feature was also reported in the studies of Gifford et al.<sup>27</sup> who investigated the changes in aberrations induced by the PureVision High Add. This negative spherical aberration



( $Z_4^0$ ) in the relaxed eye has been suggested to be an influencing factor on accommodative lag.<sup>28</sup> Thus, it would help to enhance the add effect, increase the DoF and create a pseudo accommodation effect. This also explains the lags of about 1.25 D and 1.50 D that we encountered at the two accommodative stages (2.5 D and 4 D), respectively for both kind of MFCLs. This is because the depth of focus compensates for the accommodative effort while maintaining the image quality.

Our results concur with those from numerous studies which show a tendency for spherical aberration to shift towards negative values (which is linearly related to the accommodative effort).<sup>3, 6, 8, 29, 30</sup> In addition, this is in agreement with the only study<sup>12</sup> which evaluated ocular aberrations in PureVision High Add wearers and whose values of spherical aberration ( $Z_4^0$ ) and vertical coma ( $Z_3^{-1}$ ) are in accordance with those found in our study for both MFCLs. Despite the fact that third-order aberrations have been demonstrated to not represent a significant decrease in visual performance<sup>31</sup> and are not strongly involved in accommodation<sup>32</sup>; results of horizontal coma ( $Z_3^1$ ) in our study slightly differ from those of Ruiz-Alcocer et al.<sup>12</sup> According to the investigations of Guirao et al.<sup>33</sup>, higher-order aberrations are likely to be created due to translational lens movement. This effect is pronounced as a result of blinking which leads to movement of the lens. Studies of different soft CLs show varying degrees of excursion lag with eye movement and lens uplift with blink which can exceed  $550 \mu\text{m}$ <sup>29</sup> and lead to higher results of third-order RMS.<sup>33</sup> Translational lens movement could account for the differences in the amount of comatic aberrations found between this and previous studies as we did not do a

particularly tight fit of the two MFCLs evaluated at the diverse accommodative states.

The maximum addition that the MFCLs can reach is 2.50 D. Thus, it is of interest to examine the effect of both MFCLs at the focal point that will coincide with the subject's remote point when looking at near. At this stage all the participants were supposed not to accommodate. However, we enrolled pre-presbyopic subjects who would be able to trigger an accommodative response in the presence of blur rather than presbyopes lacking of accommodation capacity. Therefore, our results in accommodative response and increase in primary spherical aberration ( $Z_4^0$ ) with accommodation in both MFCLs indicate that an accommodative response was being produced when wearing both MFCLs. This is also consistent with our results of DCNVA which was measured for the same vergence (40 cm). DCNVA was significantly better for the PureVision 2 High Add and similarly, when statistically significant differences have been found in aberrations between both MFCLs (Figure 5.4), the magnitude of aberrations was lower for the PureVision 2 High Add. These results show that the main differences in DCNVA achieved by the subjects wearing the two different MFCLs were due to the MFCLs' optics and not to the accommodative function that was not better for any of the MFCLs evaluated in this study. A formal assessment or validated questionnaire to assess subjectively both MFCLs was not administered to the participants; however, most of them referred an increase of comfort wearing the PureVision 2. Hence, the physical properties of the PureVision 2 High Add were investigated further and this particular MFCL resulted to have a higher oxygen transmissibility (Dk/t) and is thinner. This can also

be translated into an improvement of the lens feature as has been demonstrated in the literature<sup>34</sup> that high oxygen levels are strongly connected with symptoms of comfort during soft contact lens wear.

We have provided data of the combined effects of any correcting lens and the eye for a 4 mm pupil size and due to the optical design of this kind of simultaneous vision MFCLs, the aberration data we got was averaged. This means that the error was not paraxially measured. By design the near vision area of the PureVision Multifocal High Add is 2.4 mm,<sup>35</sup> thus smaller than the area chosen in this study. This implies that the subjects were not only looking through the near vision area when accommodating but also throughout an area with less positive power. Hence, pupil diameter is a key issue when fitting simultaneous vision MFCLs. Besides, pupil size has inter- and intra-individual variations and it depends on the age of the individual, lighting and viewing conditions. It has been reported<sup>36</sup> that the change in pupil diameter per dioptre of accommodation is  $0.39 \text{ mm D}^{-1}$ . Consequently, if these MFCLs would have been fitted in early presbyopic subjects we probably would have obtained very small pupils as due to the senile miosis they would have started out from a smaller pupil diameter and the system would have been almost diffraction limited. This would make subjects to look only throughout the near vision area of the lenses providing a better visual performance and reaching the near VA values shown by presbyopes in numerous studies.<sup>15, 21, 37, 38</sup>

To sum up, we fitted simultaneous vision MFCLs in non-presbyopic subjects, both in the highest available addition. We found no relaxed accommodative response which results in a significant increase in some higher-order aberrations. Aberrations

introduced by both MFCLs, without considering the ones introduced by the eye, are different because the accommodative function was pretty much the same for both MFCLs. Consequently, from the results achieved with PureVision 2 High Add, it seems that the contact lens market is improving. Pupil diameter is a critical parameter when fitting simultaneous vision MFCLs and the differences in pupil size between younger and older people suggest that all these results should be treated carefully when trying to extrapolate them to presbyopic wearers which will be the potential users.

## 5.6 REFERENCES

1. Donders FC, Moore WD. On the anomalies of accommodation and refraction of the eye: With a preliminary essay on physiological dioptrics: The New Sydenham Society; 1864.
2. Duane A. Normal values of the accommodation at all ages. *JAMA* 1912;59:1010-1013.
3. Kalsi M, Heron G, Charman W. Changes in the static accommodation response with age. *Ophthalmic Physiol Opt* 2001;21:77-84.
4. Ramsdale C, Charman W. A longitudinal study of the changes in the static accommodation response. *Ophthalmic Physiol Opt* 1989;9:255-263.
5. Turner M. Observations on the normal subjective amplitude of accommodation. *Br J Physiol Opt* 1958;15:70.
6. Charman WN. Developments in the correction of presbyopia I: spectacle and contact lenses. *Ophthalmic Physiol Opt* 2014;34:8-29.
7. Montes-Mico R, Madrid-Costa D, Dominguez-Vicent A, Belda-Salmeron L, Ferrer-Blasco T. In vitro power profiles of multifocal simultaneous vision contact lenses. *Cont Lens Anterior Eye* 2014;37:162-167.
8. Morgan PB, Efron N, Woods CA. An international survey of contact lens prescribing for presbyopia. *Clin Exp Optom* 2011;94:87-92.
9. Sreenivasan V, Irving EL, Bobier WR. Binocular adaptation to near addition lenses in emmetropic adults. *Vision Res* 2008;48:1262-1269.

10. Madrid-Costa D, Ruiz-Alcocer J, Radhakrishnan H, Ferrer-Blasco T, Montes-Mico R. Changes in accommodative responses with multifocal contact lenses: a pilot study. *Optom Vis Sci* 2011;88:1309-1316.
11. Montes-Mico R, Madrid-Costa D, Radhakrishnan H, Charman WN, Ferrer-Blasco T. Accommodative functions with multifocal contact lenses: a pilot study. *Optom Vis Sci* 2011;88:998-1004.
12. Ruiz-Alcocer J, Madrid-Costa D, Radhakrishnan H, Ferrer-Blasco T, Montes-Mico R. Changes in accommodation and ocular aberration with simultaneous vision multifocal contact lenses. *Eye Contact Lens* 2012;38:288-294.
13. Gupta N, Naroo SA, Wolffsohn JS. Visual comparison of multifocal contact lens to monovision. *Optom Vis Sci* 2009;86:E98-105.
14. Garcia-Lazaro S, Ferrer-Blasco T, Madrid-Costa D, Albarran-Diego C, Montes-Mico R. Visual Performance of Four Simultaneous-Image Multifocal Contact Lenses Under Dim and Glare Conditions. *Eye Contact Lens* 2014.
15. Ferrer-Blasco T, Madrid-Costa D. Stereoacuity with simultaneous vision multifocal contact lenses. *Optom Vis Sci* 2010;87:E663-668.
16. Ferrer-Blasco T, Madrid-Costa D. Stereoacuity with balanced presbyopic contact lenses. *Clin Exp Optom* 2011;94:76-81.
17. Bara S, Pailos E, Arines J, Lopez-Gil N, Thibos L. Estimating the eye aberration coefficients in resized pupils: is it better to refit or to rescale? *J Opt Soc Am A Opt Image Sci Vis* 2014;31:114-123.
18. Anderson HA, Glasser A, Manny RE, Stuebing KK. Age-related changes in accommodative dynamics from preschool to adulthood. *Invest Ophthalmol Vis Sci* 2010;51:614-622.

19. Thibos LN, Hong X, Bradley A, Applegate RA. Accuracy and precision of objective refraction from wavefront aberrations. *J Vis* 2004;4:329-351.
20. Castejon-Mochon JF, Lopez-Gil N, Benito A, Artal P. Ocular wave-front aberration statistics in a normal young population. *Vision Res* 2002;42:1611-1617.
21. Llorente-Guillemot A, Garcia-Lazaro S, Ferrer-Blasco T, Perez-Cambrodi RJ, Cervino A. Visual performance with simultaneous vision multifocal contact lenses. *Clin Exp Optom* 2012;95:54-59.
22. Plainis S, Ntzilepis G, Atchison DA, Charman WN. Through-focus performance with multifocal contact lenses: effect of binocularity, pupil diameter and inherent ocular aberrations. *Ophthalmic Physiol Opt* 2013;33:42-50.
23. Pepin SM. Neuroadaptation of presbyopia-correcting intraocular lenses. *Curr Opin Ophthalmol* 2008;19:10-12.
24. McGraw P, Winn B, Whitaker D. Reliability of the Snellen chart. *BMJ* 1995;310:1481-1482.
25. Williams MA, Moutray TN, Jackson AJ. Uniformity of visual acuity measures in published studies. *Invest Ophthalmol Vis Sci* 2008;49:4321-4327.
26. Berntsen DA, Kramer CE. Peripheral defocus with spherical and multifocal soft contact lenses. *Optom Vis Sci* 2013;90:1215-1224.
27. Gifford P, Cannon T, Lee C, Lee D, Lee HF, Swarbrick HA. Ocular aberrations and visual function with multifocal versus single vision soft contact lenses. *Cont Lens Anterior Eye* 2013;36:66-73; quiz 103-104.
28. Lopez-Gil N, Fernandez-Sanchez V. The change of spherical aberration during accommodation and its effect on the accommodation response. *J Vis* 2010;10:12.

29. Cui L, Shen M, Wang MR, Wang J. Micrometer-scale contact lens movements imaged by ultrahigh-resolution optical coherence tomography. *Am J Ophthalmol* 2012;153:275-283 e271.
30. Phillips S, Stark L. Blur: a sufficient accommodative stimulus. *Doc Ophthalmol* 1977;43:65-89.
31. Fernandez-Sanchez V, Ponce ME, Lara F, Montes-Mico R, Castejon-Mochon JF, Lopez-Gil N. Effect of 3rd-order aberrations on human vision. *J Cataract Refract Surg* 2008;34:1339-1344.
32. Lopez-Gil N, Rucker FJ, Stark LR, et al. Effect of third-order aberrations on dynamic accommodation. *Vision Res* 2007;47:755-765.
33. Guirao A, Williams DR, Cox IG. Effect of rotation and translation on the expected benefit of an ideal method to correct the eye's higher-order aberrations. *J Opt Soc Am A Opt Image Sci Vis* 2001;18:1003-1015.
34. Dillehay SM. Does the level of available oxygen impact comfort in contact lens wear?: A review of the literature. *Eye Contact Lens* 2007;33:148-155.
35. Plainis S, Atchison DA, Charman WN. Power profiles of multifocal contact lenses and their interpretation. *Optom Vis Sci* 2013;90:1066-1077.
36. Kasthurirangan S, Glasser A. Characteristics of pupil responses during far-to-near and near-to-far accommodation. *Ophthalmic Physiol Opt* 2005;25:328-339.
37. Garcia-Lazaro S, Albarran-Diego C, Ferrer-Blasco T, Radhakrishnan H, Montes-Mico R. Visual performance comparison between contact lens-based pinhole and simultaneous vision contact lenses. *Clin Exp Optom* 2013;96:46-52.



38. Madrid-Costa D, Garcia-Lazaro S, Albarran-Diego C, Ferrer-Blasco T, Montes-Mico R. Visual performance of two simultaneous vision multifocal contact lenses. *Ophthalmic Physiol Opt* 2013;33:51-56.

## **6 FINAL SUMMARY AND FUTURE WORK**

Gaining a better understanding of the changes the human accommodative system undergoes with age was the main purpose of the present PhD thesis.

The first experimental chapters (2 and 3) explored accommodation from a structural perspective. Results of Chapter 2 showed that the cornea is stable during accommodation in young adults with full accommodative ability, which allowed us to go further and study the changes that happen in the ciliary muscle with accommodation, not only in young but also in an older cohort (Chapter 3). This is because from Chapter 2 one can assume that anatomical images of the eye do not need to be corrected when the eye is accommodating due to corneal effects. Similarly, the steadiness of corneal aberrations during accommodation found in Chapter 2 suggests that the main contributor to the changes in aberrations is unlikely to be the cornea. Chapter 3 shows that the changes in paraxial M (calculated from defocus and primary SA data) at different accommodative demands are primarily due to changes in the crystalline lens. Furthermore, in Chapter 3 by comparing structural (slope of the CMT with accommodation) and functional (slope of the paraxial M with accommodation) features of the accommodation process, we were able to confirm Fincham's theory of presbyopia. We found out that younger people with more deformable crystalline lenses produce a smaller change in ciliary muscle thickness to accurately accommodate than older people. However, changes in ciliary muscle thickness can be attributed to accommodation and do not occur as a result of ageing.

Following the studies outlined in Chapters 2 and 3 in which accommodation was assessed only from a static point of view, we took interest in investigating the dynamics of accommodation. Studies in chapters 4 and 5 aimed to both understand the development of presbyopia and the optical performance of some of the current solutions for presbyopia correction. Thus, in Chapter 4 accommodative dynamics were assessed in different age groups including participants over 50 years, since most of the optical changes are expected to be happening after the onset of presbyopia. No significant variation in time constants and a reduction in amplitude of accommodation with age were found in Chapter 4. Subjects over 40 years demonstrated reduced accommodation capacity when fluctuations in accommodation were assessed. A rise in the magnitude of fluctuations was found in subjects aged less than 40 when the smaller stimulus demand was presented, being those in their 30's the ones that had the higher fluctuations in accommodation. This may indicate that accommodative fluctuations play a role in accommodation control since a bigger effort of the accommodative system was being produced with higher accommodation accuracy. Lower fluctuations were found in order to accommodate more accurately when a high accommodative demand was presented to those with possibly more blur tolerance (myopes and presbyopes). The accommodative performance when young participants were fitted with MFCLs resembled that of the naked eye situation. Therefore, Chapter 5 looked into the changes in accommodation and ocular aberrations with two generations of MFCLs. Accommodative response in pre-presbyopic subjects fitted with two different MFCLs was assessed in Chapter 5 and found to be almost identical for both MFCLs.

However, the latest MFCL introduced to the market presented smaller magnitude of aberrations and delivered significantly better near VA.

Experimental Chapters 2 to 5 were intended to meet the specific objectives posed at the beginning of this thesis, which are addressed below:

- ***Clarifying how accommodation affects the cornea (including the peripheral area) and its aberrations.***

Despite the small sample, the results were conclusive enough to clarify that anterior and posterior corneal keratometry as well as total corneal power (TCP) and pachymetry, are stable during accommodation even in the periphery of the cornea (7 to 10 mm) in a sample of 7 healthy young emmetropes. Likewise, total corneal aberrations obtained from topographic height data did not change at different accommodative states.

- ***Looking into the relationship between the accommodative response and evaluate the changes in the ciliary muscle characteristics in an age divided cohort at different accommodative levels.***

In spite of the lack of standardized methods to measure and analyse the ciliary muscle characteristics, I managed to gather data from 18 subjects whose ciliary muscle thickness (CMT) was measured at three different locations and at three different accommodative states. These results obtained along with those from the accommodative response, allowed me to assess the relationship between both and find out that there are not changes in CMT because of age but with accommodation. This supports Fincham's theory of presbyopia as younger subjects exhibited a smaller

ciliary muscle change in relation with their accommodative response accuracy compared to older subjects.

- ***Knowing the extent of microfluctuations for distance and near to understand the changes in microfluctuations with age by extending the age range to 70 years.***

Working towards the completion of this objective was very difficult due to the complexity of the acquisition and analysis of dynamic accommodation measurements. However, the results allowed me to understand better the high inter- and intra-subject variability that exists in the accommodative function and to describe the nature of the small amplitude changes that happen in accommodation in subjects of different ages. These results suggested that there is an increase in the accommodative fluctuations in the 3<sup>rd</sup> decade of life when the accommodative demand is in the middle of the subject's amplitude of accommodation range. Additionally, assessment of the relationship between fluctuations and accommodative response accuracy suggested that accommodative fluctuations might play a role in controlling the accommodative system to some extent.

- ***Assessing the accommodative and disaccommodative performance in both static and dynamic conditions in young subjects fitted with MFCLs.***

This objective was achieved by looking into the static and dynamic measurements of both the accommodative and disaccommodative performance of the same young subjects fitted with two different designs of MFCLs. Results show that the accommodative performance mimicked that of the naked eye situation. This suggests that accommodation is used by

young people fitted with MFCLs as they do not interfere in the accommodative performance.

- ***Investigating if changes are produced in accommodation and ocular aberrations while wearing two generations of simultaneous vision MFCLs.***

Although pupil size is a key parameter in MFCLs fitting and I used a fixed one to assume a constant effect of the CLs in every subject, no difference in accommodative performance was found between the two centre-near design MFCLs. However, aberrations introduced by each MFCL were different.

All the research included in this thesis studies the accommodative system from a fundamental science point of view with a view to improve the current methods of presbyopia correction and the level of vision care that can be provided. In order to produce future research in this field, the limitations spotted in the planning, development and completion of the studies included in this thesis would be worth considering. Substantial intersubject variability in aberrations and accommodation data has been extensively reported in the literature<sup>1</sup>, which is shared with the outcomes of this thesis. This high variability has led to a large amount of lost data, especially in accommodative dynamics measurements. Moreover, the number of subjects over 40 years of age meeting the inclusion criteria and willing to participate in the studies was reduced. This low rate of older subjects recruited was a concern when trying to assess the effects of age in presbyopic subjects. Finally, the lack of standardized methods for non-invasive ciliary muscle and continuous accommodation assessment and analysis was another limitation. The incipient state

of commercialized methods for ciliary muscle characteristics and continuous accommodation evaluation along with the lack of consensus in data analysis makes the implementation of these exams in the daily clinical practice very difficult. Therefore, further research towards this objective is warranted. It would be extremely useful to be able to measure the stability of accommodation and the ciliary muscle characteristics in a standardized fashion prior to cataract surgery. This would improve the level of surgery customization not only when an IOL is being implanted but also in nascent, experimental yet unproven approaches that aim to restore the dynamic young accommodative function in an adult eye such as lens refilling or photodisruption.<sup>2</sup>

The next step forward could be evaluating accommodation dynamics and ciliary muscle characteristics in individuals implanted with multifocal and accommodating intraocular lenses (IOLs), which are currently being implanted, to further investigate their optical performance along with the functionality of the ciliary muscle, especially in accommodating IOLs.

## 6.1 REFERENCES

1. Charman WN, Heron G. Microfluctuations in accommodation: an update on their characteristics and possible role. *Ophthalmic Physiol Opt* 2015;35:476-499.
2. Charman WN. Developments in the correction of presbyopia II: surgical approaches. *Ophthalmic Physiol Opt* 2014.

## APPENDIX

### MATLAB® Program to read .txt files of continuous measurements from irx3 and process them

#### Initialize variables

```
datapath =  
'C:\AGEYEproject\THESIS\STUDIES\ContinuousMeasurements\Age1\Raw  
data\';  
  
patientfilename = dir(datapath);
```

#### Create empty variables to allocate results

```
Tconstants2 = zeros(180,39);  
info2 = cell(180,2);  
Tconstants4 = zeros(180,39);  
info4 = cell(180,2);
```

#### Select .txt file

```
for i = 3:length(patientfilename);delimiter = sprintf('\t', '');  
delimiter = sprintf('\t', '');  
patientname = patientfilename(i).name;
```

#### Open the file and get the number of columns

```
fileID = fopen([datapath, patientfilename(i).name], 'r');  
for j = 1:10;  
    tLines = fgets(fileID);  
end  
nCols = numel(strfind(tLines,delimiter)+1)+1;  
fclose(fileID);
```

#### Format string for each column of text

```
formatspec = [repmat('%s', [1 nCols]), '%[\n\r]'];
```

#### Open the text file

```
fileID = fopen([datapath, patientfilename(i).name], 'r');
```



## Read columns of data according to format string

```
dataArray = textscan(fileID, formatSpec, 'Delimiter', delimiter,...  
    'EmptyValue' ,NaN, 'ReturnOnError', false);
```

## Close the text file

```
fclose(fileID);
```

## Create output variable

```
patientname = [dataArray{1:end-1}];
```

## Transpose the cell so Zernikes are sorted by columns

```
sortedpatientname = patientname.';  
[zernikes_col,zernikes_rows]=size(sortedpatientname);
```

## Create a structure to organize and separate data (by columns)

```
patient = struct;  
patient.date = sortedpatientname(2,1);  
patient.softwareVers = sortedpatientname(2,2);  
patient.name = sortedpatientname(2,3);  
patient.initials = sortedpatientname(2,4);  
patient.birthDate = sortedpatientname(2,5);  
patient.visit = sortedpatientname(2,6);  
patient.measurementNo = str2double(sortedpatientname(2,7));  
patient.eye = sortedpatientname(2,8);  
patient.pupil = str2double(sortedpatientname(2:end,[10,21]));  
patient.stimulusVergence = str2double(sortedpatientname(2:end,11));  
patient.sphEq = patient.stimulusVergence(2,1);  
patient.time = str2double(sortedpatientname(2:end,12));  
patient.rx = str2double(sortedpatientname(2:end,[13,14,15]));%  
Sph,cyl,axis  
patient.fittingQ = str2double(sortedpatientname(2:end,26));  
patient.Zmicrons = str2double(sortedpatientname...  
    (2:end,27:((zernikes_rows-29)/2)+26));% ANSI order for Zernikes  
patient.Zdiopters = str2double(sortedpatientname...  
    (2:end,(((zernikes_rows-29)/2)+30):end));  
% ANSI order for Zernikes, the number of Zernikes  
% for microns and diopters is always the same  
patient.Mpx = [((patient.Zmicrons(:,2))*-4*sqrt(3) +...  
    patient.Zmicrons(:,10)*12*sqrt(5))./(...  
    (patient.pupil(:,2)./2).^2))-patient.sphEq]; %Get M paraxial
```

```

patient.SAeq = [((24*sqrt(5)./((patient.pupil(:,2)./2).^4)).* ...
    patient.zmicrons(:,10))]; %Equivalent dioptres of spherical
aberration
%calculated from the primary sph aberration z(4,0)
patient.rxSph = patient.rx(:,1) - patient.sphEq;

```

### Correct the stimulus vergence and identify when the stimulus was switched

```

idx = find(patient.stimulusVergence(2:end,1)~= patient.sphEq);
firstEle = idx(1,:)+1;
lastEle = idx(end,:)+1;
verg = (((patient.stimulusVergence(firstEle,:)-patient.sphEq)*-
1)*10);
patient.stimulusVergence = patient.stimulusVergence-patient.sphEq;

```

## PROCESS DATA DEPENDING ON THE ACCOMMODATIVE STIMULUS PRESENTED

### Stimulus: 2.5 D

```
if verg == 25;
```

### Correction for elements in which the Badal was moving

```
(info provided by manufacturer)
stimatedMvt = 0.3066666666666667;
% ACCOMMODATION:
patient.Mpx(firstEle-1,1) = patient.Mpx(firstEle-1,1) + (-8 *
stimatedMvt);
patient.Mpx(firstEle-2,1) = patient.Mpx(firstEle-2,1) + (-7 *
stimatedMvt);
patient.Mpx(firstEle-3,1) = patient.Mpx(firstEle-3,1) + (-6 *
stimatedMvt);
patient.Mpx(firstEle-4,1) = patient.Mpx(firstEle-4,1) + (-5 *
stimatedMvt);
patient.Mpx(firstEle-5,1) = patient.Mpx(firstEle-5,1) + (-4 *
stimatedMvt);
patient.Mpx(firstEle-6,1) = patient.Mpx(firstEle-6,1) + (-3 *
stimatedMvt);
patient.Mpx(firstEle-7,1) = patient.Mpx(firstEle-7,1) + (-2 *
stimatedMvt);
patient.Mpx(firstEle-8,1) = patient.Mpx(firstEle-8,1) + (-1 *
stimatedMvt);

% DISACCOMMODATION:
patient.Mpx(lastEle,1) = patient.Mpx(lastEle,1) - (-8 *
stimatedMvt);
patient.Mpx(lastEle-1,1) = patient.Mpx(lastEle-1,1) - (-7 *
stimatedMvt);
patient.Mpx(lastEle-2,1) = patient.Mpx(lastEle-2,1) - (-6 *
stimatedMvt);
patient.Mpx(lastEle-3,1) = patient.Mpx(lastEle-3,1) - (-5 *
stimatedMvt);
patient.Mpx(lastEle-4,1) = patient.Mpx(lastEle-4,1) - (-4 *
stimatedMvt);
patient.Mpx(lastEle-5,1) = patient.Mpx(lastEle-5,1) - (-3 *
stimatedMvt);
patient.Mpx(lastEle-6,1) = patient.Mpx(lastEle-6,1) - (-2 *
stimatedMvt);
patient.Mpx(lastEle-7,1) = patient.Mpx(lastEle-7,1) - (-1 *
stimatedMvt);
```

## Correction for elements in which the Badal was moving

(info provided by manufacturer)

**% ACCOMMODATION:**

```
patient.stimulusVergence(firstEle-1,1) = -8 * stimatedMvt;  
patient.stimulusVergence(firstEle-2,1) = -7 * stimatedMvt;  
patient.stimulusVergence(firstEle-3,1) = -6 * stimatedMvt;  
patient.stimulusVergence(firstEle-4,1) = -5 * stimatedMvt;  
patient.stimulusVergence(firstEle-5,1) = -4 * stimatedMvt;  
patient.stimulusVergence(firstEle-6,1) = -3 * stimatedMvt;  
patient.stimulusVergence(firstEle-7,1) = -2 * stimatedMvt;  
patient.stimulusVergence(firstEle-8,1) = -1 * stimatedMvt;
```

**% DISACCOMMODATION:**

```
patient.stimulusVergence(lastEle,1) = -1 * stimatedMvt;  
patient.stimulusVergence(lastEle-1,1) = -2 * stimatedMvt;  
patient.stimulusVergence(lastEle-2,1) = -3 * stimatedMvt;  
patient.stimulusVergence(lastEle-3,1) = -4 * stimatedMvt;  
patient.stimulusVergence(lastEle-4,1) = -5 * stimatedMvt;  
patient.stimulusVergence(lastEle-5,1) = -6 * stimatedMvt;  
patient.stimulusVergence(lastEle-6,1) = -7 * stimatedMvt;  
patient.stimulusVergence(lastEle-7,1) = -8 * stimatedMvt;
```

## RMS deviation and time constants calculation

**% DEFINE EACH SECTION (stimulusVergence):**

```
svdisacc1 = patient.stimulusVergence(1 : idx(1,1)-8, 1);  
svacc = patient.stimulusVergence(idx(1,1)+1 : idx(end,1)-7, 1);  
svdisacc2 = patient.stimulusVergence(idx(end,1)+2 : end, 1);
```

**% Avg refraction in defined baseline sections**

```
baseX = mean(patient.Mpx(31 : idx(1,1)-18, 1));  
baseXstd = std(patient.Mpx(31 : idx(1,1)-18, 1));  
baseY = mean(patient.Mpx(idx(1,1)+31 : idx(end,1)-17, 1));  
baseYstd = std(patient.Mpx(idx(1,1)+31 : idx(end,1)-17, 1));  
baseZ = mean(patient.Mpx(idx(end,1)+32 : end-10, 1));  
baseZstd = std(patient.Mpx(idx(end,1)+32 : end-10, 1));
```

**% RMS deviation in defined baseline sections**

**% X**

```
baseX_HOARMS = sqrt(sum(patient.Zmicrons(31 : idx(1,1)-18,  
4:12).^2,2));  
AvgbaseX_HOARMS = mean(baseX_HOARMS);  
baseX_HOARMSsd = sqrt(1/length(baseX_HOARMS)*...  
(sum((baseX_HOARMS(:,1) - mean(baseX_HOARMS)).^2)));
```

```
baseX_MpxRMS = patient.Mpx(31 : idx(1,1)-18, 1);  
AvgbaseX_MpxRMS = mean(baseX_MpxRMS);
```

```

baseX_MpxRMSsd = sqrt(1/length(baseX_MpxRMS)*...
    (sum((baseX_MpxRMS(:,1) - mean(baseX_MpxRMS)).^2)));

baseX_SAEqRMS = patient.SAEq(31 : idx(1,1)-18, 1);
AvgbaseX_SAEqRMS = mean(baseX_SAEqRMS);
baseX_SAEqRMSsd = sqrt(1/length(baseX_SAEqRMS)*...
    (sum((baseX_SAEqRMS(:,1) - mean(baseX_SAEqRMS)).^2)));

% Y
baseY_HOARMS = sqrt(sum(patient.Zmicrons(idx(1,1)+31 : ...
    idx(end,1)-17, 4:12).^2,2));
AvgbaseY_HOARMS = mean(baseY_HOARMS);
baseY_HOARMSsd = sqrt(1/length(baseY_HOARMS)*(sum...
    ((baseY_HOARMS(:,1) - mean(baseY_HOARMS)).^2)));

baseY_MpxRMS = patient.Mpx(idx(1,1)+31 : idx(end,1)-17, 1);
AvgbaseY_MpxRMS = mean(baseY_MpxRMS);
baseY_MpxRMSsd = sqrt(1/length(baseY_MpxRMS)*(sum...
    ((baseY_MpxRMS(:,1) - mean(baseY_MpxRMS)).^2)));

baseY_SAEqRMS = patient.SAEq(idx(1,1)+31 : idx(end,1)-17, 1);
AvgbaseY_SAEqRMS = mean(baseY_SAEqRMS);
baseY_SAEqRMSsd = sqrt(1/length(baseY_SAEqRMS)*(sum...
    ((baseY_SAEqRMS(:,1) - mean(baseY_SAEqRMS)).^2)));

% Z
baseZ_HOARMS = sqrt(sum(patient.Zmicrons(idx(end,1)+32 : end-10,
    4:12).^2,2));
AvgbaseZ_HOARMS = mean(baseZ_HOARMS);
baseZ_HOARMSsd = sqrt(1/length(baseZ_HOARMS)*...
    (sum((baseZ_HOARMS(:,1) - mean(baseZ_HOARMS)).^2)));

baseZ_MpxRMS = patient.Mpx(idx(end,1)+32 : end-10, 1);
AvgbaseZ_MpxRMS = mean(baseZ_MpxRMS);
baseZ_MpxRMSsd = sqrt(1/length(baseZ_MpxRMS)*...
    (sum((baseZ_MpxRMS(:,1) - mean(baseZ_MpxRMS)).^2)));

baseZ_SAEqRMS = patient.SAEq(idx(end,1)+32 : end-10, 1);
AvgbaseZ_SAEqRMS = mean(baseZ_SAEqRMS);
baseZ_SAEqRMSsd = sqrt(1/length(baseZ_SAEqRMS)*...
    (sum((baseZ_SAEqRMS(:,1) - mean(baseZ_SAEqRMS)).^2)));

% Calculate Amplitudes
A = abs(baseY)-abs(baseX);
B = abs(baseY)-abs(baseZ);

```

```

% Time interval in defined baseline sections
basexTime = -(patient.time(32,1) - patient.time(idx(1,1)-18, 1));
portionX = basexTime; % ms of sustained accommodative response
begX = patient.time(32,1); % ms after the stimulus presentation that
we
%take to start considering the sustained accommodative response
portion
baseYTime = -(patient.time(idx(1,1)+31,1) - patient.time(idx(end,1)-
17, 1));
portionY = baseYTime;
begY = patient.time(idx(1,1)+31,1) - patient.time(idx(1,1)+1,1); %
ms after
%the stimulus presentation that we take to start considering the
sustained
%accommodative response portion
baseZTime = -(patient.time(idx(end,1)+32,1) - patient.time(end-10,
1));
portionZ = baseZTime;
begZ = patient.time(idx(end,1)+32,1) -
patient.time(idx(end,1)+2,1); % ms
%after the stimulus presentation that we take to start considering
the
%sustained accommodative response portion

% DEFINE EACH SECTION (Mpx): from the beginning of the transition
when the
% stimulus was presented to the 41th data point in the next section
Mpxdisacc1 = patient.Mpx(1 : idx(1,1)-8, 1);
Mpxtrans1 = patient.Mpx(idx(1,1)-7:idx(1,1)+40,1); %from the
beginning of
%the transition when the stimulus was presented to the beginning of
the
%baseline section Y (starting on point 40)
Mpxacc = patient.Mpx(idx(1,1)+1 : idx(end,1)-7, 1);
Mpxtrans2 = patient.Mpx(idx(end,1)-6:idx(end,1)+41,1);%from the
beginning of
%the transition when the stimulus was moved to OD to the beginning
of the
%baseline section Z (starting on point 40)
Mpxdisacc2 = patient.Mpx(idx(end,1)+2 : end, 1);

% DEFINE EACH SECTION (time): from the beginning of the transition
when the
% stimulus was presented to the 41th data point in the next section
TimeTrans1 = patient.time(idx(1,1)-7:idx(1,1)+40,1); %from the end
of

```

```

%baseline section X to the beginning of baseline section Y
Timetrans2 = patient.time(idx(end,1)-6:idx(end,1)+41,1);%from the
end of
%baseline section Y to the beginning of baseline section Z

% DEFINE CALCULATION SECTIONS
% ACCOMMODATION

x = diff(Mpxtrans1)<0; %logical vector that returns wether the
difference
%between that number with respect to the previous one is negative
(decrease)
for j = 1:(length(x)-3)
    y(j) = ([x(j,1)+x(j+1,1)+x(j+2,1)+x(j+3,1)]==3 && ...
        [x(j+1,1)+x(j+2,1)+x(j+3,1)]==3);% logical vector that
returns ones
    %when there are 4 consecutive decreasing numbers (at least 3
zeros in
    %the logical vector x) even if the first one does not decrease
with
    %respect to the previous one
end
indexey = find(y == true); %find which is the first series that
decreases.
%That point will delimitate the portion in which the time constant
cut off
%points will be calculated
if isempty(indexey)
    display([patientfilename(i).name,...
        '___accommodation(a): No consecutive... decreasing data
points found'])
else
    x1 = diff(Mpxtrans1)>0;%logical vector that returns wether the
difference
    %between that number with respect to the previous one is positive
(increase)
    for j = 1:(length(x1)-3)
        y1(j) = ([x1(j,1)+x1(j+1,1)+x1(j+2,1)+x1(j+3,1)]==3 &&...
            [x1(j+1,1)+x1(j+2,1)+x1(j+3,1)]==3);
    end
    indexey1 = find(y1 == true);
    if isempty(indexey1)
        display([patientfilename(i).name,...
            '___accommodation(b): No consecutive decreasing data
points found'])
    else

```

```

% Define section in which the cut off values will be
calculated (Mpx and time)
Mpxcalc1 = Mpxtrans1(indicey(1,1)+1 : indicey(1,1)+1,1);
%portion
%from the first number that makes 4 consecutive decreasing
numbers
%to the first number that makes 4 consecutive increasing
numbers.
Timecalc1 = Timetrans1(indicey(1,1)+1 : indicey(1,1)+1,1);
% Plot stimulus vergence, Mpx and calculation zone
boundaries
% vs time and save it
figure('Name', [patientfilename(i).name, '_M_25_TC'])
xlim([0,20]);
ylim([-6,6]);
title('Dynamic accommodative response');
xlabel('Time (s)');
ylabel('Paraxial Equivalent Refraction (D)');
hold on
plot(patient.time/1000,patient.stimulusVergence,'k');
hold on;
plot(patient.time(1:31, 1)/1000, patient.Mpx(1:31, 1),'b');
%blue line when no baseline section
hold on;
plot(patient.time(31 : idx(1,1)-18, 1)/1000,...
      patient.Mpx(31 : idx(1,1)-18, 1),'r'); %red line when
baseline section
hold on;
plot(patient.time(idx(1,1)-18:idx(1,1)+31,1)/1000,...
      patient.Mpx(idx(1,1)-18:idx(1,1)+31,1),'b');
hold on;
plot(patient.time(idx(1,1)+31 : idx(end,1)-17, 1)/1000,...
      patient.Mpx(idx(1,1)+31 : idx(end,1)-17, 1),'r');
hold on;
plot(patient.time(idx(end,1)-17:idx(end,1)+32,1)/1000,...
      patient.Mpx(idx(end,1)-17:idx(end,1)+32,1),'b');
hold on;
plot(patient.time(idx(end,1)+32 : end-10, 1)/1000,...
      patient.Mpx(idx(end,1)+32 : end-10, 1),'r');
hold on
if isempty(Timecalc1)
    display([patientfilename(i).name, '___invalid
accommodation'])
else
% Locate cut-off points in the calculation sections
a = baseX + (0.1*A);

```



```

[w index] = min(abs(Mpxcalc1-a));
ida = index; % Finds first one only
a = Timecalc1(ida,1)/1000;
aplot = [a,a];
yaxisplot = [6,-6];
plot(aplot,yaxisplot,'c--')
hold on;

b = baseY - (0.1*A);
[w index] = min(abs(Mpxcalc1-b));
idb = index; % Finds first one only
b = Timecalc1(idb,1)/1000;
bplot = [b,b];
yaxisplot = [6,-6];
plot(bplot,yaxisplot,'c--')
hold on;

% Time constants
Tacc = (b-a)/log(9);

% save relevant data
Tconstants2(i,1:11) = [verg, baseX, baseXstd, baseY,
baseYstd,...
baseZ, baseZstd, A, B, a, b];
Tconstants2(i,14) = Tacc;

% Plot stimulus vergence, Mpx and calculation zone
boundaries vs
% time and save it
plot(Timecalc1(1,1)/1000,Mpxcalc1(1,1),'g*',...
Timecalc1(end,1)/1000,Mpxcalc1(end,1),'g*')
hold on
end
end
end

% DISACCOMMODATION
w = diff(Mpxtrans2)>0;
for j = 1:(length(w)-3)
q(j) = ([w(j,1)+w(j+1,1)+w(j+2,1)+w(j+3,1)]==3 &&...
[w(j+1,1)+w(j+2,1)+w(j+3,1)]==3);
end
indiceq = find(q == true);
if isempty(indiceq)
display([patientfilename(i).name,...
'___dissaccommodation(c): No consecutive decreasing data

```

```

points found'])
else
    w1 = diff(Mpxtrans2)<0;
    for j = 1:(length(w1)-3)
        q1(j) = ([w1(j,1)+w1(j+1,1)+w1(j+2,1)+w1(j+3,1)]==3 &&...
                [w1(j+1,1)+w1(j+2,1)+w1(j+3,1)]==3);
    end
    indiceq1 = find(q1 == true);
    if isempty(indiceq1)
        display([patientfilename(i).name,...
                '___dissaccommodation(d): No consecutive decreasing
data points found'])
    else
        % Define section in which the cut off values will be
calculated (Mpx)
        Mpxcalc2 = Mpxtrans2(indiceq(1,1)+1 : indiceq1(1,1)+1,1);
        Timecalc2 = Timetrans2(indiceq(1,1)+1 : indiceq1(1,1)+1,1);
        if isempty(Timecalc2)
            display([patientfilename(i).name,...
                    '___invalid dissaccommodation'])
        else
            % Locate cut-off points in the calculation sections
            c = baseY + (0.1*B);
            [w index] = min(abs(Mpxcalc2-c));
            idc = index; % Finds first one only
            c = Timecalc2(idc,1)/1000;
            cplot = [c,c];
            yaxisplot = [6,-6];
            plot(cplot,yaxisplot,'c--')
            hold on;

            d = baseZ - (0.1*B);
            [w index] = min(abs(Mpxcalc2-d));
            idd = index; % Finds first one only
            d = Timecalc2(idd,1)/1000;
            dplot = [d,d];
            yaxisplot = [6,-6];
            plot(dplot,yaxisplot,'c--')
            hold on;

            % Time constants
            Tdisacc = (d-c)/log(9);

            % Save relevant data
            Tconstants2(i,12:13) = [c, d];
            Tconstants2(i,15) = Tdisacc;

```

```

% Plot stimulus vergence, Mpx and calculation zone
boundaries vs time
    plot(Timecalc2(1,1)/1000,Mpxcalc2(1,1),'g*',...
         Timecalc2(end,1)/1000,Mpxcalc2(end,1),'g*')
    end
end
end

```

## Clear temporary variables

```

clearvars filename delimiter formatSpec fileID dataArray ans
lastEle
firstEle idx stimatedMvt j tLines nCols patientname
sortedpatientname svdisacc1 svdisacc2 svacc Mpxdisacc1 Mpxdisacc2
Mpxacc Mpxtrans1 Mpxtrans2 Timetrans1 Timetrans2 baseXtime baseYtime
baseZtime;

```

## Save relevant data

```

Tconstants2(i,16:39) = [AvgbaseX_HOARMS, baseX_HOARMSsd,
AvgbaseX_MpxRMS,...
    baseX_MpxRMSsd,AvgbaseX_SAeqRMS, baseX_SAeqRMSsd,
AvgbaseY_HOARMS,...
    baseY_HOARMSsd, AvgbaseY_MpxRMS,
baseY_MpxRMSsd,AvgbaseY_SAeqRMS,...
    baseY_SAeqRMSsd, AvgbaseZ_HOARMS, baseZ_HOARMSsd,
AvgbaseZ_MpxRMS,...
    baseZ_MpxRMSsd, AvgbaseZ_SAeqRMS, baseZ_SAeqRMSsd, portionX,
portionY,...
    portionZ, begX, begY, begZ];
info2(i,:) = [patient.name, patient.measurementNo];
save(['C:\AGEYEproject\THESIS\STUDIES\ContinuousMeasurements\Age1\AN
ALYSED\25 D\',patientfilename(i).name,'_25corrected.mat'],
'patient', 'Tconstants2', 'info2');
savefig(['C:\AGEYEproject\THESIS\STUDIES\ContinuousMeasurements\Age1
\ANALYSED\25 D\figures\',patientfilename(i).name,'_Mpx_25_TC.fig']);

```

## Stimulus: 4 D

```

else verg == 40;

```

## Correction for elements in which the Badal was moving

(info provided by manufacturer)

```

    stimulatedMvt = 0.3066666666666667;
    % ACCOMMODATION:
    patient.Mpx(firstEle-1,1) = patient.Mpx(firstEle-1,1) + (-13 *
stimulatedMvt);
    patient.Mpx(firstEle-2,1) = patient.Mpx(firstEle-2,1) + (-12 *
stimulatedMvt);
    patient.Mpx(firstEle-3,1) = patient.Mpx(firstEle-3,1) + (-11 *
stimulatedMvt);
    patient.Mpx(firstEle-4,1) = patient.Mpx(firstEle-4,1) + (-10 *
stimulatedMvt);
    patient.Mpx(firstEle-5,1) = patient.Mpx(firstEle-5,1) + (-9 *
stimulatedMvt);
    patient.Mpx(firstEle-6,1) = patient.Mpx(firstEle-6,1) + (-8 *
stimulatedMvt);
    patient.Mpx(firstEle-7,1) = patient.Mpx(firstEle-7,1) + (-7 *
stimulatedMvt);
    patient.Mpx(firstEle-8,1) = patient.Mpx(firstEle-8,1) + (-6 *
stimulatedMvt);
    patient.Mpx(firstEle-9,1) = patient.Mpx(firstEle-9,1) + (-5 *
stimulatedMvt);
    patient.Mpx(firstEle-10,1) = patient.Mpx(firstEle-10,1) + (-4 *
stimulatedMvt);
    patient.Mpx(firstEle-11,1) = patient.Mpx(firstEle-11,1) + (-3 *
stimulatedMvt);
    patient.Mpx(firstEle-12,1) = patient.Mpx(firstEle-12,1) + (-2 *
stimulatedMvt);
    patient.Mpx(firstEle-13,1) = patient.Mpx(firstEle-13,1) + (-1 *
stimulatedMvt);

    % DISACCOMMODATION:
    patient.Mpx(lastEle,1) = patient.Mpx(lastEle,1) - (-13 *
stimulatedMvt);
    patient.Mpx(lastEle-1,1) = patient.Mpx(lastEle-1,1) - (-12 *
stimulatedMvt);
    patient.Mpx(lastEle-2,1) = patient.Mpx(lastEle-2,1) - (-11 *
stimulatedMvt);
    patient.Mpx(lastEle-3,1) = patient.Mpx(lastEle-3,1) - (-10 *
stimulatedMvt);
    patient.Mpx(lastEle-4,1) = patient.Mpx(lastEle-4,1) - (-9 *
stimulatedMvt);
    patient.Mpx(lastEle-5,1) = patient.Mpx(lastEle-5,1) - (-8 *
stimulatedMvt);
    patient.Mpx(lastEle-6,1) = patient.Mpx(lastEle-6,1) - (-7 *
stimulatedMvt);
    patient.Mpx(lastEle-7,1) = patient.Mpx(lastEle-7,1) - (-6 *

```

```

stimatedMvt);
    patient.Mpx(lastEle-8,1) = patient.Mpx(lastEle-8,1) - (-5 *
stimatedMvt);
    patient.Mpx(lastEle-9,1) = patient.Mpx(lastEle-9,1) - (-4 *
stimatedMvt);
    patient.Mpx(lastEle-10,1) = patient.Mpx(lastEle-10,1) - (-3 *
stimatedMvt);
    patient.Mpx(lastEle-11,1) = patient.Mpx(lastEle-11,1) - (-2 *
stimatedMvt);
    patient.Mpx(lastEle-12,1) = patient.Mpx(lastEle-12,1) - (-1 *
stimatedMvt);

```

## Correction for elements in which the Badal was moving

(info provided by manufacturer)

### % ACCOMMODATION:

```

patient.stimulusVergence(firstEle-1,1) = -13 * stimatedMvt;
patient.stimulusVergence(firstEle-2,1) = -12 * stimatedMvt;
patient.stimulusVergence(firstEle-3,1) = -11 * stimatedMvt;
patient.stimulusVergence(firstEle-4,1) = -10 * stimatedMvt;
patient.stimulusVergence(firstEle-5,1) = -9 * stimatedMvt;
patient.stimulusVergence(firstEle-6,1) = -8 * stimatedMvt;
patient.stimulusVergence(firstEle-7,1) = -7 * stimatedMvt;
patient.stimulusVergence(firstEle-8,1) = -6 * stimatedMvt;
patient.stimulusVergence(firstEle-9,1) = -5 * stimatedMvt;
patient.stimulusVergence(firstEle-10,1) = -4 * stimatedMvt;
patient.stimulusVergence(firstEle-11,1) = -3 * stimatedMvt;
patient.stimulusVergence(firstEle-12,1) = -2 * stimatedMvt;
patient.stimulusVergence(firstEle-13,1) = -1 * stimatedMvt;

```

### % DISACCOMMODATION:

```

patient.stimulusVergence(lastEle,1) = -1 * stimatedMvt;
patient.stimulusVergence(lastEle-1,1) = -2 * stimatedMvt;
patient.stimulusVergence(lastEle-2,1) = -3 * stimatedMvt;
patient.stimulusVergence(lastEle-3,1) = -4 * stimatedMvt;
patient.stimulusVergence(lastEle-4,1) = -5 * stimatedMvt;
patient.stimulusVergence(lastEle-5,1) = -6 * stimatedMvt;
patient.stimulusVergence(lastEle-6,1) = -7 * stimatedMvt;
patient.stimulusVergence(lastEle-7,1) = -8 * stimatedMvt;
patient.stimulusVergence(lastEle-8,1) = -9 * stimatedMvt;
patient.stimulusVergence(lastEle-9,1) = -10 * stimatedMvt;
patient.stimulusVergence(lastEle-10,1) = -11 * stimatedMvt;
patient.stimulusVergence(lastEle-11,1) = -12 * stimatedMvt;
patient.stimulusVergence(lastEle-12,1) = -13 * stimatedMvt;

```

## RMS deviation and time constants calculation

```
% DEFINE EACH SECTION (stimulusVergence):
svdisacc1 = patient.stimulusVergence(1 : idx(1,1)-13, 1);
svacc = patient.stimulusVergence(idx(1,1)+1 : idx(end,1)-12, 1);
svdisacc2 = patient.stimulusVergence(idx(end,1)+2 : end, 1);
% Avg refraction in defined baseline sections
baseX = mean(patient.Mpx(31 : idx(1,1)-23, 1));
baseXstd = std(patient.Mpx(31 : idx(1,1)-23, 1));
baseY = mean(patient.Mpx(idx(1,1)+31 : idx(end,1)-22, 1));
baseYstd = std(patient.Mpx(idx(1,1)+31 : idx(end,1)-22, 1));
baseZ = mean(patient.Mpx(idx(end,1)+32 : end-10, 1));
baseZstd = std(patient.Mpx(idx(end,1)+32 : end-10, 1));
% RMS deviation in defined baseline sections
% X
baseX_HOARMS = sqrt(sum(patient.Zmicrons(31 : idx(1,1)-23,
4:12).^2,2));
AvgbaseX_HOARMS = mean(baseX_HOARMS);
baseX_HOARMSsd = sqrt(1/length(baseX_HOARMS)*...
    (sum((baseX_HOARMS(:,1) - mean(baseX_HOARMS)).^2)));

baseX_MpxRMS = patient.Mpx(31 : idx(1,1)-23, 1);
AvgbaseX_MpxRMS = mean(baseX_MpxRMS);
baseX_MpxRMSsd = sqrt(1/length(baseX_MpxRMS)*...
    (sum((baseX_MpxRMS(:,1) - mean(baseX_MpxRMS)).^2)));

baseX_SAEqRMS = patient.SAEq(31 : idx(1,1)-23, 1);
AvgbaseX_SAEqRMS = mean(baseX_SAEqRMS);
baseX_SAEqRMSsd = sqrt(1/length(baseX_SAEqRMS)*...
    (sum((baseX_SAEqRMS(:,1) - mean(baseX_SAEqRMS)).^2)));

% Y
baseY_HOARMS = sqrt(sum(patient.Zmicrons(idx(1,1)+31 : idx(end,1)-
22, 4:12).^2,2));
AvgbaseY_HOARMS = mean(baseY_HOARMS);
baseY_HOARMSsd = sqrt(1/length(baseY_HOARMS)*...
    (sum((baseY_HOARMS(:,1) - mean(baseY_HOARMS)).^2)));

baseY_MpxRMS = patient.Mpx(idx(1,1)+31 : idx(end,1)-22, 1);
AvgbaseY_MpxRMS = mean(baseY_MpxRMS);
baseY_MpxRMSsd = sqrt(1/length(baseY_MpxRMS)*...
    (sum((baseY_MpxRMS(:,1) - mean(baseY_MpxRMS)).^2)));

baseY_SAEqRMS = patient.SAEq(idx(1,1)+31 : idx(end,1)-22, 1);
AvgbaseY_SAEqRMS = mean(baseY_SAEqRMS);
baseY_SAEqRMSsd = sqrt(1/length(baseY_SAEqRMS)*...
    (sum((baseY_SAEqRMS(:,1) - mean(baseY_SAEqRMS)).^2)));
```

```

% Z
baseZ_HOARMS = sqrt(sum(patient.Zmicrons(idx(end,1)+32 : end-10,
4:12).^2,2));
AvgbaseZ_HOARMS = mean(baseZ_HOARMS);
baseZ_HOARMSsd = sqrt(1/length(baseZ_HOARMS)*...
    (sum((baseZ_HOARMS(:,1) - mean(baseZ_HOARMS)).^2)));

baseZ_MpxRMS = patient.Mpx(idx(end,1)+32 : end-10, 1);
AvgbaseZ_MpxRMS = mean(baseZ_MpxRMS);
baseZ_MpxRMSsd = sqrt(1/length(baseZ_MpxRMS)*...
    (sum((baseZ_MpxRMS(:,1) - mean(baseZ_MpxRMS)).^2)));

baseZ_SAEqRMS = patient.SAEq(idx(end,1)+32 : end-10, 1);
AvgbaseZ_SAEqRMS = mean(baseZ_SAEqRMS);
baseZ_SAEqRMSsd = sqrt(1/length(baseZ_SAEqRMS)*...
    (sum((baseZ_SAEqRMS(:,1) - mean(baseZ_SAEqRMS)).^2)));

% Calculate Amplitudes
A = abs(baseY)-abs(baseX);
B = abs(baseY)-abs(baseZ);

% Time interval in defined baseline sections
baseXtime = -(patient.time(31,1) - patient.time(idx(1,1)-23, 1));
portionX = baseXtime; % ms of sustained accommodative response
begX = patient.time(31,1); % ms after the stimulus presentation that
we take
%to start considering the sustained accommodative repsonse portion
baseYtime = -(patient.time(idx(1,1)+31,1) - patient.time(idx(end,1)-
22, 1));
portionY = baseYtime;
begY = patient.time(idx(1,1)+31,1) - patient.time(idx(1,1)+1,1); %
ms after
%the stimulus presentation that we take to start considering the
sustained
%accommodative repsonse portion
baseZtime = -(patient.time(idx(end,1)+32,1) - patient.time(end-10,
1));
portionZ = baseZtime;
begZ = patient.time(idx(end,1)+32,1) - patient.time(idx(end,1)+2,1);
% ms after the stimulus presentation that we take to start
considering the
%sustained accommodative repsonse portion;

% DEFINE EACH SECTION (Mpx): from the beggining of the transition
when the

```

```

% stimulus was presented to the 41th data point in the next section
Mpxdisacc1 = patient.Mpx(1 : idx(1,1)-13, 1);
Mpxtrans1 = patient.Mpx(idx(1,1)-12:idx(1,1)+40,1);
Mpxacc = patient.Mpx(idx(1,1)+1 : idx(end,1)-12, 1);
Mpxtrans2 = patient.Mpx(idx(end,1)-11:idx(end,1)+41,1);
Mpxdisacc2 = patient.Mpx(idx(end,1)+2 : end, 1);

% DEFINE EACH SECTION (time)
Timetrans1 = patient.time(idx(1,1)-12:idx(1,1)+40,1);
Timetrans2 = patient.time(idx(end,1)-11:idx(end,1)+41,1);

% DEFINE CALCULATION SECTIONS
% ACCOMMODATION

x = diff(Mpxtrans1)<0;
for j = 1:(length(x)-3)
    y(j) = ([x(j,1)+x(j+1,1)+x(j+2,1)+x(j+3,1)]==3 &&...
        [x(j+1,1)+x(j+2,1)+x(j+3,1)]==3);
end
indicey = find(y == true);
if isempty(indicey)
    display([patientfilename(i).name,...
        '___accommodation(a): No consecutive decreasing data points
found'])
else
    x1 = diff(Mpxtrans1)>0;
    for j = 1:(length(x1)-3)
        y1(j) = ([x1(j,1)+x1(j+1,1)+x1(j+2,1)+x1(j+3,1)]==3 &&...
            [x1(j+1,1)+x1(j+2,1)+x1(j+3,1)]==3);
    end
    indicey1 = find(y1 == true);
    if isempty(indicey1)
        display([patientfilename(i).name,...
            '___accommodation(b): No consecutive decreasing data
points found'])
    else
        % Define section in which the cut off values will be
calculated (Mpx and time)
        Mpxcalc1 = Mpxtrans1(indicey(1,1)+1 : indicey1(1,1)+1,1);
        Timecalc1 = Timetrans1(indicey(1,1)+1 : indicey1(1,1)+1,1);
        % Plot stimulus vergence, Mpx and calculation zone
boundaries
        % vs time and save it
        figure('Name', [patientfilename(i).name, '_M_40_TC'])
        xlim([0,20]);
        ylim([-6,6]);
    end
end

```



```

title('Dynamic accommodative response');
xlabel('Time (s)');
ylabel('Paraxial Equivalent defocus (D)');
hold on;
plot(patient.time/1000,patient.stimulusVergence,'k');
hold on;
plot(patient.time(1:31, 1)/1000, patient.Mpx(1:31, 1),'b');
%blue
%line when no baseline section
hold on;
plot(patient.time(31 : idx(1,1)-23, 1)/1000,...
      patient.Mpx(31 : idx(1,1)-23, 1),'r'); %red line when
baseline section
hold on;
plot(patient.time(idx(1,1)-23:idx(1,1)+31,1)/1000,...
      patient.Mpx(idx(1,1)-23:idx(1,1)+31,1), 'b');
hold on;
plot(patient.time(idx(1,1)+31 : idx(end,1)-22, 1)/1000,...
      patient.Mpx(idx(1,1)+31 : idx(end,1)-22, 1),'r');
hold on;
plot(patient.time(idx(end,1)-22:idx(end,1)+32,1)/1000,...
      patient.Mpx(idx(end,1)-22:idx(end,1)+32,1), 'b');
hold on;
plot(patient.time(idx(end,1)+32 : end-10, 1)/1000,...
      patient.Mpx(idx(end,1)+32 : end-10, 1),'r');
hold on
if isempty(Timecalc1)
    display([patientfilename(i).name, '___invalid
accommodation'])
else
% Locate cut-off points in the calculation sections
a = baseX + (0.1*A);
[w index] = min(abs(Mpxcalc1-a));
ida = index; % Finds first one only
a = Timecalc1(ida,1)/1000;
aplot = [a,a];
yaxisplot = [6,-6];
plot(aplot,yaxisplot,'c--')
hold on;

b = baseY - (0.1*A);
[w index] = min(abs(Mpxcalc1-b));
idb = index; % Finds first one only
b = Timecalc1(idb,1)/1000;
bplot = [b,b];
yaxisplot = [6,-6];

```

```

plot(bplot,yaxisplot,'c--')
hold on;

% Time constants
Tacc = (b-a)/log(9);

% Save relevant data
Tconstants4(i,1:11) = [verg, baseX, baseXstd, baseY,...
    baseYstd, baseZ, baseZstd, A, B, a, b];
Tconstants4(i,14) = Tacc;

% Plot stimulus vergence, Mpx and calculation zone
boundaries
% Vs time and save it
plot(Timecalc1(1,1)/1000,Mpxcalc1(1,1), 'g*',...
    Timecalc1(end,1)/1000,Mpxcalc1(end,1), 'g*')
hold on
end
end
end

% DISACCOMMODATION
w = diff(Mpxtrans2)>0;
for j = 1:(length(w)-3)
    q(j) = ([w(j,1)+w(j+1,1)+w(j+2,1)+w(j+3,1)]==3 &&...
        [w(j+1,1)+w(j+2,1)+w(j+3,1)]==3);
end
indiceq = find(q == true);
if isempty(indiceq)
    display([patientfilename(i).name,...
        '___dissaccommodation(c): No consecutive decreasing data
points found'])
else
    w1 = diff(Mpxtrans2)<0;
    for j = 1:(length(w1)-3)
        q1(j) = ([w1(j,1)+w1(j+1,1)+w1(j+2,1)+w1(j+3,1)]==3 &&
[w1(j+1,1)+w1(j+2,1)+w1(j+3,1)]==3);
    end
    indiceq1 = find(q1 == true);
    if isempty(indiceq1)
        display([patientfilename(i).name,...
            '___dissaccommodation(d): No consecutive decreasing
data points found'])
    else
        % Define section in which the cut off values will be
calculated (Mpx)
Mpxcalc2 = Mpxtrans2(indiceq(1,1)+1 : indiceq1(1,1)+1,1);

```

```

Timecalc2 = Timetrans2(indiceq(1,1)+1 : indiceq1(1,1)+1,1);
if isempty(Timecalc2)
    display([patientfilename(i).name, ...
            '____invalid dissaccommodation'])
else
    % Locate cut-off points in the calculation sections
    c = baseY + (0.1*B);
    [w index] = min(abs(Mpxcalc2-c));
    idc = index; % Finds first one only
    c = Timecalc2(idc,1)/1000;
    cplot = [c,c];
    yaxisplot = [6,-6];
    plot(cplot,yaxisplot,'c--')
    hold on;

    d = baseZ - (0.1*B);
    [w index] = min(abs(Mpxcalc2-d));
    idd = index; % Finds first one only
    d = Timecalc2(idd,1)/1000;
    dplot = [d,d];
    yaxisplot = [6,-6];
    plot(dplot,yaxisplot,'c--')
    hold on;

    % Time constants
    Tdisacc = (d-c)/log(9);

    % Save relevant data
    Tconstants4(i,12:13) = [c, d];
    Tconstants4(i,15) = Tdisacc;

    % Plot stimulus vergence, Mpx and calculation zone
boundaries Vs time
    plot(Timecalc2(1,1)/1000,Mpxcalc2(1,1), 'g*', ...
         Timecalc2(end,1)/1000,Mpxcalc2(end,1), 'g*')
    end
end
end
end

```

### Clear temporary variables

```

clearvars filename delimiter formatSpec fileID dataArray ans
lastEle firstEle idx j tLines nCols patientname sortedpatientname
stimatedMvt svdisacc1 svdisacc2 svacc Mpxdisacc1 Mpxdisacc2 Mpxacc
Mpxtrans1 Mpxtrans2 Timetrans1 Timetrans2 baseXtime baseYtime
baseZtime;

```

## Save relevant data

```
Tconstants4(i,16:39) = [AvgbaseX_HOARMS, baseX_HOARMSsd,
AvgbaseX_MpxRMS, ...
    baseX_MpxRMSsd, AvgbaseX_SAEqRMS, baseX_SAEqRMSsd,
AvgbaseY_HOARMS, ...
    baseY_HOARMSsd, AvgbaseY_MpxRMS, baseY_MpxRMSsd,
AvgbaseY_SAEqRMS, ...
    baseY_SAEqRMSsd, AvgbaseZ_HOARMS, baseZ_HOARMSsd,
AvgbaseZ_MpxRMS, ...
    baseZ_MpxRMSsd, AvgbaseZ_SAEqRMS, baseZ_SAEqRMSsd, portionX,
portionY, ...
    portionZ, begX, begY, begZ];
info4(i,:) = [patient.name, patient.measurementNo];
save(['C:\AGEYEproject\THESIS\STUDIES\ContinuousMeasurements\Age1\AN
ALYSED\40 D\',patientfilename(i).name,'_40corrected.mat'],
'patient', 'Tconstants4', 'info4');
savefig(['C:\AGEYEproject\THESIS\STUDIES\ContinuousMeasurements\Age1\AN
ALYSED\40 D\figures\',patientfilename(i).name,'_Mpx_40_TC.fig']);

End

end
save(['C:\AGEYEproject\THESIS\STUDIES\ContinuousMeasurements\Age1\AN
ALYSED\25 D\total_25corrected.mat'], 'Tconstants2', 'info2');
save(['C:\AGEYEproject\THESIS\STUDIES\ContinuousMeasurements\Age1\AN
ALYSED\40 D\total_40corrected.mat'], 'Tconstants4', 'info4');
```

*Published with MATLAB® R2014b*